AD NUMBER

AD840024

LIMITATION CHANGES

TO:

Approved for public release; distribution is unlimited.

FROM:

Distribution authorized to U.S. Gov't. agencies and their contractors; Critical Technology; AUG 1968. Other requests shall be referred to Office of Naval Research, Washington, DC. This document contains export-controlled technical data.

AUTHORITY

onr ltr, 28 jul 1977

SU-SEL-68-052

Quasi-Linear Interference Suppressor

by

A. C. Phillips

AUGUST 1968

TECHNICAL REPORT NO. 150

Prepared under
Office of Naval Research Contract
Nonr-225(64), NR 088 019, and
Advanced Research Projects Agency ARPA Order 196

RADIOSCIENCE LABORATORY

STANFORD ELECTRONICS LABORATORIES

STANFORD UNIVERSITY · STANFORD, CALIFORNIA

QUASI-LINEAR INTERFERENCE SUPPRESSOR

by

A. C. Phillips

August 1968

Technical Report No. 150

Prepared under
Office of Naval Research Contract
Nonr-225(64), NR 088 019

Radioscience Laboratory
Stanford Electronics Laboratories
Stanford University Stanford, California

ABSTRACT

The purpose of this research was to devise and test new interference suppression techniques. A major motivation was the desire to minimize the deleterious effects of HF radio-station interference to an ionosphere sounder. Previous research has shown that the FM-CW waveform is particularly attractive for ionosphere sounding because of the ability to generate waveforms having very large time bandwidth products using electronically controlled frequency synthesizers. In studying interference problems during this research it was appreciated for the first time that simple nonlinear processing (e.g., clipping) in the FM-CW sounder is directly analogous to the much more complicated nonlinear processing (e.g., frequency-by-frequency limiting) necessary in the corresponding simple-pulse or coded-pulse sounding systems.

A new interference suppression method has been devised and shown to be effective in removing pulse or FM-CW interference from narrow-band signals. Interference energy at frequencies outside the desired-signal bandwidth is processed and used to balance out the interference energy included with the desired signal. The balancing action is intermittent and the principle of operation is to switch from one linear mode to another, hence the name quasi-linear suppressor (QLS).

The performance of the quasi-linear suppressor in removing pulse or FM-CW signals generated in the laboratory, was shown to be very satisfactory. An FM-CW sounder receiver was tested at a field site where antennas of a type typically used for ionosphere sounding were available. It was found that the new suppressor was able to decrease the amplitude of the IF response due to interference at least 20 dB for about 70 percent of the stations. The FM-CW receiver was also used to compare the suppression of HF radio-station interference by means of the new quasi-linear suppressor, with a hitherto preferred nonlinear technique. A CW signal, to simulate a desired sounder signal, was added to the interference background received from the antenna. The criterion for performance in this test was the ratio of the spectrum analyzer response at the desired CW frequency, to analyzer responses caused by the interference. (The interference usually affects all filters in the analyzer roughly alike.) The improvement in this ratio

when using the quasi-linear suppressor was found to be approximately 3 dB. It is felt that this is a pessimistic result because in the process of testing, it was observed that the laboratory FM-CW generator contained spurious outputs which greatly increased the effects of the interference in a way which reduced the advantage of the quasi-linear scheme over non-linear methods.

CONTENTS

CONTENTS (Cont)

TABLE

Number

ILLUSTRATIONS

ILLUSTRATIONS (Cont)

LIST OF SYMBOLS

A_i, B_i	constant for circuit transfer function
b	system constant
B	circuit 3 dB bandwidth
e(t)	sinusoid envelope
E_o	system output voltage
$F_r(\gamma)$	Fresnel integral
f_m	modulation frequency
f_o	band center frequency
$\triangle f$	frequency increment
A(t)	amplitude function of time
g(s)	numerator of system transfer function
G	circuit gain
h(s)	denominator of system transfer function
H	system transfer function
i	integer
P	probability
PSNR	peak signal to rms-noise energy ratio
Q	ratio of inductive reactance ωL to circuit resistance R in a single tuned circuit
s	Laplace transform variable
S	FM-CW sweep rate (Hz/sec)
SNR	signal-to-noise energy ratio
t	time
t_a	time measurement accuracy
t_e	time measurement error
T	fixed time increment

$T(s)$	system transfer function
v	ac voltage
V_c	cancelled QLS output
V_i	network voltage input
V_N	noise voltage
V_o	network voltage output
V_r	cancellation residue
V_s	signal voltage
V_u	uncancelled QLS output
α	real part of complex number
β	imaginary part of complex number
γ	complex number
ϵ	FM-CW sweep constant $\left(= \frac{\pi S}{2}\right)$
θ	general phase constant
θ_e	phase error
θ_L	phase lag of delay circuits
Σ	summation
τ	time delay
$\varphi(t)$	phase function of time
ω_o	band center radian frequency $(= 2\pi f_o)$
$\Delta\omega$	radian frequency increment

ACKNOWLEDGMENT

The author wishes to thank Professor O. G. Villard, Jr. for his guidance and encouragement throughout this work. I am also grateful to Professor L. A. Manning and Professor M. M. McWhorter for their suggestions in improving the technical quality of the manuscript.

I. INTRODUCTION

A. PURPOSE

The object of the research reported herein was to devise and test new interference-suppression methods to be used in the processing of signals in the presence of additive interference. An effective interference-suppressing technique may be defined as one which has the ability to distinguish between the additive interference and the desired signal, and to select the signal while rejecting the interference.

In the present study, emphasis is on those situations in which the desired information is contained in the amplitude and phase of a complex signal whose frequency components are contained within a known bandwidth. It is assumed that the additive interference has frequency components both inside and outside the signal bandwidth, and that the components outside the bandwidth are correlated with those inside the bandwidth.

B. BACKGROUND

1. Motivation

A specific motivation for the present work was the desire to improve the quality of interference rejection in the linear-sweep continuous wave (FM-CW) ionosphere sounder. This device is used for determining the refractive properties of various layers of the ionosphere, which in turn affect the transmission of high-frequency (HF) radio signals.

Electronic analog communication, where radiation (as contrasted with guiding) of energy takes place, is of very great economic importance. Unfortunately the frequency spectrum useful for radiation has a finite width. The demands for spectrum space are steadily increasing as the world's needs for communication increase. The frequency interval within which signals can be transmitted via the ionosphere is particularly limited and is therefore especially crowded, and interference is already a serious problem. Furthermore, the properties of the ionosphere are extraordinarily variable: there are major changes with time of day,

season, geographic location, and position in the sunspot cycle. To ensure optimum utilization of the available frequency spectrum, these changes should be known as a function of real time.

The circumstances described above have led to widespread adoption of techniques for sounding the refracting ability of the ionosphere, preferably in many geographic areas at one time. Once this information is available, it is possible to adopt procedures (such as choice of radio frequencies, antennas, etc.) which insure best utilization of the ionospheric layers and hence the most effective communication. Knowledge of the condition of the layers is useful for other purposes as well. For example, the ionosphere is perturbed by large explosions [Ref. 1] such as nuclear tests. Since the occurrence of such tests over inaccessible terrain can be monitored by radio means, ionosphere sounding has acquired additional importance in this connection.

A unique problem with ionosphere sounders is that they must operate with variable radio frequency, in order properly to assess the refractive properties of the plasma. Further, they must operate in a portion of the spectrum which is for all practical purposes already filled with other signals. They must not themselves be put out of action by the signals received, and they must not cause too much interference to other users of the spectrum. One type of sounding signal which has proven quite promising in both regards is the linear FM-CW sweep, which appears likely to find increasing application in the future. Improvement in the interference-rejection ability of the FM-CW ionosphere sounder, therefore, should prove valuable in increasing knowledge of the properties of the ionosphere and hence in ensuring optimum utilization of the frequency spectrum available for HF radio propagation.

2. Previous Work in the Field

Previous efforts toward overcoming the deleterious effects of the fixed-station interference in an ionosphere sounder have been limited to the development of methods for increasing the transmitted energy, and the adoption of nonlinear signal processing. The disadvantages of these techniques are that the increased transmitted energy may worsen the

interference to fixed-station communicators, and the nonlinear operations often distort the desired data, thus making its interpretation more difficult.

A complete discussion of previous work in the field of interference suppression, with especial reference to the ionosphere sounder, will be found in Chapter III.

C. APPROACH USED IN THE PRESENT STUDY

In view of the limitations and disadvantages inherent in existing methods of interference suppression, the author of the present study has developed a quasi-linear anti-interference technique which actually balances out interference while leaving the desired signal intact. (There is a slight degradation in signal-to-noise ratio during the balancing operation.) The technique, called the "Quasi-Linear Suppressor" (QLS) is particularly useful in reducing interference caused by fixed-station signals in an FM-CW ionosphere sounder. The technique can also be used to suppress FM-CW or impulsive interference in communication systems, provided a bandwidth of three times the desired signal bandwidth, and centered about the latter, is available free of other narrow-band transmissions.

The balancing action of the QLS is intermittent, and must be triggered by the interfering signal. The efficiency of interference removal therefore depends to some extent on the effectiveness of the triggering. The anti-interference circuit described here performs well with that fairly large class of interfering signals which have frequency components extending well outside the desired-signal passband, and whose statistical properties are reasonably well understood and amenable to prediction. Two types of interfering signals possessing these properties are impulse signals and FM-CW signals.

The quasi-linear interference suppression technique to be discussed is particularly well adapted to handle FM-CW signals. In a sounder of the FM-CW type, the QLS technique can reduce the effects of a large class of fixed-frequency interfering signals. In addition, for fixed-frequency services (provided that certain requirements can be met) the technique

offers the possibility of greatly reducing FM-CW sounder interference (or with a slight modification, impulse interference) with little effect on a communication receiver.

In this report the design of the QLS and its component circuitry is analyzed, and test results measuring its effectiveness are presented.

D. CONTRIBUTIONS

Original contributions involved in the research described herein are as follows:

1. A new method of eliminating impulse interference by cancellation, using a quasi-linear technique, was devised. A circuit was constructed to demonstrate the feasibility of the method. In a preferred configuration of the circuit, its operation during impulse cancellation can be described by the theory of linear time-varying systems, thus distinguishing the method from any of the previously proposed methods for eliminating impulse interference.

2. The quasi-linear method was extended to include interference caused by FM-CW ("chirp") waveforms. The feasibility of using the quasi-linear method to decrease the interference caused by HF radio stations to an FM-CW ionosphere sounder was demonstrated in tests using a simulated FM-CW sounder receiver.

II. TYPES AND PROPERTIES OF INTERFERENCE

As pointed out in the introduction, an effective interference-suppressing technique may be defined as one which has the ability to distinguish between the disturbance and the desired signal and to select the signal while rejecting the disturbance. The basis for the selection can be any property of the radio-frequency signals such as their relative amplitudes, frequencies, phase relations, etc. In this chapter, the types and properties of interference important in this research are discussed.

A. THE HF RADIO BAND

As a preliminary step, the nature of the HF radio spectrum will be discussed in order to illustrate the importance of HF radio and to describe the properties of the interference encountered by the ionosphere sounder. It should be noted that the interference suppression methods to be discussed in later chapters of this work do not attempt to alleviate the problems of interference between adjacent narrow-bandwidth HF communication channels (i.e., they are effective only against wide-bandwidth signals).

Radio transmissions at frequencies within the HF band (3-30 MHz) encounter unique conditions of refraction and low attenuation during propagation in the ionosphere. These conditions make extremely long distance communication possible. However, dispersion, multipath, maximum usable frequency (MUF), and attenuation are effects which limit the range of frequencies that may be used for reliable long-distance communication.

Economic considerations are an important reason for communication by HF radio. Other communication methods for point-to-point communication (such as cable, microwave relay chain or relay satellite) are superior to HF radio in reliability and quality; but often the amount of communication traffic between two given points does not justify the comparatively greater expense or complication of these methods. The HF band is particularly useful in mobile situations. In the case of

broadcasting service such as provided by the British Broadcast Corporation, the Voice of America, and others, HF radio is also used for economic reasons, since fewer transmitters are required to cover a given geographic area compared to the number required for standard broadcasting at frequencies below 3 MHz. Transmissions in the HF band are also useful for international information exchanges, where it is desired to communicate to populations whose governments would not allow foreign operation of broadcast stations on their soil.

Because of the utility of, and demand for, HF radio, the frequencies for which long-distance propagation is of good quality are almost completely in use. Band-occupancy surveys have shown that the output of a 5 kHz bandwidth receiver connected to a sensitive antenna yields a signal level well above that corresponding to random noise more than 90 percent of the time as the receiver is tuned across the more active portions of the HF band [Ref. 2].

Many types of modulation are employed in HF radio, but a detailed discussion of them is not necessary here. The majority of transmissions, however, are of less than 10 kHz bandwidth, with most of the energy contained in a carrier wave of fixed or slowly varying frequency. The most notable exceptions to this statement are multiplex telegraph systems.

B. IMPULSE NOISE

Impulse noise can be characterized as having greater excursions above the rms value than would be expected from a gaussian random noise. This is a consequence of spikes or bursts of energy from single sources, each of which has energy which cannot be considered negligible compared to the total noise energy. Some typical and highly ubiquitous sources for this type of disturbance are lightning discharges, automobile ignition systems, arcing electrical contacts, etc.

If the energy bursts are sufficiently narrow in time (i.e., wide in frequency bandwidth) their effect on a system may be indistinguishable from that expected of an ideal impulse (i.e., zero duration, infinite amplitude) [Ref. 3]. A single ideal impulse will cause identical envelope responses when applied to two symmetrical filters of equal bandwidths but

differing center frequencies. When a sequence of impulses with random spacing is applied to the same filters, the filter responses will not be identical unless the filter ringing caused by each impulse has decayed to an insignificant level before the next arrives. This is because the phase of the ringing with respect to the phase of the new impulse response is a function of the center frequency of the filter. Similarly, the envelope probability distribution of a single filter output becomes the same as a gaussian random process (Rayleigh) as the rate of randomly spaced impulses is increased to some value determined by the filter bandwidth. Thus a disturbance with a particular rate of impulse occurrence may retain its impulsive properties in a wide bandwidth filter, but be indistinguishable from a gaussian process in a narrow bandwidth filter.

Many disturbances which are nearly equivalent to a true impulse at the source lose much of their impulsive property before reaching the receiver. The phenomena of dispersion and multipath, such as occur with an ionospherically propagated signal, may introduce substantial waveform distortion. Theoretically, the dispersion could be compensated by using a network of equal but opposite dispersion; but of course the dispersion is usually not known, and in addition, interference may be arriving from several sources with differing dispersions. Multipath increases the number of impulses received at a given point, requiring a larger bandwidth to preserve the impulsive properties; and if dispersion is present at the same time, the impulsive properties may be degraded for any bandwidth, and thus make its elimination more difficult.

C. IONOSPHERE SOUNDER OPERATION

Ionosphere measurement techniques involve transmitting and receiving signals within the same frequency bands used by communicators. Methods are required which enable these measurements to be made with as little disruption as possible of the fixed-station communicator reception.

Electromagnetic propagation through the ionosphere can be represented as a "block" (i.e., a self-contained unit) in a communication channel. It is a very complex and time-variable block which has required continued research since the first ionosphere measurement technique was developed.

As new and more precise measurements are made, new questions tend to arise, the solution of which calls for even better methods of measurement. The characteristics of the ionosphere are normally determined by a sounder which uses radar techniques to obtain a graph of time delay between transmitter and receiver as a function of transmitted frequency. Such a graph is called an ionogram. The first ionosphere soundings were made by Breit and Tuve [Ref. 4] using a conventional pulse waveform. Sophisticated equipment developed and waveform theory has recently led to the use of coded pulse and FM-CW ("chirp") waveforms [Refs. 10 and 13]. The configuration of the transmitter and receiver may be monostatic or bistatic. In monostatic sounding, the probing beam is vertical and is reflected by the ionospheric layers back to the same spot from which it originated, so that transmitter and receiver are in the same location. In bistatic sounding, the probing beam is oblique and is therefore reflected by the ionospheric layers to some spot on the earth's surface other than the transmitting site, so that the sounder receiver and the sounder transmitter are in different locations. Bistatic sounding using an oblique-incidence probe simulates the communication situation more accurately than does monostatic sounding using a vertical-incidence probe.

Communication equipment operators use the data resulting from the operation of vertical-sounding sites around the world to select the time and frequency best for communicating. The parameters most used from the sounder data are the critical frequencies, which are the highest frequencies reflected by the different layers of the ionosphere. For research purposes the ionograms also provide data enabling calculation of the free electron density as a function of height. A resolution of about 100 μsec is adequate to determine the critical frequencies and electron densities. The corresponding typical receiver bandwidth of 10 to 40 kHz gives enough rejection of interference so that the available power in the sounder transmitter provides an adequate ratio of signal strength to interference strength to yield usable ionograms. Sounding every 15 minutes is normally adequate for the prediction of communication conditions, since the time required for significant changes in communication parameters due to ionosphere variations is on the order of one half hour.

During a sounding, a communication service would typically be interrupted no more than a few seconds by the sounder transmission. This length of time is negligible compared with the extent of other HF radio interruptions due to deep fades, atmospheric noise, and other interference.

Research which is being performed to obtain more detailed information on the properties of the ionosphere (in addition to the critical frequencies and the related electron densities) often requires higher-resolution soundings, usually of the oblique type, than those usable for the more routine analyses. The problems of interference become much greater in the wide bandwidth oblique sounder used for fine-scale study of ionospheric phenomena. First, since the ionosphere is a time-varying medium and the time of occurrence of many phenomena of interest is not known, continuous operation of the sounder over long periods is required. Second, the wide bandwidth contained by the sounder signal includes frequencies being used by many fixed-station communicators. This results in mutual interference. The Quasi-Linear Suppressor described in this report would improve the ratio of signal strength to interference strength in a sounder using the FM-CW waveform. The improved interference suppression could be used to improve the quality of soundings; or it could permit decreasing the transmitted power necessary to obtain usable data, thereby reducing the interference to other receivers, caused by the sounder.

III. PREVIOUS WORK IN INTERFERENCE SUPPRESSION

As was mentioned in the introduction, previous work in interference suppression applied to the ionosphere sounder has consisted primarily of (a) methods of increasing the average transmitted power of the sounder; and (b) introduction of nonlinear signal processing. One objective of this chapter is to present an account of this previous work in sounder interference suppression. A second objective is to present and discuss other interference suppression methods, previously used to suppress impulsive noise in communication practice, which are likely to be useful in ionosphere sounding, but which have not necessarily been applied as yet to sounding systems.

The ionosphere sounder measures, in the presence of heavy HF radio interference, the amplitude and the arrival time of a pulse or equivalent waveform. This measurement of time delay and amplitude as functions of frequency can be used to determine the amplitude and phase of the transfer function of the "block" representing the ionosphere in a communication system such as that shown by the block diagram in Fig. 1. The objective of a communication system is to transmit the message in an intelligible manner. The same block diagram as that in Fig. 1 can also be used to represent the ionosphere sounder, where the "message" becomes a pulse of sufficient bandwidth to give the time resolution required for the sounding information. The return time of the pulse, and its condition, are used to determine the properties of the ionospheric propagation path.

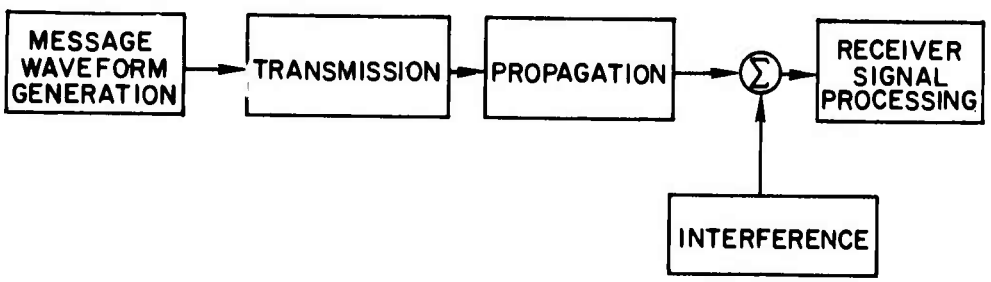

Fig. 1. BLOCK DIAGRAM OF COMMUNICATION SYSTEM.

It should be noted that in the ionosphere sounder it is not enough to indicate merely the presence or absence of a known waveform (e.g., the case analyzed by Hall [Ref. 5]). The true objective of the sounder is to measure the parameters of dispersion and multipath which make the received waveform a function of the propagation path. If methods can be developed to compensate in the communication receiver for the dispersion and multipath effects, measurements provided by the sounder can be used to determine the compensation required to restore the waveform to its original, transmitted form, thus enabling methods such as those developed by Hall to be most effective in the communication receiver.

In some systems the waveform generation block of Fig. 1 may simply be a modulation process, such as amplitude or frequency modulation. In other systems, linear operations (i.e., waveform design) may be performed before or after the modulation in order to make the transmitted waveform more easily distinguished from interference and noise or to make its waveform more convenient to transmit. The receiver signal processor will perform the inverse of any required linear operation before or after detection of the signal.

Within the context of HF radio, the present work assumes that any possible, relevant requirements concerning antenna design or receiver noise figure have already been considered. In this connection, recent developments in adaptive antennas are worth consideration [Ref. 6].

A. THE MATCHED FILTER

The matched filter is discussed here because it is the fundamental linear system-theory contribution to the problem of detecting the presence of a known waveform when that waveform is combined with other signals, or with noise having a flat frequency spectrum. It was shown by North [Ref. 7] in 1943 that the best linear system to determine the presence or absence of a known waveform in the presence of white noise is the matched filter. The peak response from the matched filter exceeds the background noise by a maximum amount [Ref. 8], so that the matched filter is an appropriate candidate for use in radar or sounder signal processing when a measurement of amplitude and time delay is required. In fact, it is a matched filter

(or equivalent) that is used to process all the waveform designs discussed in Part B of this chapter (Pulse Code, Smear-Desmear and FM-CW).

A matched filter is defined as a linear system whose impulse response is identical, within the limits of a constant multiplier, with the waveform to which it is matched with time flow reversed. An example of a matched filter for video pulse is shown in Fig. 2a [Ref. 9]. With application of an impulse a charge is immediately deposited on capacitance C. If the delay chosen is equal to the pulse width to which the circuit is to be matched, the inverted impulse from the delay network removes the charge on C after a time equal to one pulse width. Thus the circuit impulse response is equal to that of the pulse to which it was to be matched; and since reversing the time scale does not alter the shape of the pulse, this circuit constitutes the matched filter for the video pulse.

The circuit of Fig. 2a [Ref. 9] can be altered to be a matched filter for an RF pulse. The integration for the RF pulse to replace the RC integrator for the video pulse is a single, tuned, high-Q filter. Figure 2b shows the resulting matched filter for an RF pulse of pulse width τ. The selection of τ is limited to values which provide a phase shift equal to an integral number of cycles of the pulse carrier frequency. This is not ordinarily a serious limitation, since most pulses are long enough to make an error of a fraction of a cycle in the impulse response negligible. The order of the delay-line filter and the integrator may of course be reversed in either Fig. 2a or b, since they are both linear systems. The configuration in which the integrator follows the filter might be the more desirable, since there would be less energy storage in the integrator. The difficulty of constructing a delay line with adequate amplitude and phase stability would often eliminate using Fig. 2b for an RF pulse matched filter.

The improvement provided by a matched filter in the ability to detect a pulse in the presence of white noise is often assumed to be applicable to the situation where a large number of narrow-band signals are contained within the pulse bandwidth (e.g., see Coll and Storey [Ref. 10]). A precise analysis to verify this assumption for the HF sounder receiver has not been made, since an accurate statistical

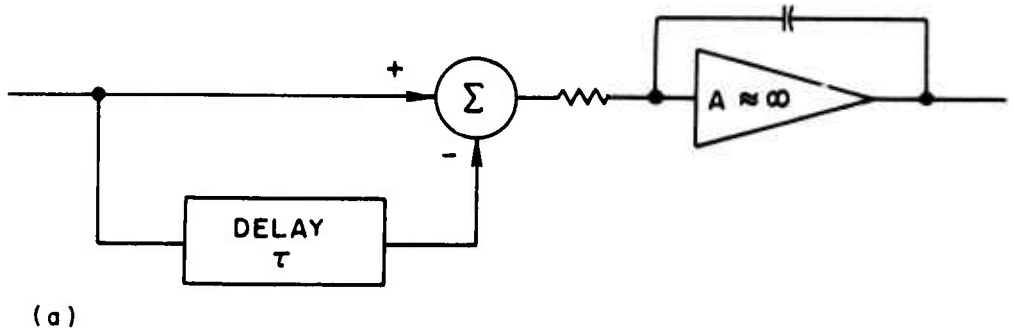

(a)

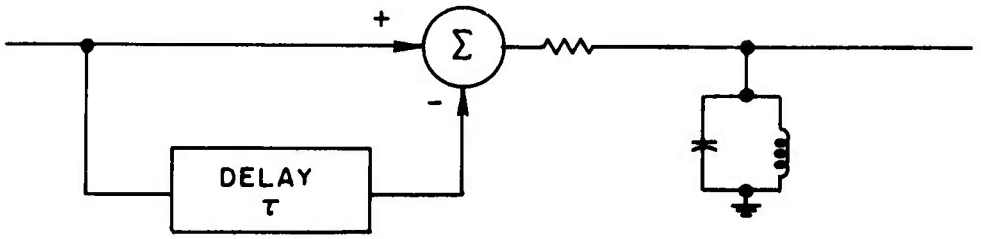

(b)

Fig. 2. EXAMPLES OF MATCHED FILTERS.
a. Matched filter for a video pulse.
b. Matched filter for an RF pulse.

description of the interference encountered in the HF band is not feasible because of the variability of the interference with time and frequency. If a priori (to pulse reception) knowledge of the HF interference is used, such as knowledge of the frequencies of narrow-band signals, the matched filter is not optimum, since the interfering narrow-band signals could be suppressed with band-rejection filters. The complexity of building and automatically adjusting the required number of band-rejection filters is to be avoided if other equally effective methods can be found. It will be noted that when nonlinear techniques are applied to the FM-CW sounder, they perform a function similar to that performed by band-rejection filters in the simple pulse system.

B. SOUNDER WAVEFORM DESIGN

Waveform design methods will be discussed here because these techniques include perhaps the most significant advances that have as yet been made in overcoming the deleterious effects of interference in ionosphere sounding practice. The subject of waveform design is in general important in interference suppression for two reasons:

1. The waveform representing a message may be designed to give a desirably low ratio of peak to average power. This can increase the average transmitted power of a peak-power-limited transmitter, thereby improving the ability of the receiver to detect the signal in the presence of the interference.

2. The desired signal waveform can perhaps be selected to be more easily distinguished from interference or noise.

The first step in considering a waveform design in general is to determine what features of the transmission through the "communication" channel are a measure of the quality of the detected "message." For a digital system, the probability of error obtainable is usually appropriate. For an analog system, the ratio of rms signal energy to rms noise energy (SNR) may be useful; but for the pulse case, the ratio of peak signal energy to rms noise energy (PSNR) is most appropriate [Ref. 9]. Once a way of determining the quality of the received "message" is found, a particular waveform design can be evaluated by considering two factors: first, the quality of the detected message for a given average

transmitted energy; and second, the peak transmitted energy required for a given quality of detected message. The first factor is of general importance, whereas the second is involved only when peak transmitter power is a limitation or represents increased expense.

The waveform designs discussed in this section are obtained by linear transformations of the message waveform either before or after modulation. In all cases the message is a pulse, since the pulse is the fundamental waveform used to measure time delay as is required in an ionosphere sounder. Waveform design is also commonly used in communication situations. In high fidelity FM broadcasting, for example, the SNR of the detected message is improved by emphasizing high frequencies before the modulation process, and de-emphasizing high frequencies an equal amount after detection.

The waveform design methods presented in subsections 1 and 2 below work by lowering the ratio of peak to average power of the transmitted signal. The FM-CW waveform discussed in subsection 3 has the best possible ratio of peak to average power (i.e., one); but an even more important feature will be observed later. This is the ease by which interference may be suppressed by using nonlinear or quasi-linear techniques.

1. Pulse Code

Coded-pulse-compression radar systems using tapped-delay-line methods were described by Rochefort [Ref. 9] in 1954. The description of the coded-pulse system presented here is essentially that which Coll and Storey [Ref. 10] applied to ionosphere sounding in 1964. A pulse train of N pulses is transmitted. Each single pulse is narrow enough in time duration to give the desired resolution. The pulses are coded in such a way that at the receiver they can be added coherently to give a pulse amplitude equal to the sum of the individual received pulse amplitudes.

Figure 3a shows a possible configuration of a transmitter for a coded-pulse system. The delay-line taps are spaced with a delay of one pulse width between taps. The pulses are coded through multiplication by gain constants, K_i, having amplitude and sign. The amplitude

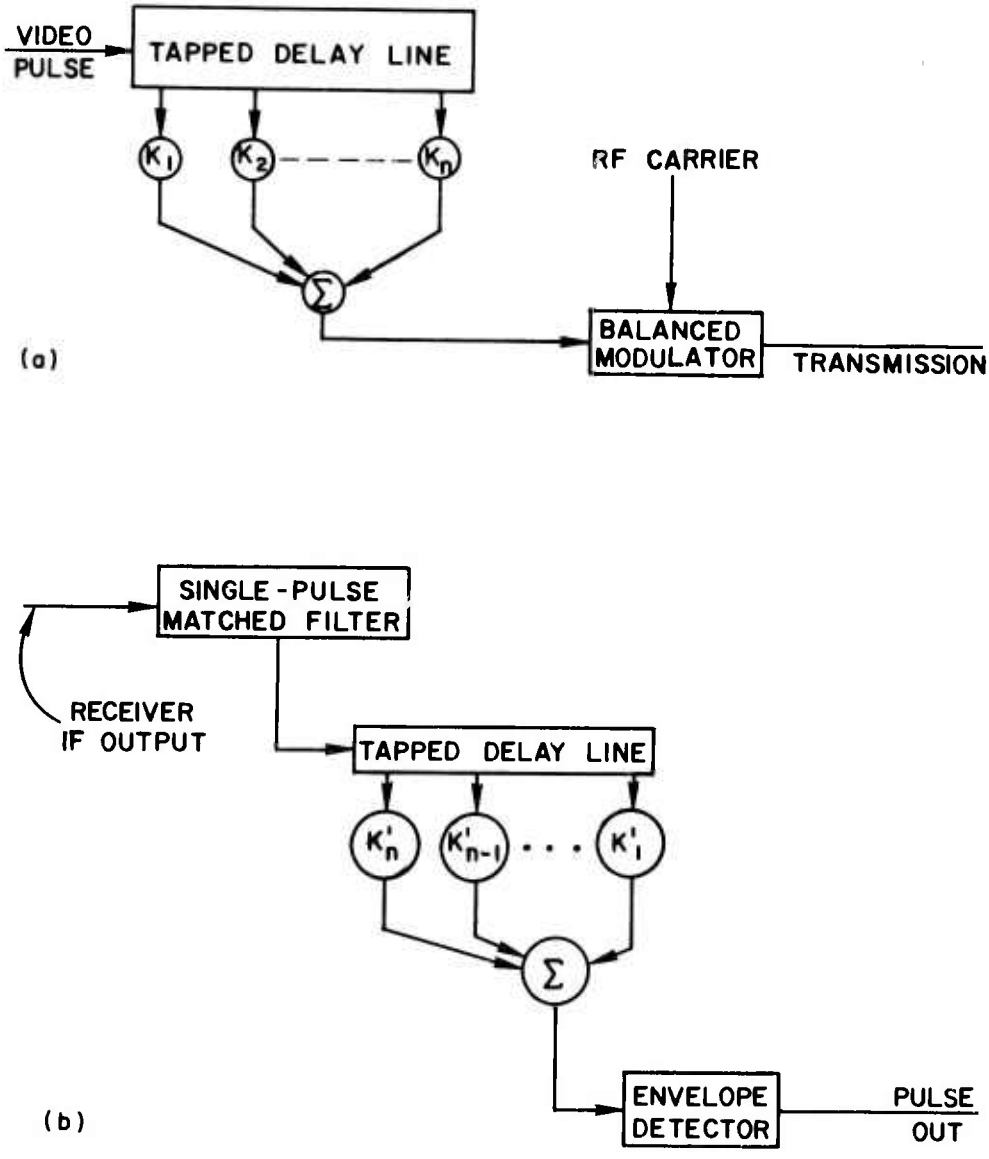

Fig. 3. BLOCK DIAGRAMS FOR CODED-PULSE SYSTEM.
a. Coded-pulse transmitter.
b. Matched filter for coded-pulse receiver.

becomes amplitude modulation of the transmitted carrier; the sign becomes either 0° or 180° phase modulation. Figure 3b shows the matched-filter signal processor which could be used for the coded-pulse reception. The constants K_i' have an amplitude and phase which correspond to the amplitude and sign of the K_i.

The matched filter effectively produces the autocorrelation function of the coded pulse train as it moves through the delay line. Codes are selected to have autocorrelation functions which are near zero except in the nonshifted position (pulse centered in the delay line). The undesired responses are called sidelobes because of the similarity between the desired form of the autocorrelation function and a narrow-beam antenna pattern. One obvious sidelobe is that which occurs when there is only one pulse in the delay line. The sidelobe responses will limit the usable dynamic range of the pulse radar or sounder.

A gain constant equal to 1 will be used to demonstrate the ability of the coded-pulse system to discriminate against random noise. When the pulse train is centered in the delay line the summation coherently adds the pulse so that the peak voltage of the output pulse becomes N times the voltage of the input pulse train. However, random noise does not add coherently, so that the output rms noise voltage is $\sqrt{N}$ times the input rms noise voltage. The improvement in the ratio of peak signal voltage to rms noise voltage is therefore $\sqrt{N}$ --an improvement of N in the ratio of peak signal power to rms noise power (PSNR). It is also noted that this improvement equals the time bandwidth product of the matched filter, which is the property commonly used to infer the effectiveness of a pulse-compression system.

2. Smear-Desmear

The coded-pulse system derived its wideband extended-time transmitted signal by sending the basic pulse signal through a multipath transfer network. A similar system uses another common property of a transmission path--that is, dispersion. The sounder pulse is applied to a dispersive network before it is sent to the transmitter, so that the frequency components of the pulse are smeared in time [Ref. 8]. At the receiver, a network producing equal but opposite dispersion compresses

or "desmears" the pulse back to its original shape. An appropriate manner of variation of time delay with frequency is shown in Fig. 4 for each of the two networks. Either network could be used for the transmitter filter, the other filter being appropriate for the receiver matched filter. The improvement of PSNR in a peak-power-limited radar obtained by using the smear-desmear technique is equal to the time bandwidth product of the transmission as in the coded-pulse system.

The smear-desmear method of waveform design is also used to transmit pulse information in the presence of impulse noise [Ref. 11], in addition to possible uses in peak-power-limited radar. The principle to be used in reducing impulse interference is that the impulse noise is added to the signal when the latter is in the smeared form. When the signal plus the impulse noise is applied to the desmearing filter, the signal again becomes a defined pulse, while the impulse noise is smeared. In this procedure, impulse noise is rejected without an increase in average power, which is not the case with the radar or sounder operation in the presence of interference and non-impulsive noise.

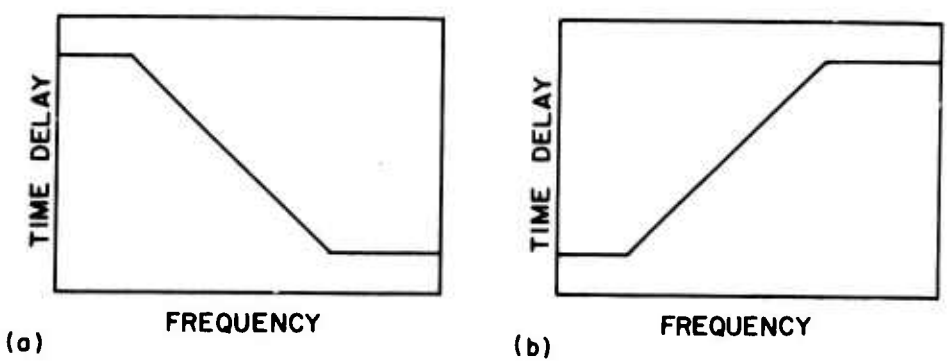

Fig. 4. PLOTS OF TIME DELAY VS FREQUENCY FOR LINEARLY DISPERSIVE NETWORKS.
a. Decreasing delay.
b. Increasing delay.

The smear-desmear type of pulse compression system has not, to the author's knowledge, been applied to ionosphere sounding. Methods have not been developed to construct the required dispersive filters with time bandwidth products much greater than one at bandwidths appropriate for ionosphere sounding (i.e., less than one MHz). However, the dispersive-filter method of waveform design is presented here as background for the FM-CW waveform to be discussed below.

3. FM-CW

If a very narrow pulse approaching an impulse (a flat frequency spectrum) is applied to one of the filters in Fig. 4 and the output is restricted to frequencies for which the time delay is linear with respect to frequency, a linear-sweep continuous wave (FM-CW) or "chirp" signal is approximately produced. The other filter of Fig. 4 becomes the corresponding matched filter. The filter method of generating or detecting FM-CW signals is not used for ionosphere sounding because techniques have not been found to build filters with adequate pulse lengths or large enough time-bandwidth products.

In 1954 Gnanalingam [Ref. 12] described an FM-CW sounding system which uses two FM-CW signal generators. One generator drives the transmitter, while the other is used as a local oscillator for a balanced mixer at the receiver and thereby produces a beat frequency which is proportional to the product of sweep rate and time delay. This beat frequency is then spectrum-analyzed to obtain the desired time delay resolution.

Gnanalingam's technique was not immediately utilized because FM-CW generators of sufficient linearity and bandwidth had not been developed. In 1964, Barry and Fenwick at Stanford University [Ref. 13] devised the first FM-CW generating equipment suitable for ionosphere sounding. This FM-CW generating equipment produces a phase-coherent sweep over 1 MHz bandwidths by digital control of a frequency synthesizer.

It is interesting to compare the spectrum-analysis method of detecting FM-CW signals to the method of using a match filter (assuming one could be built). This comparison is easiest to make by assuming system constants as follows:

FM-CW sweep rate = S = 1 MHz/sec

Analyzer bandwidth = B = 1 Hz

Path time delay = τ

The analyzed frequency equals 1 MHz/sec times τ, so that a change in τ of a microsecond will shift the analyzed frequency 1 Hz. This, in turn, results in a time-delay resolution of one microsecond with an analyzer bandwidth of 1 Hz. An effective integration time of one second is found by assuming that the analyzer filter integration time equals 1/B. During this one second, 1 MHz of the RF signal is used to obtain the one microsecond resolution, just as would be required with a conventional pulse. The noise accepted by the 1 Hz filters is equal to 10^{-6} of that in the 1 MHz bandwidth used in a conventional pulse receiver. This accomplishes an improvement of 10^6 in the PSNR as compared with the simple pulse radar having the same peak power. By finding the product of integration time and sweep rate, the time bandwidth product is found to be 10^6, so that the results of spectrum-analyzer detection are found to be equivalent to those of the matched-filter detection.

C. AN INEFFECTIVE "LINEAR IMPULSE-NOISE SUPPRESSION TECHNIQUE"

The circuit represented by the block diagram in Fig. 5 was described by Baghdady [Ref. 14] in 1960 as being effective in suppressing impulse interference. The upper amplifier has adequate bandwidth to pass the signal, while the lower is wider by a factor k in order to provide the cancelling signal. The general idea in this circuit was that when the gain of the two paths is adjusted to obtain the best cancellation of the filter ringing due to an impulse, the resulting difference in gain causes only partial cancellation of a desired narrow-band signal. However, an analysis was conducted by the present author to confirm suspicions that the suppression of impulse noise attributed to this network is misleading.

In evaluating this system Baghdady calculates the improvement in the ratio of signal amplitude to peak impulse-response amplitude at point 2 over that at point 1 shown in Fig. 5. The waveforms illustrate the principle in the case where the amplifiers have high Q, single-tuned circuits as loads. Nearly perfect cancellation results when the impulse response

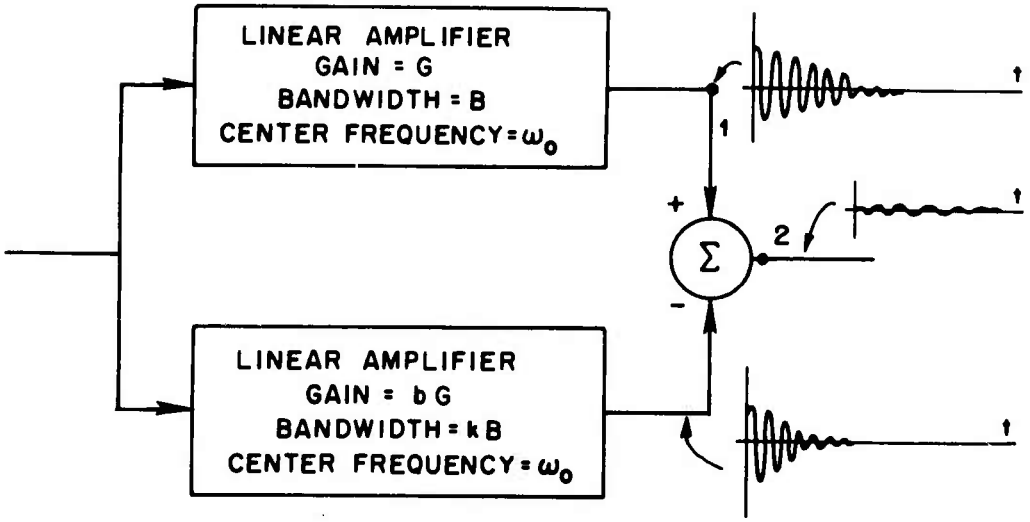

Fig. 5. BLOCK DIAGRAM OF A PURPORTED LINEAR IMPULSE SUPPRESSOR.

is largest, and the resulting peak amplitude of the impulse response is decreased more than the signal attenuation resulting from the subtraction. Optimum results are obtained in this case by making b equal to 1/k. The improvement in the ratio of signal amplitude to peak impulse amplitude then approaches 8.686 dB as k approaches 1 from above.

For the simple tuned-circuit case, Fig. 6a shows the transfer functions to match the optimum conditions. Figure 6b shows the results of reducing the block diagram by subtracting the lower transfer function from the upper. It can be seen from this result that the same two filters in series give the same transfer function (except for a constant) just as they do in the subtracting configuration. Thus the justification for the decreased impulse response is simply that more filtering is carried out.

The concept of the "linear impulse-noise suppression technique" described above was based on consideration of waveforms in the time domain. However, without checking the frequency response to each of the points where impulse responses are observed, the peak values do not have any significance. The following is a quote from Baghdady: "Bandwidth restriction to the minimum necessary value of B in circuits that follow the arrangement shown in Fig. 23* is expected to result in the removal of any

*Figure 5 of present report.

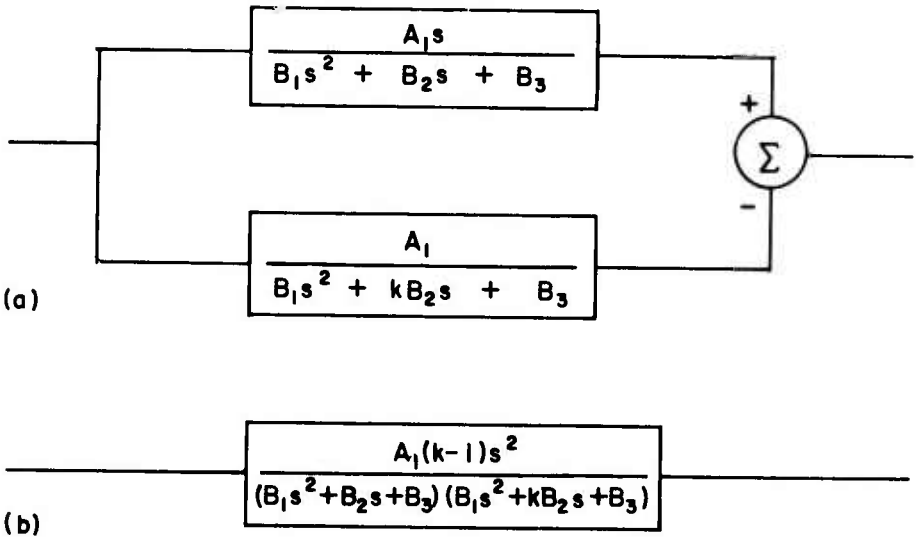

Fig. 6. REDUCTION OF BLOCK DIAGRAM OF IMPULSE SUPPRESSOR.
a. Complete diagram.
b. Reduced diagram.

added random noise or interference that may pass through the excess bandwidth of the lower amplifier branch." It is obvious from this sentence that it was not realized that the effective bandwidth to the output after subtracting is narrower than that in either separate path, which is of course the real reason for the decreased impulse response.

A linear network is described by its transfer function, which contains the amplitude and phase of the transmission from input to output at all frequencies. Clearly, energy within a band of frequencies must be transmitted according to this transfer function, regardless of the differing properties of the time function that may describe the input signal. This consideration should rule out a search for a linear interference suppression technique to improve the SNR of an existing signal with respect to interference, except that one should use the narrowest bandwidth filter consistent with signal requirements.

D. NONLINEAR METHODS FOR SUPPRESSING IMPULSE INTERFERENCE

1. Clipping and Blanking

Techniques for suppressing impulse noise are described here because the effects of interfering stations on the FM-CW ionosphere sounder receiver are very similar to those which would be caused by impulses, so that methods that have been devised for suppressing impulse noise are likely also to be applicable to eliminating the effects of interfering stations in an FM-CW sounder receiver. Additional new approaches to the problem of impulse suppression may be justified because of the ease and economy with which complicated network functions may be realized and constructed by using recently developed integrated circuits.

Effective nonlinear techniques are available for interference suppression when it is possible to distinguish between signal and interference on the basis of the amplitude of the time function. This is particularly true for impulse interference. The suppression of this type of interference is usually accomplished by restricting the dynamic range of the signal plus interference, thereby preventing large responses caused by impulse occurrence. If the result of losing part or all of the signal for short lengths of time is not serious, the method may be adequate and easy to implement.

Nonlinear techniques are also available which discriminate between interference and signal on the basis of the amplitudes of their respective spectral components. A device which uses this technique is the frequency-selective limiter (FSL), which limits individual narrowband spectral components to some maximum value while allowing linear operation in other parts of the frequency spectrum. Such a device would be convenient for ionosphere sounding in order to limit the magnitude of fixed-station signals in the sounder receiver. A narrow bandwidth FSL (less than 2 kHz) can be made using the phenomenon of nuclear magnetic resonance [Ref. 16]. For the wide bandwidths (approximately 1 MHz) required in high resolution ionosphere sounders, the FSL is presently realized by a filter band with each filter having a conventional limiter on its output. The FSL is not needed in the FM-CW sounder however, since other, more easily constructed nonlinear methods of interference suppression are available.

A basic way of reducing impulse interference is to use a limiter or clipper which prevents the output signal from making excursions greater than those expected from the signal (Fig. 7a). Weagant [Ref. 17] mentions the limiter in 1919 in a paper which describes his experiments with using an antenna array to suppress atmospheric noise. In 1940 Wald [Ref. 18] showed that the effectiveness of the limiter is greatest when the bandwidth is as wide as possible. The wide bandwidth makes the impulse exceed the signal by a greater amount, thus facilitating its identification. Furthermore, the duration of the impulse response in the wider bandwidth is shorter than is the case for narrower bandwidths, which results in a shorter length of time during which the signal is degraded. The maximum bandwidth usable will be determined by random noise or interference in adjacent bands. Should the random noise included in the bandwidth exceed the signal, the clip level would have to be raised to prevent intermodulation of the noise and signal, so that the increased bandwidth would not improve performance. After the limiting operation, additional filtering consistent with signal requirements is performed to eliminate the additional random noise contained in the prelimiting bandwidth.

Nicholson and Kay [Ref. 19] reported in 1964 experiments showing that in the case of message transmissions whose frequency spectrum falls off at higher frequencies, the clipping method can be improved by differentiating the message plus impulse before clipping and then integrating back to get the message with little attendant error caused by the impulse (Fig. 7b). The reason this procedure is effective is that the impulse noise spectrum is flat, and therefore in the frequency domain the impulse noise spectrum is larger relative to the signal at high frequencies than at low. Differentiation emphasizes the high frequencies, so that the impulse stands out more above the message signal, making clipping more effective.

The suppression methods shown in Figs. 7c and 7d were also evaluated by Nicholson and Kay [Ref. 19]. The blanking system of Fig. 7c has a threshold similar to the clipping method, except that in this case a switch is operated when the interference exceeds the threshold, and the output is then disconnected. The power in the output which cannot be attributed to signal is much less with blanking than with clipping.

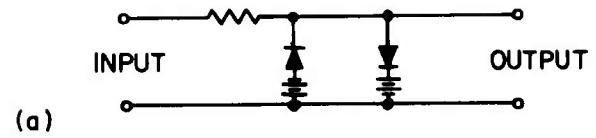

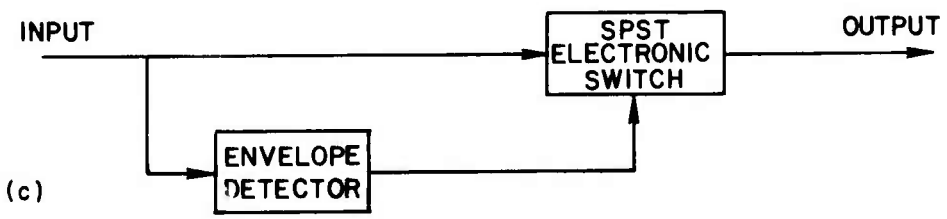

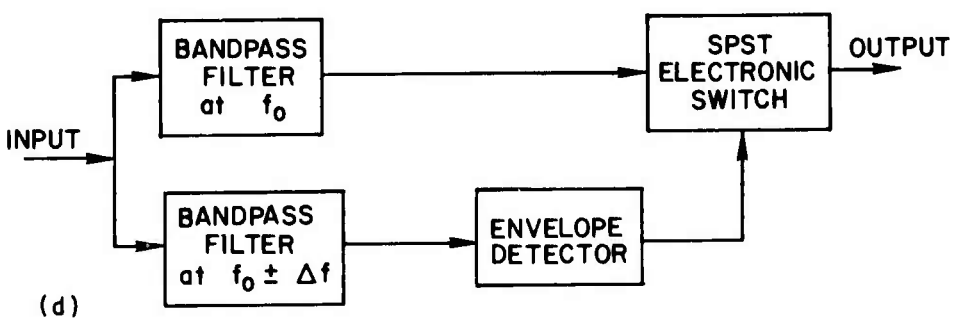

Fig. 7. FOUR TYPES OF NONLINEAR INTERFERENCE SUPPRESSORS.
a. Clipper.
b. Improved impulse clipper.
c. Self blanker.
d. Separate-channel blanker.

If an adjacent channel is free of interference, the blanking control can be obtained independently from the signal channel as shown in Fig. 7d. When detecting interference in the presence of the signal, it is found that the interference may add or subtract from the signal depending on the phase relations of the two; so that in some cases the interference may have to be greater than twice the signal in order to be detected. The separate-channel blanking eliminates the signal-interference interaction, thus enabling direct detection of the interference. The detection threshold can also be set at an optimum value without encountering the problem of signal self-blanking. In the case of a CW desired signal, the minimum rms error between the desired signal and the actual output will be obtained with a blanking threshold equal to the desired signal amplitude.

Still further improvement in impulse rejection can be obtained with the increased complexity shown in the block diagram in Fig. 8. This method is the same as that in Fig. 7d, except that the switch is moved to precede the signal bandpass filter and a delay is added to give the interference detector time to prevent impulse energy from causing ringing in the signal filter. A true impulse is perfectly eliminated in this system, with almost no effect on the desired signal. An interference-free adjacent frequency must be available for use, however.

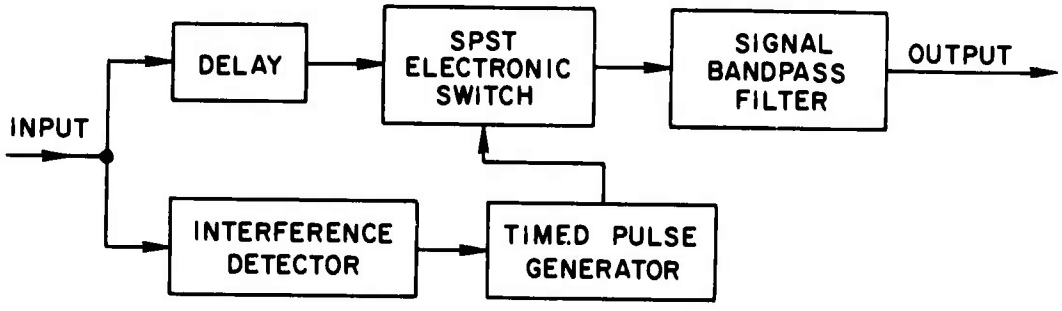

Fig. 8. TIMED-BLANKING INTERFERENCE SUPPRESSOR.

2. Cancellation

A successful nonlinear impulse-noise cancellation technique was reported by Black [Ref. 26] in 1963. Figure 9 shows the block diagram for this nonlinear cancelling circuit. The three filters tuned respectively

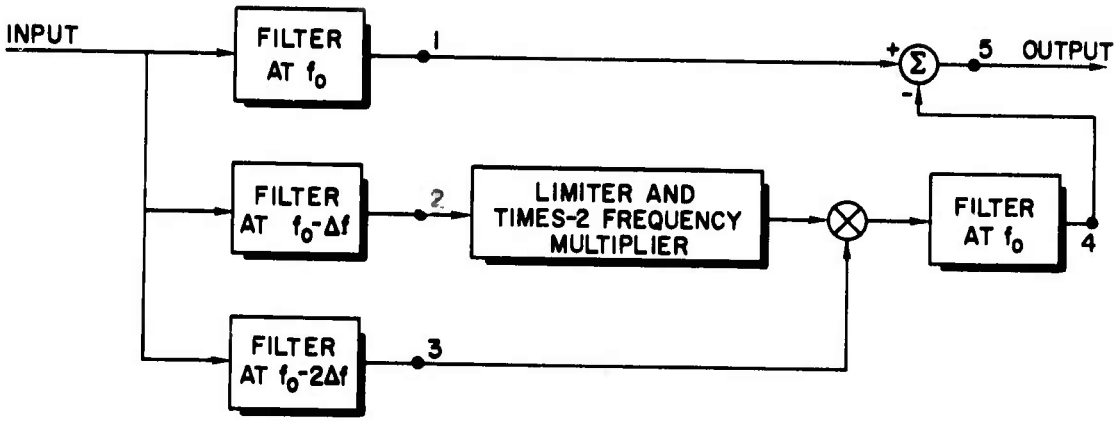

Fig. 9. NONLINEAR IMPULSE CANCELLER.

at f_o, $f_o - \Delta f$, and $f_o - 2\Delta f$ have narrow bandwidths so that their impulse responses can be expressed as constant frequency sinusoids of slowly varying amplitudes. The filter at f_o passes the band of frequencies required to transfer the desired signal. The frequency difference, Δf, is chosen just great enough to prevent desired signal energy from passing through the lower frequency filters. The equations expressing the impulse responses of the three filters can be written:

$$v_1 = e_1(t) \cos [\omega_o t] ,$$

$$v_2 = e_2(t) \cos [(\omega_o - \Delta\omega)t] ,$$

$$v_3 = e_3(t) \cos [(\omega_o - 2\Delta\omega)t] ,$$

where the subscripts correspond with the numbered points on the block diagram. The limiter and the times-two frequency multiplier provide a constant amplitude "local oscillator" signal for the mixer. The filter at f_o which follows the mixer selects the difference frequency, but has adequate bandwidth to pass the envelope of v_3 without distortion. Therefore:

$$v_4 = e_3(t) \cos [2(\omega_o - \Delta\omega)t - (\omega_o - 2\Delta\omega)t]$$

$$= e_3(t) \cos [\omega_o]$$

and

$$v_5 = [e_1(t) - e_3(t)] \cos \omega_o t \ .$$

Assuming identical bandpass shapes for filters at frequencies f_o and $f_o - 2\Delta f$, the impulse envelope responses, $e_1(t)$ and $e_3(t)$, will be equal, giving

$$v_5 = 0$$

for an impulse input.

E. NONLINEAR METHODS APPLIED TO FM-CW INTERFERENCE SUPPRESSION

The block diagram for an FM-CW sounder receiver is shown in Fig. 10. The interferences from fixed-frequency transmissions become FM-CW signals after passing through the balanced mixer. The ability of the receiver to detect low-amplitude echoes is lowered by the undesired responses which result as each station is swept through the receiver frequency. Most of the stations are modulated, but modulation does not alter the performance of the interference suppression in most cases. Since in a typical ionosphere sounder situation the time during which the interfering FM-CW signal has significant energy within the receiver IF bandwidth is about equal

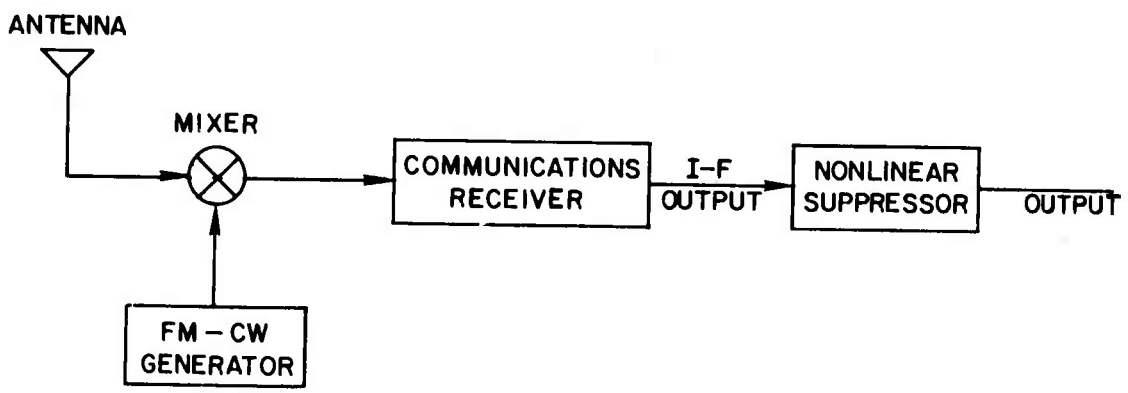

Fig. 10. BLOCK DIAGRAM OF FM-CW RECEIVER.

to the IF filter decay time, the resulting receiver response from an interfering station has a duration only slightly greater than that of an impulse response. Therefore, nonlinear methods for suppressing this type of interference are similar to those used for impulse-noise suppression. In the case of the impulse noise, it was noted that the receiver IF amplifier filter should be as wide as possible in order to make the duration of the impulse short, so that the nonlinear processor would interrupt the signal for the shortest possible time. This is not true in the case of FM-CW interference, because as the IF bandwidth is widened the interfering signal stays within the bandwidth for a longer time in proportion to the bandwidth. However, if the IF filter bandwidth is made too narrow, ringing will again cause increased blanking or clipping time as in the impulse case, and the smearing of energy caused by a narrow filter removes the possibility of detecting and suppressing interference caused by some of the weaker interfering stations.

The blanking or clipping time T is approximately equal to the sum of the time the instantaneous frequency of the FM-CW having sweep rate of S Hz per sec is within the bandwidth B and the time required for the filter to decay. The latter may be approximated by $1/B$. Thus

$$T = \frac{1}{B} + \frac{B}{S}. \tag{3.1}$$

If the minimum signal-interruption time is found by varying the bandwidth in Eq. (3.1) it is found that the bandwidth giving that time is

$$B = \sqrt{S}\ . \tag{3.2}$$

The filter decay time of $1/B$ which was used to find the optimum filter bandwidth to precede the nonlinear operation is only a crude approximation, for the following reason: The length of time the filter ringing exceeds the signal is a function of the magnitude of the interference. A situation in which the ringing would have decayed to the signal value in a time equal to $1/B$ represents the presence of an interference having an amplitude of about three times that of the desired signal. The amplitude of interference will vary depending on the particular receiving system and propagation conditions; but in most ionosphere

sounders there will be a good deal of interference of amplitude larger than three times that of the desired sounder signal, so that the optimum bandwidth for suppressing this interference may be greater than the value specified above. For example, if the amplitude of the interference is ten times that of the desired signal and the filter output has a simple exponential decay, the optimum bandwidth becomes about $\sqrt{2S}$.

A possible technique for decreasing the clipping or blanking time for the purpose of eliminating FM-CW interference has been discussed in the Stanford Radioscience Laboratory. This technique involves widening the receiver IF amplifier and inserting a compressive filter network with a linear variation of time delay with frequency as shown in the graphs of Fig. 4. If the IF bandwidth were widened by a factor of K, the width of the response from the appropriate compressive filter would be K^{-1} times the width of the response in the unwidened amplifier case. It is the author's opinion, however, that the use of this type of compressive filter preceding the nonlinear operation is not worthwhile for two reasons. First, when the duration of the response is reduced by a factor K^{-1}, the wider bandwidth accepts K times as much interference energy. The peak energy of the response is therefore increased by a factor of approximately K^2, with the result that the width of the compressed pulse at the desired clipping level (determined by the signal amplitude and not changed by adding the compressive filter) has not been reduced by the factor K^{-1}. In fact, depending on the shape of the compressed pulse, the pulse width may not have been reduced at all. Second, the rms sideband energy of the interfering signal (present in most HF radio interferences) is increased by a factor of K, and thereby may be increased to the clipping level. This would result in more severe signal interruption than might have occurred with the unwidened receiver.

The behavior of the clipping and self-blanking circuit for FM-CW would be no different than that in the impulse examples discussed above. For separate-channel blanking, however, a delay must be added as shown in Fig. 11, in order to make the two filter envelope responses from a particular interference coincide. If decreasing-frequency FM-CW interference is to be blanked, a filter with higher frequency than the signal filter would be used to detect the interference.

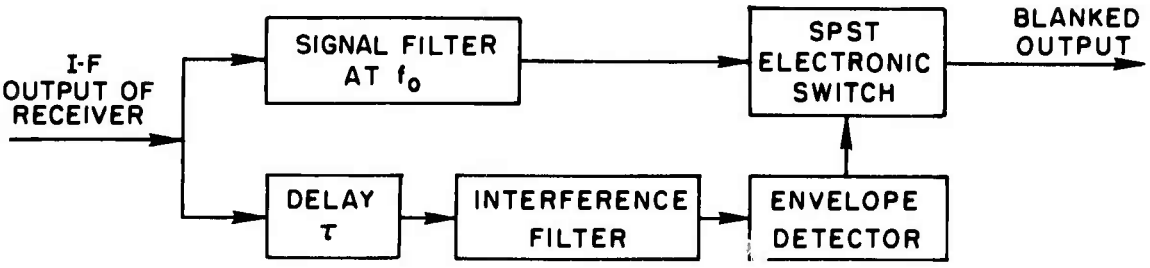

Fig. 11. SEPARATE-CHANNEL FM-CW BLANKER.

The time-pulse separate-channel blanking (Fig. 8) can also be used for FM-CW rejection. In typical FM-CW sounder conditions the off time of the switch must be considerably longer than the time required for the interference to sweep through the signal filter bandwidth. This effect can be ascribed to the presence of sidelobes in the frequency spectrum of the square pulse of FM-CW which was removed. Because of these sidelobes, little improvement results in the FM-CW case by putting the blanking switch before the IF filter, providing the filter is not significantly narrower than the optimum one discussed above.

A limiter method of interference suppression has been used in most of the FM-CW ionograms made by the Stanford Radioscience Laboratory. Limiting has been accomplished by manually setting the receiver gain so that the desired signal is near the maximum dynamic range of the receiver IF amplifier. The amount of filtering preceding the limiting may not have been constant, since limiting may have occurred at different stages within the IF amplifier and filter depending on the interfering signal amplitude. The desirability of this multiple limiting at different bandwidths has not been analyzed.

F. SUMMARY OF SUPPRESSION METHODS

Previous efforts to suppress interference, in an ionosphere sounder caused by fixed-frequency stations, have included special waveform design and nonlinear received-signal processing. Sounding practice in ionosphere research has been to use both techniques to obtain the best data with the state-of-the-art equipment available at the time. The

complexity of the nonlinear operations is very much a function of the waveform selected, and relatively simple operations are very effective in the FM-CW sounder.

In the case of pulse ionosphere sounders, the waveform design procedure involves finding methods of building pulse-compression systems having large time bandwidth products. A fundamental way of constructing a pulse-compression system is to use multipath or dispersive networks. The complexity and stability of the required networks limit the time-bandwidth product to about 10^3. The search for a pulse-compression system having a larger time-bandwidth product led to the development of the digitally controlled frequency synthesizer which is capable of producing "pulses" of one MHz bandwidth having a large time-bandwidth product ($>10^6$).

Nonlinear techniques for the simple pulse receiver require the use of a filter bank to break up the frequency spectrum in order to make it possible to eliminate those parts of the spectrum which are contaminated by interference. The use of a limiter on the output of each filter results in the frequency-selective limiter (FSL). An alternative plan would be not to use filter outputs which contain interference. Pulse-compression systems using filter-network methods also require the FSL, because frequencies of the interference are not inherently separated from interference-free parts of the spectrum in any other way (e.g., in time).

The FM-CW equivalent pulse-compression system which uses an FM-CW local oscillator to produce a fixed beat frequency for a fixed time delay permits the use of nonlinear techniques that had already been developed for impulse-noise suppression. At the output of the IF amplifier in the FM-CW sounder receiver, the frequencies of the interference are separated in time from interference-free parts of the spectrum. The resolution of this separation is determined by the IF bandwidth of the receiver and the FM-CW sweep rate S. The most selective separation obtainable for a given sweep rate S is approximately $2\sqrt{S}$, and is obtained with an IF bandwidth approximately equal to $1\sqrt{S}$. A clipping circuit at the receiver IF output gives results nearly equivalent to a frequency-selective limiter. Using the example of a 1 MHz sweep rate, the resolution of the effective FSL obtained by a clipper can be about 2 kHz. Therefore, in cases where

the pulse bandwidth is equal to 1 MHz, the clipper provides the function of an FSL composed of 500 individual filters.

Because of the large time-bandwidth product and the ease of implementing effective nonlinear functions, the use of an FM-CW signal generated by a synthesizer was a great advance in the ionosphere sounding art. It is still true, however, that the major factor determining the PSNR of the sounder data for a given transmitted power is the fixed-frequency interference. Chapter IV describes a new system, devised by the author, for increasing the advantages of an FM-CW system by cancelling the fixed frequency interference without an interruption of the desired signal.

IV. THE QUASI-LINEAR INTERFERENCE SUPPRESSOR

The quasi-linear interference suppressor (QLS) developed in the present research will be described in this chapter. The QLS employs a principle of balancing interference energy received on two frequencies against interference energy received on a slightly different frequency. When interference is absent, the system consists of three parallel-connected bandpass filters of differing center frequencies. Each filter has a bandwidth adequate to pass the desired signal. Frequencies of the desired signal are contained within a filter whose center frequency is centrally located between the center frequencies of the other two filters. When interference occurs, the system changes to a different mode of operation, which involves a frequency translation of two of the filter outputs before the three outputs are summed.

The desirability of an interference suppression system can be determined by considering two factors: first, the degree of elimination of the interference; and second, the amount of disturbance produced in the desired signal. It will be shown that the QLS can effectively eliminate, by a cancellation process, isolated impulses or FM-CW interference with negligible effect on the desired signal.

A. PREVIOUS SYSTEMS FOR BALANCING IMPULSE NOISE

The principle of balancing impulse noise received on one frequency including signal, against impulse noise on a slightly different frequency (free of signal) is not new. Most systems previously proposed never proved to be effective, either because the increased noise received in the additional filter more than counterbalanced the benefit gained, or because the systems were ineffectual in the situation of signal plus interference. For example, Armstrong [Ref. 20] in January 1928 published test results of a noise-balancing circuit; but Carson [Ref. 21] published a rebuttal in July of the same year showing why such a balancing system could not be effective. The only effective impulse noise canceller found in the literature was that described by Black in 1963 [Ref. 26].

Differences between the quasi-linear method presented here, and the system described by Black are: 1) the frequency band of the interference

energy which is used to develop the cancelling signal is displaced from the signal filter bandpass no more than one signal filter bandwidth, 2) the operation is intermittent so that no noise is added to the desired signal when interference is not actually being eliminated, and 3) in a preferred configuration the QLS performance can be described by linear system theory.

The QLS required for impulse cancellation will be described first although emphasis in the development of the QLS was its usefulness in reducing FM-CW sounder interference. Fortunately the conversion from an impulse suppressor to an FM-CW suppressor consists merely of adding two delay networks, as will later be shown.

B. SUPPRESSION OF IMPULSE INTERFERENCE

For background purposes, some of the properties of the impulse responses of a linear filter will now be reviewed. Using the symbol H for system transfer function and subscripts LP and BP for lowpass and bandpass, respectively, Eq. (4.1) below is used to define a bandpass filter in terms of a lowpass filter:

$$H_{BP}(j\omega) = H_{LP}(j\omega + j\omega_o) + H_{LP}(j\omega - j\omega_o) \qquad (4.1)$$

where $\omega = 2\pi \times$ frequency, and $\omega_o = 2\pi \times$ center frequency f_o.

A bandpass filter with this transfer function can be approximately realized over frequencies of significant transmission in the low fractional bandwidth case. Bandpass filters of large fractional bandwidth generally fail to have the symmetry indicated by Eq. (4.1).

The impulse response of a narrow-band filter can be expressed as a constant-frequency sinusoid, having an envelope amplitude equal to twice the impulse response of the related lowpass filter of Eq. (4.1) [Ref. 14]. In other words, the filter output $v(t)$ is given by

$$v(t) = 2V(t) \cos (\omega_o t + \varphi_o)$$

where $V(t)$ is the impulse response of the lowpass filter. The frequency $f_o = \omega_o/2\pi$ is the carrier frequency for the impulse response and is the midband frequency of the symmetrical filter. The phase, φ_o, is a constant dependent on the time reference t.

C. ELEMENTS OF THE QLS

In the QLS, three narrow-bandwidth filters, of equal bandwidths, are used. One filter at the center frequency f_o is designed with adequate bandwidth to transmit the desired signal information. The other filters are placed at frequencies $f_o + \Delta f$ and $f_o - \Delta f$, with Δf as low as may be possible without admitting significant desired-signal energy. Assuming identical filter bandpass characteristics, the equations for the impulse responses of the filters can be written as:

$$v_1 = 2V(t) \cos [(\omega_o - \Delta\omega)t + \varphi_{o1}] ,$$

$$v_2 = 2V(t) \cos [\omega_o t + \varphi_{o2}] ,$$

$$v_3 = 2V(t) \cos [(\omega_o + \Delta\omega)t + \varphi_{o3}] ,$$

where the subscripts correspond to the numbered points on Fig. 12a. By using wideband phase-shift networks as illustrated in Fig. 12a, the phase of the impulse responses of the three filters plus the associated phase-shift networks can be made equal at any time after the occurrence of an impulse. For the interference suppressor, the three phases are made equal at a time, $t = 0$, near the beginning of the interference response; i.e.,

$$v_4 = 2V(t) \cos [(\omega_o - \Delta\omega)t + \varphi_{o2}] ,$$

$$v_2 = 2V(t) \cos [\omega_o t + \varphi_{o2}] ,$$

$$v_5 = 2V(t) \cos [(\omega_o + \Delta\omega)t + \varphi_{o2}] .$$

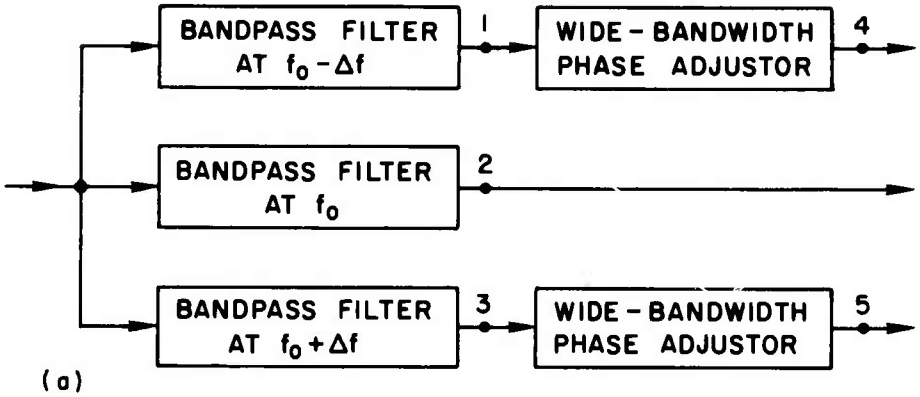

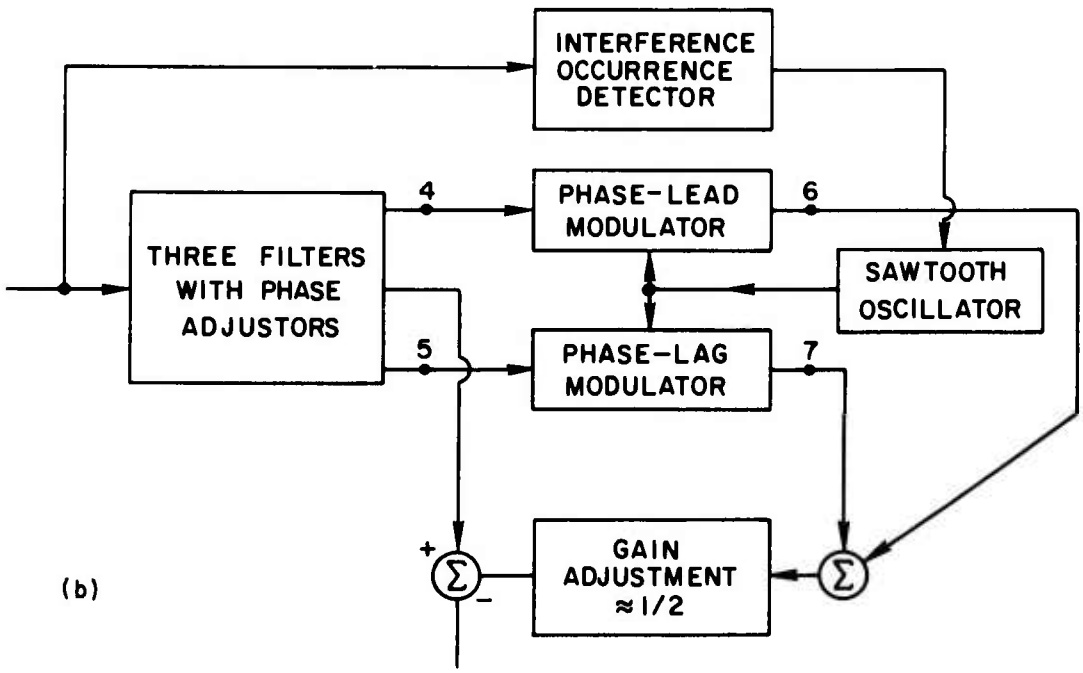

Fig. 12. PARTIAL BLOCK DIAGRAMS OF IMPULSE-TYPE QUASI-LINEAR INTERFERENCE SUPPRESSOR (QLS).
a. Filters with phase adjustments.
b. Development of the cancelling signal.

If a phase shift of $\Delta\omega t$ is inserted following point 4 of Fig. 12a, and a phase shift of $-\Delta\omega t$ following point 5, the signals obtained, v_6 and v_7, are identical and are given by

$$v_6 = v_7 = 2V(t) \cos [\omega_o t + \varphi_{o2}]$$

If the time, $t = 0$, at which the impulse occurs is determined by an interference-occurrence detector, an impulse-interference cancelling signal can be developed (as shown in Fig. 12b) by the equal but opposite phase modulation of the signals from points 4 and 5. The two waveforms, v_6 and v_7, each identical to the interfering waveform in the signal filter, are summed, then multiplied by 1/2 and subtracted from the signal-filter output.

Because of the 0 deg, 360 deg identity, an appropriate phase modulation characteristic is a 0 deg - 360 deg sawtooth with a fundamental frequency equal to the difference between the side-filter frequencies and the signal-filter frequency. The output of each phase modulator has the same envelope as its input, but the carrier frequencies have been shifted by an amount equal to the sawtooth modulation frequency. For translation to higher frequencies, a decreasing phase-lag modulation as shown in Fig. 13a is used ($\varphi = -\Delta\omega t + n2\pi$). Similarly, Fig. 13b shows the <u>increasing</u> phase-lag modulation required to translate frequencies downward ($\varphi = \Delta\omega t - n2\pi$). The circuitry which is used to translate

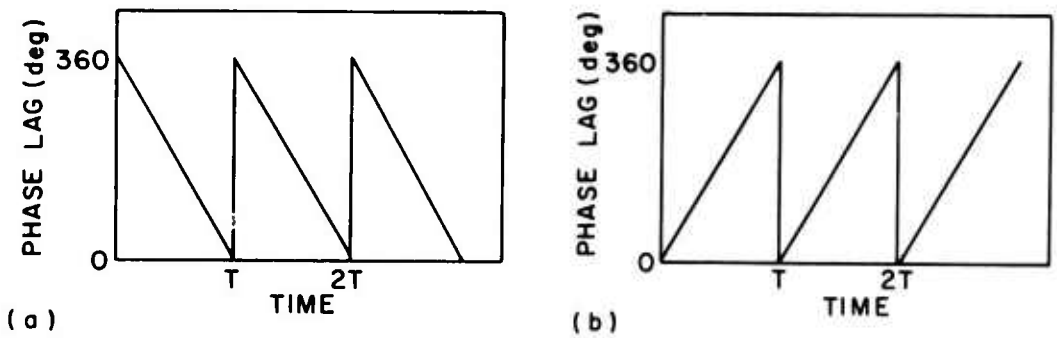

Fig. 13. QLS PHASE-MODULATION WAVEFORMS.
a. Decreasing phase-lag modulation ($\varphi = -\Delta\omega t + n2\pi$).
b. Increasing phase-lag modulation ($\varphi = \Delta\omega t - n2\pi$).

frequency in this phase-modulation manner is called a serrodyne [Refs. 22 and 23]. The wideband property of the serrodyne is particularly convenient in the interference suppressor. It would be difficult to maintain proper phase relations among the three paths in the interference suppressor, with the narrow-band filters that would be required, if conventional nonlinear-element frequency translation was used.

D. ERRORS IN THE QLS

Two identical waveforms are developed independently in the QLS, as discussed above. One might ask, why not use only one side filter and develop one waveform which is independent of the interference response in the signal filter? There are two reasons for the symmetrical configuration: 1) It will be shown later that a feedback circuit can adjust the phase modulators (Fig. 12), thus requiring less accuracy in the interference-occurrence detector. 2) A phase-adjustment error in the phase modulators does not degrade the cancellation as much as in the single filter configuration.

Assuming equal but opposite errors in the phase adjustments of the two phase modulators θ_e, vector relations illustrated in Fig. 14a are used to derive Eq. (4.2), which gives the magnitude of the interference residue V_r using cancellation derived from two side filters:

$$V_r = 1 - \cos \theta_e \, . \tag{4.2}$$

A similar derivation illustrated in Fig. 14b gives Eq. (4.3) for the residual voltage V_{rs} when a single side filter is used to develop the cancelling signal.

$$V_{rs} = 2 \sin \frac{\theta_e}{2} \, . \tag{4.3}$$

A sample calculation shows that for 10 deg phase-adjustment error, the cancellation residual voltage is down 36 dB in the two-filter case; but only 15 dB in the one-filter configuration.

Fig. 14. INTERFERENCE RESIDUE, V_r OR V_{rs}, CAUSED BY PHASE-ADJUSTMENT ERROR, θ_e.
a. Two side filters.
b. Single side filter.

Since the two-side-filter configuration yields two ac voltages having the same phase, the serrodyne adjustment can be accomplished by sensing the difference between the phase of the two signals and feeding back an adjusting signal to make the phase difference as close to zero as possible. This is accomplished by replacing the free-running oscillator with a sampling phase detector as shown in Fig. 15. The exact properties of the sampling phase detector are described in the section on circuit implementation.

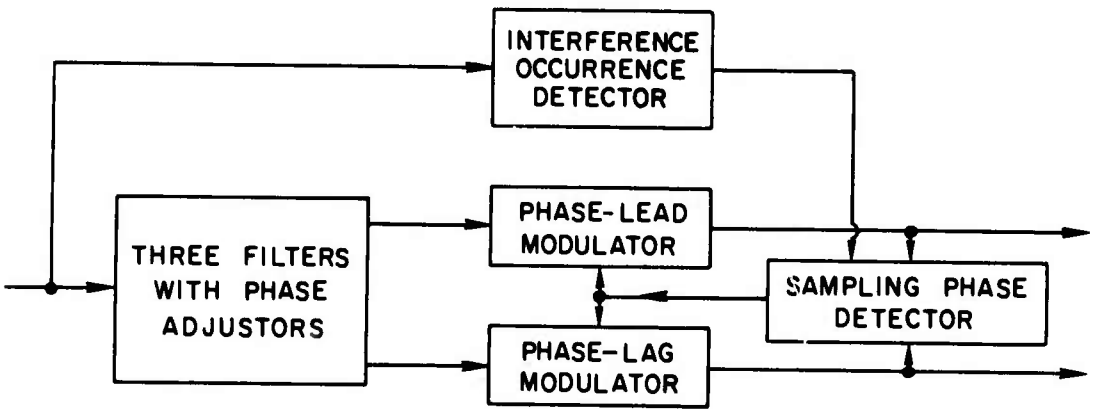

Fig. 15. BLOCK DIAGRAM FOR PHASE-DETECTOR METHOD OF PHASE ADJUSTMENT.

There are two phases 180 deg apart, one of which the phase detector may select. If the interference detector does not enable the cancelling action at the correct time, interference addition rather than cancellation may result. The time accuracy t_a required to be sure of obtaining the correct phase is given by Eq. (4.4). During this time the phase adjustment error increases to 90 deg. Accuracies much less than that expressed

by Eq. (4.4) would of course give very poor cancellation if the free-running oscillator method of serrodyne adjustment were used.

$$t_a = \frac{1}{4\Delta f} \quad . \tag{4.4}$$

Under conditions where it is not possible to achieve sufficient timing accuracy in the interference detector so that the 180 deg error is made, interference addition, rather than cancellation, results. If the interference can be expected to be greater than a desired signal, cancellation is still possible by using the logic shown in the block diagram, Fig. 16. The comparator selects the output signal having the smaller envelope magnitude. If interference is not larger than the desired signal, there is still a greater than fifty percent probability that the interference will be cancelled. Equation (4.5) gives the probability that cancellation will result as a function of the relative amplitude of desired signal voltage V_s and interference voltage V_n.

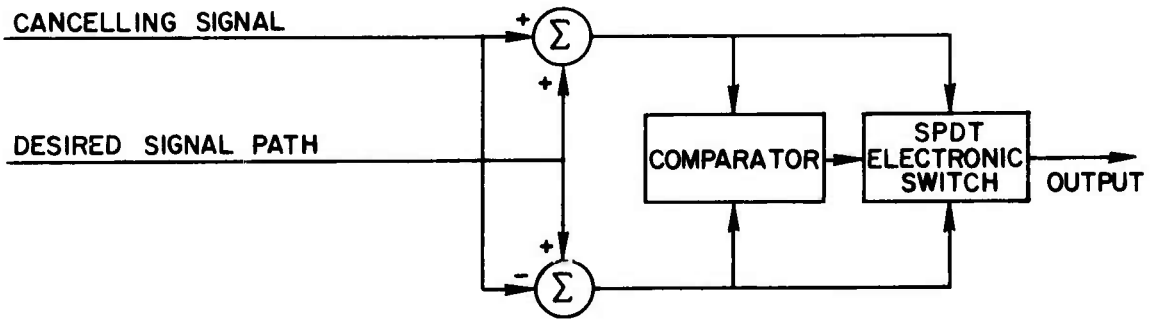

Fig. 16. BLOCK DIAGRAM FOR MINIMUM-OUTPUT SELECTOR.

$$\text{Probability of cancellation} = \begin{cases} 1 - \dfrac{\cos^{-1} V_n/V_s}{\pi} & V_n \leq V_s \\ 1 & V_n > V_s \end{cases} \tag{4.5}$$

Equation (4.5) is plotted in Fig. 17a. In deriving this equation, it is assumed that the phase difference between interference and desired signal

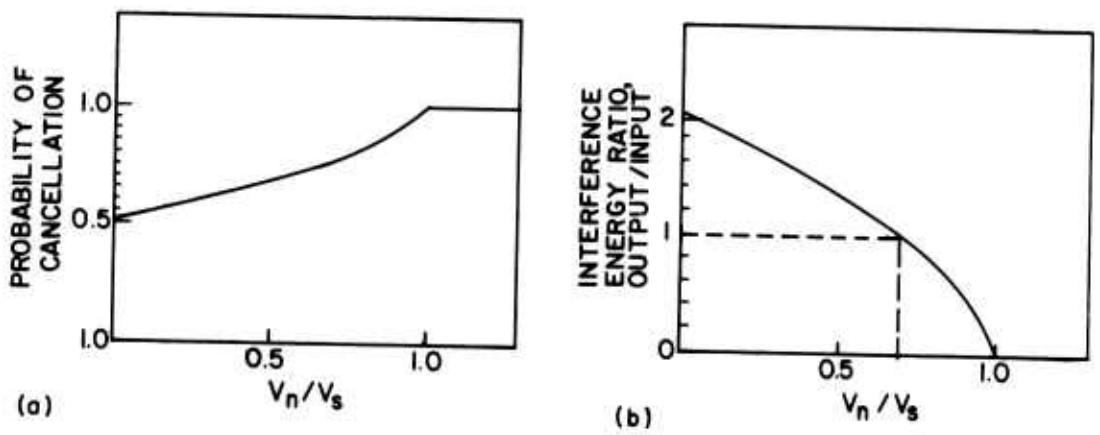

Fig. 17. PERFORMANCE OF MINIMUM-OUTPUT SELECTOR.
a. Probability of interference cancellation.
b. Interference suppression.

is uniformly distributed over a span of 0 to 2π, so that the probability of making a correct selection is the fraction of the possible phase angles of the interference which will cause decreased output in the interference cancellation path.

In most cases the important consideration is the amount of average interference energy contained at the output of the QLS relative to the input. This is given by

$$\frac{\text{Output Interference Energy}}{\text{Input Interference Energy}} = 4 \times \text{Probability of not cancelling.} \tag{4.6}$$

Equation (4.6) is plotted in Fig. 17b. It can be seen from this plot that it would be best not to use the QLS in the minimum-output mode for interference which is smaller than 0.7 times the desired signal.

The complete QLS for impulse interference is shown in Fig. 18. The minimum-output-selecting part is shown dotted, since this circuitry is undesirable if the interference detector can measure the time of the interference with sufficient accuracy. The digital phase-modulation method which was used in the final breadboard configuration of the QLS is shown.

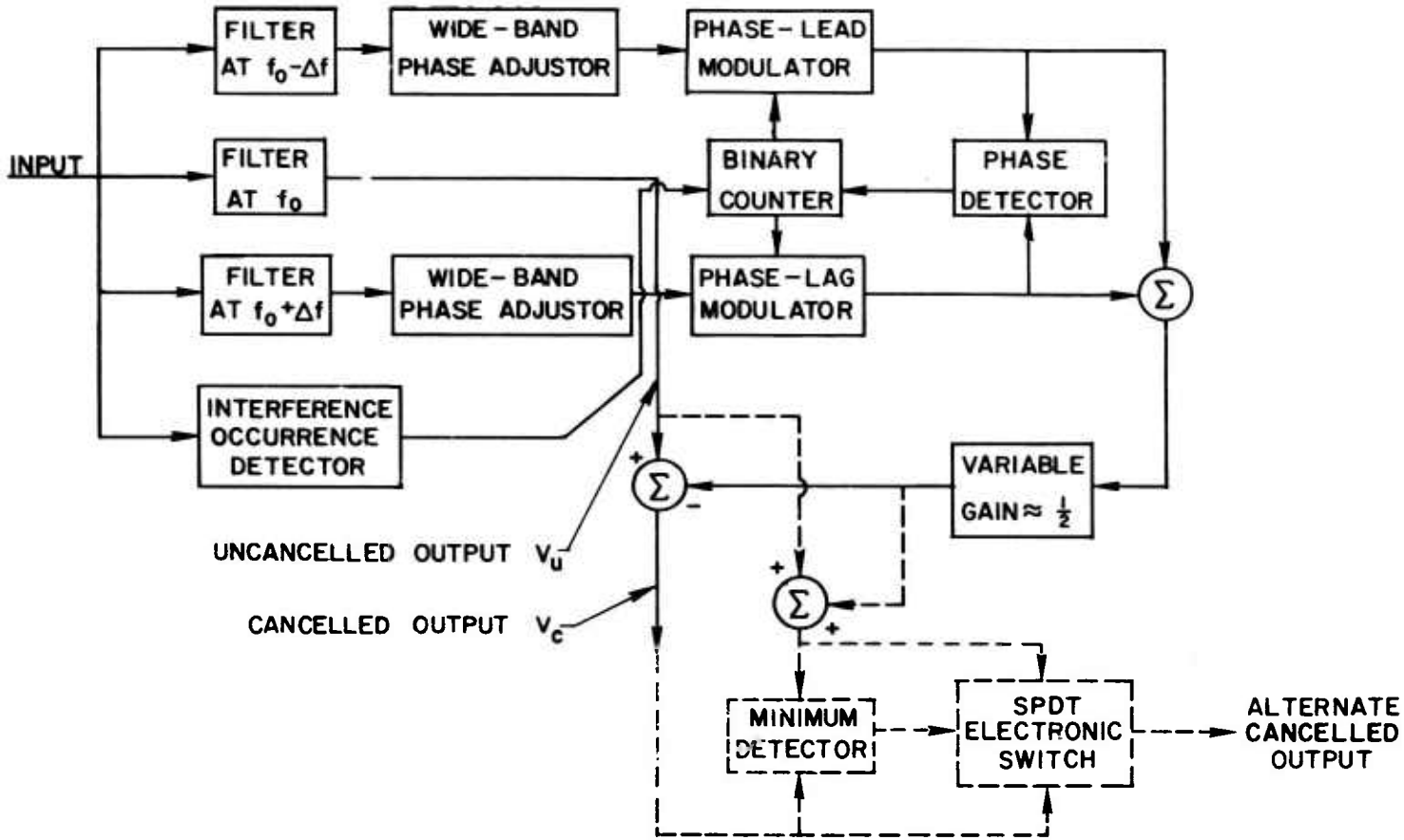

Fig. 18. BLOCK DIAGRAM OF IMPULSE-TYPE QUASI-LINEAR SUPPRESSOR.

The interference detector allows the serrodynes (phase modulators) to operate through the time when significant cancellation of interference can result. Ideally, the length of the cancelling time could be determined by a threshold detector similar to that used for separate-channel blanking. Serrodyne operation would be initiated by a measurement of the interference occurrence time and would be continued while the interference energy is above some threshold level. If the three filters are not perfectly matched the cancellation may not continue over all the time during which the threshold is exceeded. This may make it appropriate to use a fixed duration of cancelling time, rather than employ the threshold detector.

Assuming additional filtering is performed following the QLS to eliminate noise contained within the side filters, the ratio of desired signal to random noise within the signal bandwidth is not degraded during those times when the serrodynes are disabled. When the serrodynes are operating, the random noise from the side filters is translated to frequencies within the desired-signal bandwidth. Under most conditions the noise components of the serrodyne outputs remain uncorrelated. When the phase-detector method of serrodyne adjustment is used, the random noise may become correlated by the feedback adjustment unless the interference is large compared to random noise. Assuming the random noise components of the two serrodyne outputs are uncorrelated (i.e., assuming that the interference is much larger than the random noise or that the fixed-frequency oscillator method of phase adjustment is used), the output noise energy within the signal bandwidth is increased by a factor of 1.5 during cancellation. The factor of 1.5 is determined by finding the rms sum of the noise energy within the signal filter plus one fourth the energy from each side filter. (The side-filter energy is reduced by one fourth in the voltage attenuation of one half encountered before the interference subtraction.) This result points out another possible advantage of using two side filters to develop the cancelling signal, as compared with the single side-filter cancellation (as mentioned earlier). This advantage is that the single-side-filter method would increase random noise by a factor of two during interference cancellation.

E. SUPPRESSION OF FM-CW INTERFERENCE

All that is necessary to develop the block diagram to be used for FM-CW cancelling is to find the configuration which will give three outputs with properties analogous to the three filter outputs in the impulse case. These properties are 1) the desired signal is contained within the center filter; 2) the two side filters have instantaneous envelope responses due to interference equal to that caused by interference in the center filter; and 3) the phase difference between the interference in the side filters and that in the center filter is equal but opposite.

An FM-CW signal can be represented by a constant-magnitude rotating phasor whose rotation rate is linearly changing with time. Equation (4.7) below gives the angle θ of an FM-CW phasor as a function of time, where f_o and θ_o are, respectively, the frequency and phase at $t = 0$, and S is the sweep rate in Hz per second.

$$\theta = \frac{1}{2} 2\pi S t^2 + 2\pi f_o t + \theta_o . \qquad (4.7)$$

This equation is used to find the phase relationship $(\theta - \theta_1)$ and $(\theta - \theta_2)$, where θ, θ_1 and θ_2 are the phases at the points indicated in Fig. 19.

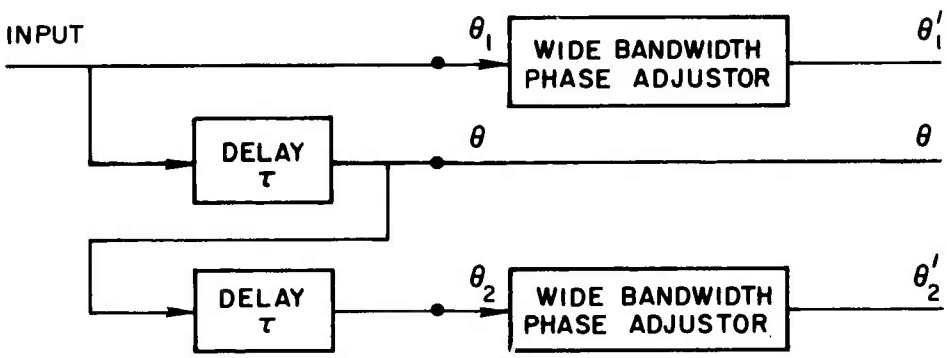

Fig. 19. PHASE RELATIONSHIP OF FM-CW SIGNAL.

$$\theta - \theta_1 = -\frac{\pi S(2t\tau + \tau^2)}{2} - 2\pi f_o \tau \qquad (4.8)$$

$$\theta - \theta_2 = \frac{\pi S(2t\tau - \tau^2)}{2} + 2\pi f_o \tau \, . \qquad (4.9)$$

By grouping the constant terms together:

$$\theta - \theta_1 = K_1 - \pi S\tau t \qquad (4.10)$$

$$\theta - \theta_2 = K_2 + \pi S\tau t \, . \qquad (4.11)$$

The constants K_1 and K_2 can be eliminated by wideband phase adjustment, with the result that side-frequency signals having equal but opposite phases are produced. At this point, however, the desired signal is present in all three paths. This condition can result in signal cancellation when interference is not being cancelled. Therefore, three filters (such as used in the impulse QLS) are required. As before, the side filters are spaced at equal frequency intervals away from the center filter frequency; and in this case the frequency difference between adjacent filters is equal to τS. At any instant of time the three interference signals are in the same portion of the corresponding filter, so that phase relationships among them are preserved.

As in the impulse cancellation system, a cancelling signal can be produced if an interference-occurrence detector determines the time of occurrence of an interference and initiates an equal but opposite phase modulation of the two side-filter outputs. Figure 20 shows the complete block diagram of the FM-CW Quasi-Linear Suppressor (QLS). The minimum-selecting circuitry is shown dotted, since this circuitry would not be used if the FM-CW interference-occurrence detector can give a time reference sufficiently accurate to eliminate the possibility of interference addition. The time accuracy required to assure correct adjustment is the time it takes the response in a side filter to deviate 90 deg with respect to the center filter. Since the difference in frequency is equal to τS, the detector time accuracy t_a required is

$$t_a = \pm \frac{1}{4\tau S} = \pm \frac{1}{4\Delta f} \, . \qquad (4.12)$$

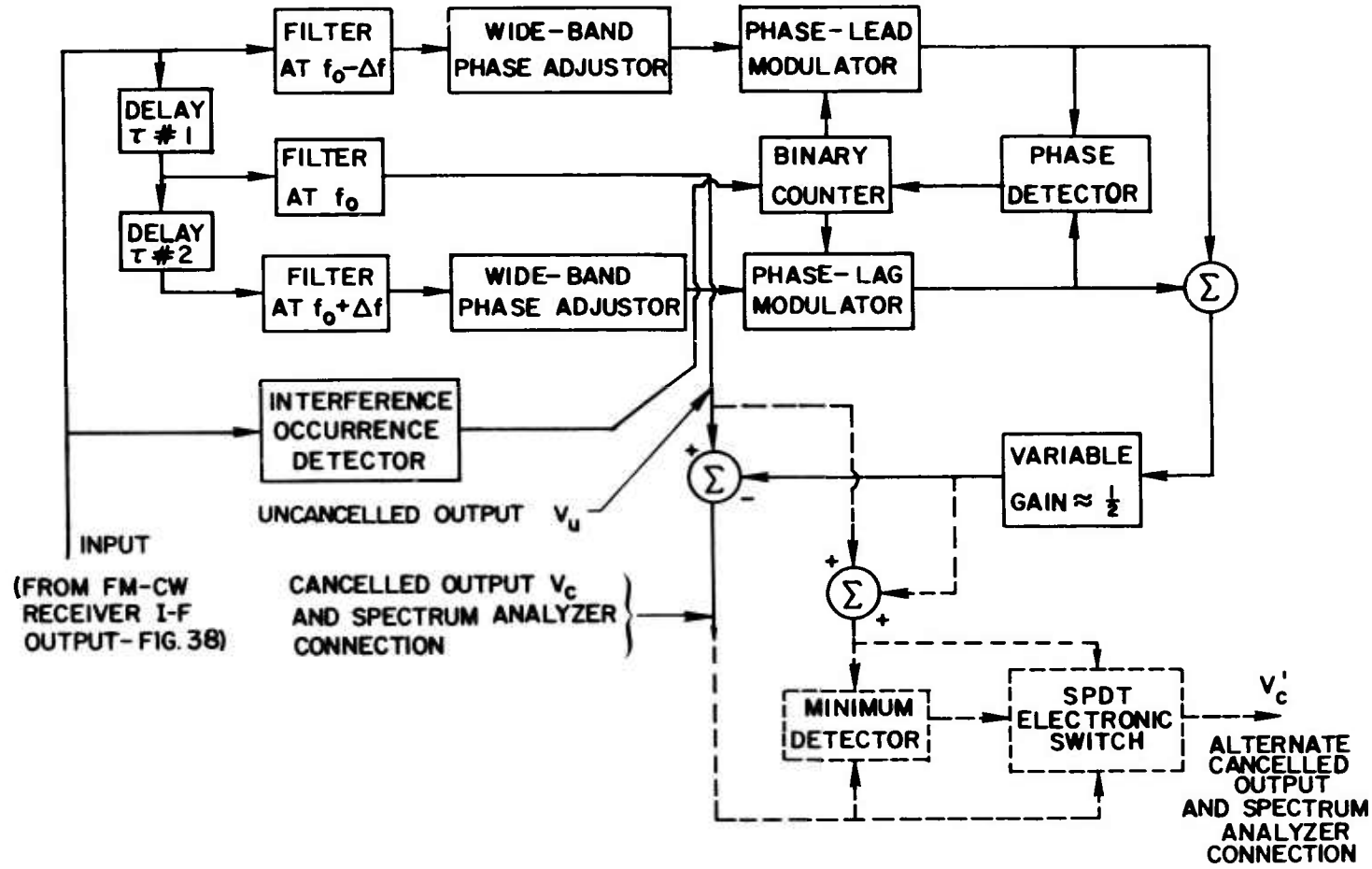

Fig. 20. BLOCK DIAGRAM OF FM-CW QUASI-LINEAR SUPPRESSOR.

F. ANALYSIS

The description in the preceding two sections shows that the QLS can nearly perfectly cancel isolated interfering impulses or unmodulated FM-CW signals. The only approximation is the distortion resulting from the phase-modulation process. A mathematical analysis of the filter responses to FM-CW inputs could be used to show theoretically the cancelling ability of the FM-CW QLS for modulated as well as for unmodulated FM-CW signals. An outline of how these calculations could be made is presented in this section. The calculations were not actually carried out for two reasons: First, the complexity of the computer programming involved might require as much time and expense as building a breadboard QLS. Second, the statistics to describe the modulated signals in the HF spectrum are not adequately known to enable using the computer results to predict the performance of a QLS in an ionosphere sounding system.

For the particular configuration of the QLS in which an oscillator rather than a phase detector drives the serrodynes, however, complete results of the transmission of FM-CW modulation sidebands are found without finding the exact responses of the filters. An interference-occurrence detector adequate to enable testing the breadboard QLS in the fixed-oscillator serrodyne-adjustment mode was not constructed because the construction of such a detector to give an accuracy sufficient to enable cancelling the carrier without using the phase-detector method of serrodyne adjustment would require expensive compressive filters. This expense did not seem appropriate at this time for two reasons. First, little if any improvement would be expected in the QLS performance; and second, interference suppression provided by the QLS was usually less than 3 dB. It should be pointed out, however, that the spurious responses of the FM-CW generator which are discussed in Chapter V limited the possible performance of the QLS; so that if FM-CW generators free of spurious responses are developed later on, the expenditure for a precise interference-occurrence detector may be justified sometime in the future.

1. Mathematical Approach

The transfer function of each of the three QLS filters can be found and expressed in the following manner

$$T(s) = \frac{g(s)}{h(s)} = \sum_{i=1}^{n} \frac{g(s_i)}{h'(s_i)(s - s_i)} \qquad (4.13)$$

where the prime indicates the derivative with respect to the Laplace transform variable s. The s_i are the roots of the equation $h(s) = 0$. (Equation (4.13) assumes there are no multiple roots. The breadboard QLS filters did, however, have multiple roots as a matter of expediency, since the higher-Q coils for a more selective stagger-tuned filter were not immediately available.) Assuming an applied FM-CW voltage, E_i, described by

$$E_i = E \exp [j(\omega_o t + 2\epsilon t^2)]$$

where

$$2\epsilon = \pi S .$$

Hok [Ref. 27] shows that the equation for the output, E_o, can be written

$$E_o = \sum_{i=1}^{n} \frac{g(s_i)}{h'(s_i)} \int_{-\infty}^{t} E \exp [j(\omega_o T + \epsilon T^2)] \cdot \exp [s_i(t - T)] \, dT . \qquad (4.14)$$

By introducing the dimensionless variable

$$\gamma = \alpha + j\beta = \frac{1}{2} \epsilon^{-\frac{1}{2}} (j\omega_o - s_i) + j\epsilon^{\frac{1}{2}} T$$

Eq. (4.14) can be rewritten as

$$E_o = E \left\{ \exp [j(\omega_o t + \epsilon t^2)] \sum_{i=1}^{n} \frac{g(s_i)}{h'(s_i)} \frac{1}{j\epsilon^{\frac{1}{2}}} \right.$$

$$\left. \cdot [\exp (j\gamma^2)] \int_{0-j\infty}^{\gamma} [\exp (-j\gamma^2)] \, d\gamma \right\} ;$$

or

$$E_o = E \exp\left[j(\omega_o t + \epsilon t^2)\right] \sum_{i=1}^{n} \frac{g(s_i)}{\epsilon^{\frac{1}{2}} h'(s_i)} F_r(\gamma) , \qquad (4.15)$$

where

$$F_r(\gamma) = -j \exp\left(j\gamma^2\right) \int_{0-j\infty}^{\gamma} \exp\left(-j\gamma^2\right) d\gamma .$$

Series expressions exist for $F_r(\gamma)$ [Ref. 27] so that a computer program could be written to find $E_o(t)$ from Eq. (4.15). Also, since $E_o(t)$ is the output from a narrow-band filter, it can be expressed as a sinusoidal wave having slowly varying (negligible change per cycle) amplitude (envelope) and a phase measured relative to a reference near the filter center frequency. Thus

$$E_o = A(t) \cos\left[\omega_o t + \varphi(t)\right] .$$

The computer can find $A(t)$ by peak detecting and $\varphi(t)$ by comparing the zero crossings of $E_o(t)$ with an internally generated reference at frequency f_o. Thus after considerable computer calculation the output of the three filters plus two time delays could be obtained as

$$E_{o1}(t) = A_1(t) \cos\left[\omega_o t + \varphi_1(t)\right] ,$$

$$E_{o2}(t) = A_2(t) \cos\left[\omega_o t + \varphi_2(t)\right] ,$$

$$E_{o3}(t) = A_3(t) \cos\left[\omega_o t + \varphi_3(t)\right] ,$$

where E_{o1}, E_{o2}, and E_{o3} are the outputs of the filters having center frequencies $f_o - \Delta f$, f_o and $f_o + \Delta f$ respectively.

A frequency equal to the center frequency of the filter tuned to f_o is used as a reference to find φ_1, φ_2 and φ_3. The serrodynes ideally add a phase term to $E_{o1}(t)$ and $E_{o3}(t)$, giving

$$V_{o1}(t) = A_1(t) \cos [\omega_o t + \varphi_1(t) + \varphi_a(t)] ,$$

$$V_{o2}(t) = A_2(t) \cos [\omega_o t + \varphi_2(t)] ,$$

$$V_{o3}(t) = A_3(t) \cos [\omega_o t + \varphi_3(t) - \varphi_a(t)] .$$

If the oscillator serrodyne drive is used, $\varphi_a(t)$ is a ramp

$$\varphi_a(t) = 2\pi S \tau t$$

starting from zero at a time, $t = 0$, when the input FM-CW frequency reaches a predetermined value. If the phase-detector serrodyne drive is used, $\varphi_a(t)$ is adjusted by feedback to satisfy

$$\varphi_1(t) + \varphi_a(t) = \varphi_3(t) - \varphi_a(t) .$$

The cancellation residue is found next by

$$V_c(t) = V_{o2}(t) - \frac{1}{2} [V_{o1}(t) + V_{o3}(t)] . \qquad (4.16)$$

Equation (4.16) assumes that the interference detector enables the serrodynes at a time selected with sufficient accuracy to prevent the 180 deg phase-adjustment error.

The case of a modulated FM-CW can be analyzed by separating the modulated FM-CW into a carrier FM-CW signal plus sideband FM-CW signals. The outputs of the filters can be found by summing the separate carrier and sideband responses, since the system is linear to this point. Phase adjustment and the subtraction would be performed using the filter outputs as in the unmodulated case. The time reference for the oscillator method of adjustment would be determined from the carrier FM-CW.

2. Simplified Case

Assuming the QLS works for an unmodulated FM-CW, the analysis of the performance for a modulated FM-CW can easily be determined for

the configuration in which a fixed oscillator is used to drive the serrodyne phase modulators. This is so because at all times except precisely at the times of enabling or disabling the serrodynes, the QLS is a linear system. It is this mode that suggested the name quasi-linear. It is assumed that a sophisticated detector is able to determine the time reference to enable the serrodynes at such a time as to cause perfect cancellation of the carrier FM-CW. This time reference will be incorrect to produce a cancelling signal for the modulation sidebands. The amount of time error, t_e, in serrodyne enabling for the sideband FM-CW signals is

$$t_e = \frac{f_m}{S} ,$$

where f_m is the modulating frequency.

The phase error, θ_e, preventing sideband cancellation is

$$\theta_e = t_e \tau S = f_m \tau ,$$

where τ is equal to the delay of each of the delay networks preceding two of the filters. The cancellation residue, V_{sc}, for a sideband of amplitude V_s is found from Eq. (4.2)

$$V_{sc} = (1 - \cos f_m \tau) V_s .$$

For the breadboard QLS, τ equals one msec.

$$V_{sc} = (1 - \cos 10^{-3} f_m) V_s . \qquad (4.17)$$

Equation (4.17) is shown plotted in Fig. 21.

Sidebands caused by modulation frequencies higher than about 2 kHz would not be affected by the QLS, because the carrier cancellation would be complete and serrodyne operation would be stopped by the time such sidebands were causing significant response from the filters. Also, pure sine-wave sidebands greater than 2 kHz would be treated by the QLS as a carrier, and would therefore be cancelled.

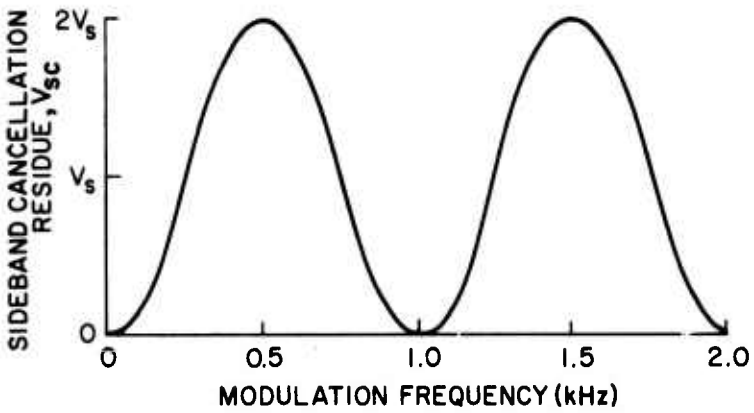

Fig. 21. TRANSMISSION OF FM-CW MODULATION SIDEBANDS THROUGH THE QLS.

V. CIRCUITS USED IN THE BREADBOARD TESTS OF THE QLS

Many of the circuits used in the realization of the Quasi-Linear Suppressor and the blanking system are commonly known, so that complete detail is not necessary in their description. An attempt has been made, however, to specify any out-of-the-ordinary properties that are required, and to discuss means for meeting these requirements. Some circuits which may not have been seen before are described in moderate detail in order to provide an understanding of the uniqueness of the circuit properties involved. For example, a description of a digital phase modulator that has an accuracy of better than ± 1 degree and requires only a simple alignment procedure has not been published before, to the author's knowledge.

A description of each of the basic circuits corresponding to the various blocks in the block diagrams appearing in this chapter will be found in the Appendix.

A breadboard version of the QLS was constructed in the manner described in the following sections. The power supply voltages used for all circuits were plus 10 V and minus 15 V. Decoupling components (not shown) were added when circuit interactions resulted from coupling through the power supply leads.

A. THE QUASI-LINEAR SUPPRESSOR CIRCUIT

The gain and phase stability of all networks in the QLS which transfer the interference response to the point of cancellation is of particular importance. For 40 dB cancellation the gain from input to the point of cancellation must not vary more than one percent between paths. Also, from the relation of Eq. (4.3) for 40 dB cancellation, the phase of the center filter relative to the average phase of the side filters must stay constant within ± .57 deg. If the phase shifts of the filters vary together, no cancellation degradation results; and also if the phase shifts of the two delay networks shift together, there will be no cancellation degradation if the phase detector-method of adjustment is used.

The constants of the FM-CW system for which the QLS was designed are:

Sweep rate, $S = 1$ MHz/sec ,

Signal bandwidth, $B = 1$ kHz.

Other constants needed to specify the circuits used in the breadboard QLS are:

Filter center frequencies: 104 kHz, 105 kHz, 106 kHz,

Delay (τ), B/S = 1 msec.

1. Delay Network

The delay of a network is defined as the derivative of phase lag with respect to angular frequency. A convenient network to provide this phase characteristic is an all-pass network such as that shown in Fig. 22a. For the delay required in the QLS, a number of these sections are used in cascade. Two choices of phase splitters are shown in Fig. 22b. Transformer type was used in the breadboard QLS because more accurate gain is obtained by the 0 deg and 180 deg outputs, and also because the resulting transistor amplifier input capacitance is lower.

The transfer function of the all-pass network, assuming no loading is

$$\frac{V_o(j\omega)}{V_i(j\omega)} = H(j\omega) = \frac{R(1 - LC\omega^2) - j\omega L}{R(1 - LC\omega^2) + j\omega L} , \qquad (5.1)$$

where $V_o(j\omega)$ is the output voltage and $V_i(j\omega)$ is the input voltage.

The phase lag θ_L of the output with respect to the input is found to be

$$\theta_L = 2 \tan^{-1} \frac{\omega L}{R(1 - LC\omega^2)} - \pi . \qquad (5.2)$$

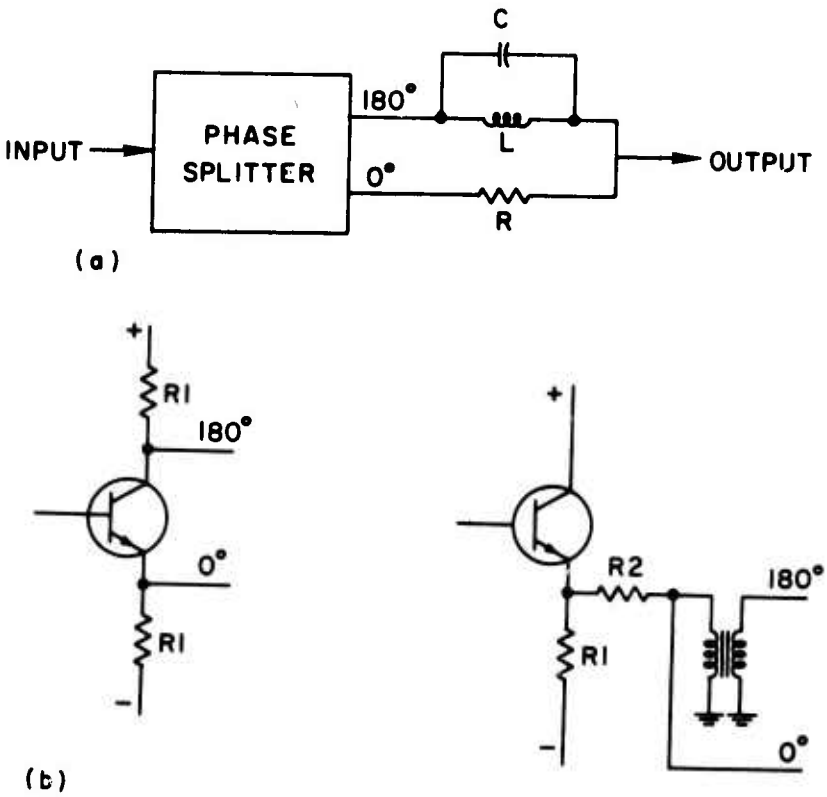

Fig. 22. SECTION OF DELAY NETWORK.
a. All-pass network.
b. Phase splitters.

By taking the derivative with respect to ω the delay τ as a function of ω is found.

$$\frac{d\theta_L}{d\omega} = \tau(\omega) = \frac{2[RL(1 - LC\omega^2) + 2RL^2C\omega^2]}{R^2(1 - LC\omega^2)^2 + \omega^2L^2} . \qquad (5.3)$$

At $\omega = \omega_o = 1/\sqrt{LC}$,

$$\boxed{\tau(\omega_o) = 4RC} \qquad (5.4)$$

The inductance value L was chosen to obtain high Q, and the capacitance C resonated with L at approximately ω_o. To obtain maximum delay R was chosen as large as possible without causing excessive attenuation or gain variation with frequency. The values used in the circuits for the breadboard study were

$R = 82K,$

$C = 500\ pF,$

$L = 2.6\ MHz$ (adjustable)

so that $\tau(\omega_o) = 4(82 \times 10^3)\ (500 \times 10^{-12}) = .164$ msec.

If all sections were adjusted for the same ω_o, about 1 msec delay would be obtained with six sections. The first delay (No. 1 on Fig. 20) used eight sections stagger-tuned to give a flat delay over the center-filter frequency range of 105 kHz ± 500 Hz. This delay network did not have constant delay within the bandwidth of the 106 kHz filter, for which it was also used, so that ten sections were required in the second delay (No. 2 on Fig. 20) to obtain the required 2 msec total delay.

Each of the delay networks was adjusted by applying a narrow bandwidth pulse obtained from the filter it precedes in the block diagram of Fig. 20. A video pulse of less than one half cycle of the filter frequency was applied to the filter to generate the pulse. Adjustments were made to obtain the correct delay and minimum preliminary responses. The oscillogram in Fig. 23a shows the output of the first 1 msec delay network superposed on the pulse originating from the 105 kHz filter. The oscillogram in Fig. 23b shows the output of the two 1 msec delays in series, superposed on the pulse originating from the 106 kHz filter.

The cores used for the inductors in the delay networks were gapped ferrite pot cores. The ferrite material used has a high permeability (a relative permeability of 1300) and is effectively used as a magnetic short circuit around an air gap. The Q obtained using litz wire was approximately 500, with the result that stray capacitances cause more deviation from the all-pass properties of the network than do coil losses.

By selecting capacitors with a vendor-specified temperature characteristic as close as possible to the opposite of that specified for the inductors, a maximum temperature coefficient for the LC product of ± 50 parts per million per deg C was obtained. Since the components used within the delay networks were all purchased at the same time, it is expected that the two delay networks should have nearly equal phase deviations with temperature changes. This characteristic would not cause a degradation in the performance of the QLS. Therefore, no attempt was

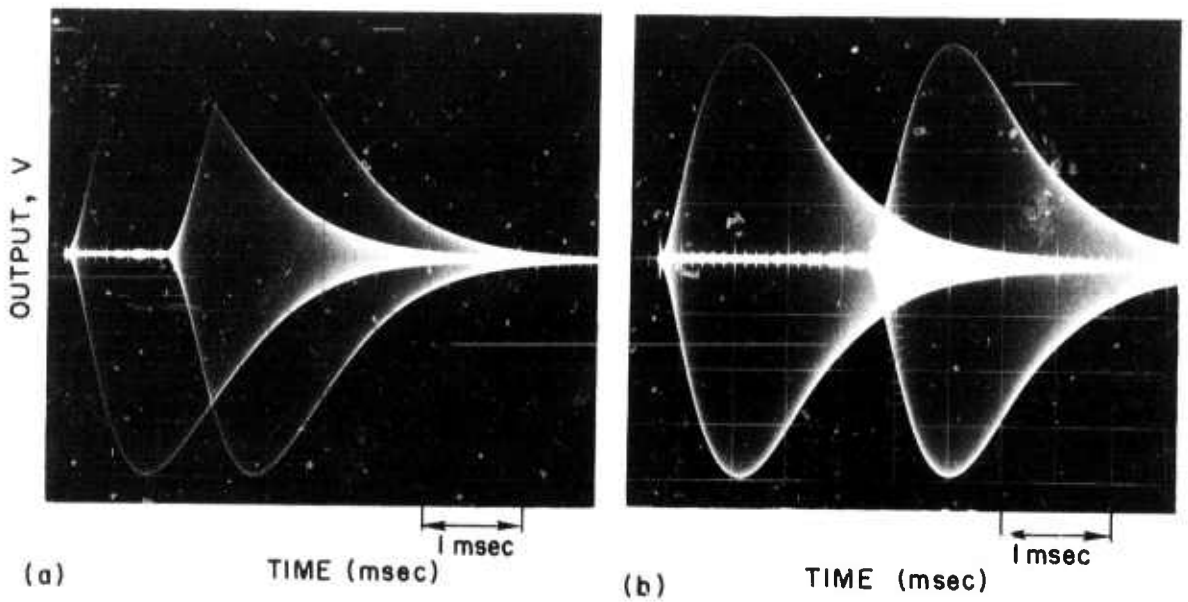

Fig. 23. DELAY-NETWORK RESPONSES.
a. One msec delay. (Pulse from 105 kHz filter.)
b. Two msec delay. (Pulse from 106 kHz filter.)

made to calculate the effects of drift in the delay lines. The circuitry was checked with a test signal each day during experimentation to be sure phase-shift changes in the networks had not degraded the cancellation effect. No adjustments were necessary over a period of about 3 weeks.

2. Filters

The filters for the breadboard demonstration QLS were designed to provide adequate isolation between the three channels, but no attempt was made to provide flat response over the entire desired signal bandwidth. Each filter consisted of three single tuned filters in cascade, isolated from one another by transistors. The overall filter had a 6 dB bandwidth of 700 Hz. A schematic diagram of one stage is shown in Fig 24. The transistors were selected to divide current equally in the no-signal condition.

The phase variation with respect to frequency in the filters is considerably less than in delay networks, so that if inductors and

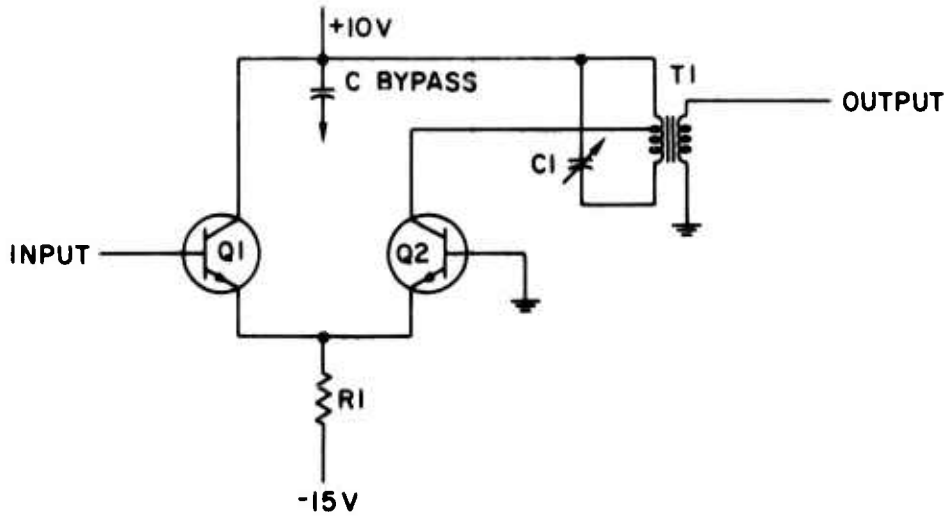

Fig. 24. SCHEMATIC DIAGRAM OF FILTER SECTION.

capacitors of equal quality were used, the filter are not a weak link in the system. However, the high-quality cores used in the delay networks had not been delivered when the filters were built. The substitute toroidal cores are marginal in two ways. First, the permeability changes with signal level; and second, the low permeability in the toroidal configuration gave low coupling between the primary and secondary windings. The changes in permeability with signal level degraded the cancellation effect at high interference levels. The low coupling caused an unsymmetrical variation of amplitude with frequency, and with it a corresponding unsymmetrical phase variation with respect to frequency. The deviation in symmetry differs from one filter to another, so that perfect cancellation is obtained at only one point in the interference response. When time permits, considerable improvement in the breadboard QLS can be obtained with redesigned filters using the higher-performance ferrite pot cores such as were used in the delay networks.

3. Phase Modulator

The equal-but-opposite phase modulation accomplished by the serrodynes in the QLS should have an accuracy of about ± 1 deg in order to maintain the correct phase relationship to obtain 40 dB cancellation.

An analog method to accomplish this did not seem readily available; so a search was made for a digital method.

The first possibility considered was that shown in Fig. 25a. This method consists of using equally spaced taps on a delay network which has a total of one cycle phase shift from input to output. For the ± 8 deg resolution required for 40 dB cancellation (determined from Eq. 4.2) at least 23 taps and switches would be required. To obtain the required accuracy of ± 1 deg, adjustments would probably be required at each tap.

Figure 25b shows the simple configuration that was devised by the author and is used in the breadboard QLS. This configuration requires only ten switches for 5 sections and gives a better-than-required phase resolution of ± 5.6°. It is easily adjusted to obtain better than ± 1 deg phase accuracy.

Referring to Fig. 25b, each binary section of the Binary Digital Controller operates switches which insert or bypass phase-shift networks. The Binary Digital Controller in the QLS is a 5 bit binary counter. The amount of phase shift inserted by a particular bit position of the controller is proportional to the value of that position in the binary system of numbers. For example, the most significant bit controls 180 deg, next 90 deg, and so on, with the amount of phase shift decreasing by a factor of two from each section to the next. Each single advance of the counter inserts a change in phase equal to that of the least significant section. In the 5 bit QLS modulator this is 11.25°.

For assuring the lowest possible transients during modulation, the modulator is designed exclusively for increasing phase lead or lag. The phase-shift sections are arranged in decreasing magnitude in the direction of signal flow. Increasing binary number drive causes increasing phase shift of the direction caused by the individual sections. By restricting the binary drive to increasing magnitude, except at the counter overflow, the input signal to a phase-shift section changes only when it is being switched out of the signal path. Therefore, transients in a phase-shift network occur only when its output is not being used. If (in some other applications) modulation in both directions is required, a separate modulator for each direction would give the lowest possible transient errors. (Since

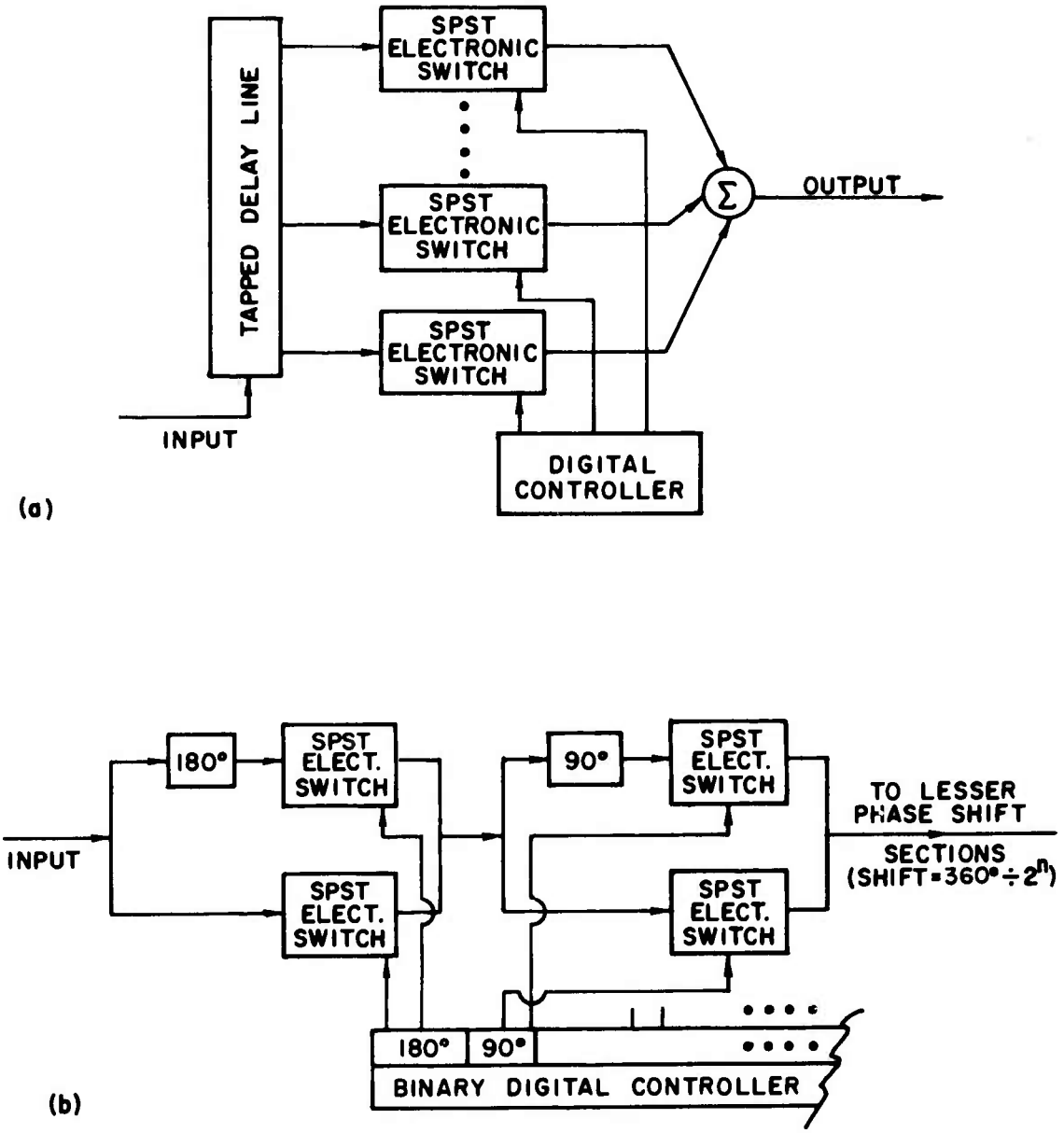

Fig. 25. DIGITAL PHASE MODULATORS.
a. Tapped-delay-line phase modulator.
b. Binary phase modulator.

the phase-shift sections are very broadband and have low delay and dispersion, transients last for only a cycle or two when reversed operation is used. The phase-lead modulator for the breadboard QLS is actually a phase-lag modulator operated in reverse; but since some degradation does result from this arrangement, the following description includes a network to be used in a phase-lead modulator which would have lower transients.)

The phase-shift network for an increasing-lag modulator is shown in Fig. 26a, including the equation specifying its phase shift. The phase splitter must be DC-coupled to its 0 deg output, because signals within the phase modulator contain frequency components from DC to above the input signal-frequency band, and if these signals are not equally transmitted at all frequencies, undesirable transients result in the switching process. Figure 26b shows the phase splitter used in the breadboard QLS. R is a small resistor to absorb any DC voltage remaining to prevent high DC current flow in the transformer primary.

A network for phase lead to complement that in Fig. 26a for phase lag is shown in Fig. 26c. This network was not used in the breadboard QLS; but the performance of the QLS could be improved by its use. The network might be considered as a 360 deg to 0 deg phase-lag network; but it is indistinguishable from a 0 deg to 360 deg phase-lead network.

Probably the most desirable feature of the digital phase modulator is the ease of adjustment. The latter is accomplished by applying a sine wave to the modulator signal input and observing the Lissajous figure obtained on an oscilloscope using the input and output signals of the phase modulator. Figure 27 shows two such oscillograms of Lissajous figures. Figure 27a is made with perfect adjustment, while Fig. 27b shows misadjustment of the least significant phase-shift section (11.25 deg). The frequency of the input is 106 kHz and the modulation rate is 360 deg per msec. (These are the required conditions in the QLS.) The output stays on one ellipse for about 3.3 cycles, so that if transients are significant, the traces will be blurred. Each ellipse in the correctly adjusted pattern is in reality two ellipses superposed. These become separate when there is an error in adjustment. In the left Lissajous figure, for example, the first ellipse away from 0 deg is ± 11.25 deg. If the

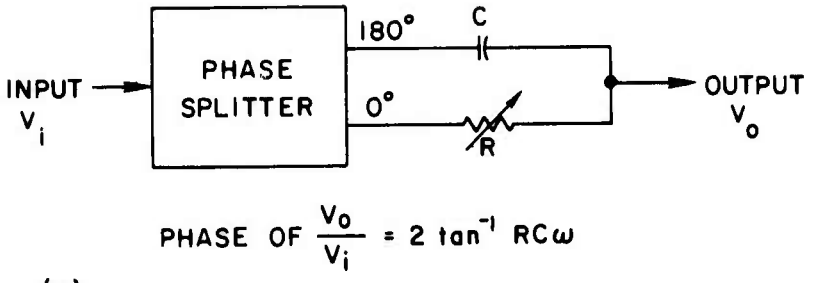

PHASE OF $\frac{V_o}{V_i} = 2 \tan^{-1} RC\omega$

(a)

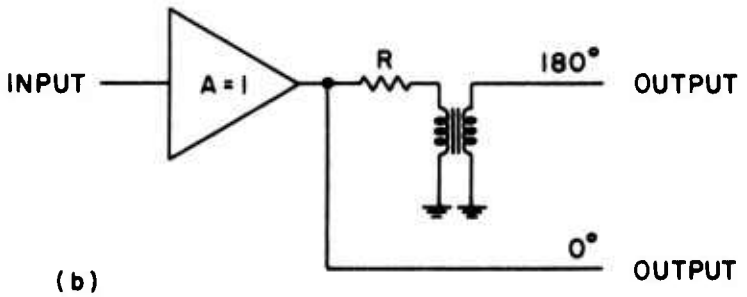

(b)

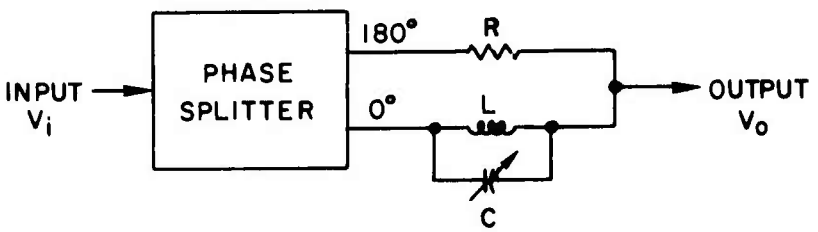

PHASE OF $\frac{V_o}{V_i} = -2 \tan^{-1} \frac{\omega L}{R(1 - LC\omega^2)}$

(c)

Fig. 26. PHASE-MODULATOR NETWORKS.
a. Phase-lag network.
b. Phase splitter.
c. Phase-lead network.

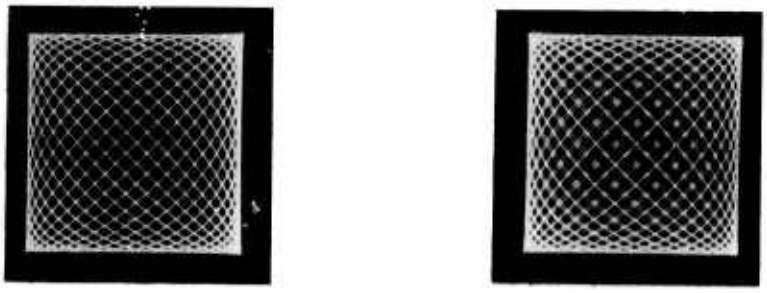

(a) (b)

Fig. 27. LISSAJOUS FIGURES OBTAINED FROM INPUT AND OUTPUT SIGNALS OF PHASE MODULATOR.
a. Perfect adjustments.
b. Adjustment error of approximately one degree.

11.25 deg section is misadjusted to 10 deg, the first ellipse away from 0 deg is 10 deg and the next, which should coincide with the first, is -12.5 deg, about like the right Lissajous figure in Fig. 27. The adjustment to make these ellipses coincide gives an accuracy of better than ± 1 deg.

In Chapter IV, Section F, "Analysis," the serrodynes are assumed to insert a phase shift independent of frequency. The phase relations in the preceding discussion are for a fixed input frequency; but the phase slope is made as low as possible in designing the phase-shift networks. The peak phase slope is about one third of that which would result by modulating, using a tapped pure time delay. The QLS breadboard modulator has a maximum phase error due to time delay of about ± 1/2 deg over the one kHz bandwidth. This phase error is considered negligible.

4. Binary Counter

The binary counter which controls the digital phase modulator consists of five cascaded integrated circuit J-K flip-flops, as shown in Fig. 28. The reset input is provided by the interference occurrence detector, and the pulse input is generated by the phase detector. The propagation time delay through the counter was measured and found to be about 100 nsec, which is insignificant for QLS purposes.

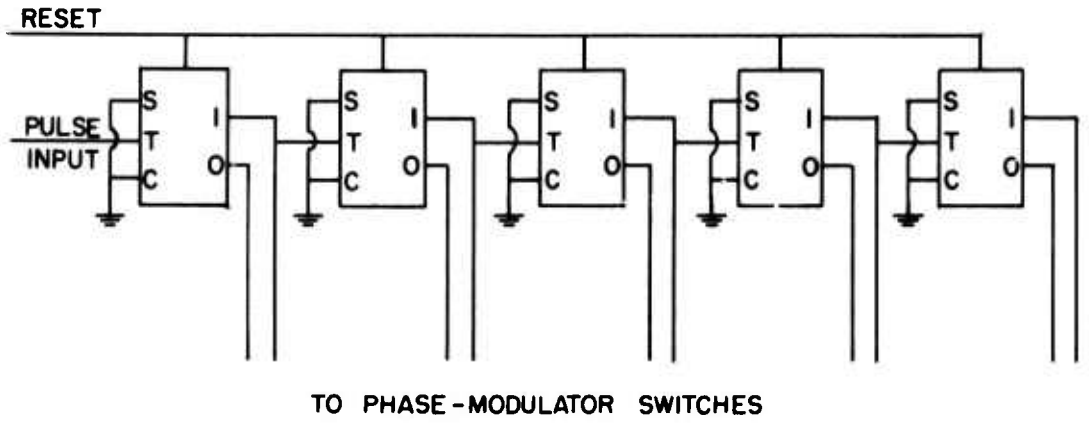

Fig. 28. SCHEMATIC DIAGRAM OF BINARY COUNTER.

5. Phase Detector

The phase detector compares the zero crossing time of its two inputs to determine whether a pulse should be sent to the binary counter. The pulse is derived from one of the inputs. Figure 29a shows the block diagram of the phase detector. The exact circuitry is not shown since it is quite conventional. The square wave is produced by a limiter. The pulse is produced by first obtaining a square wave then differentiating and finally clipping.

The principle of the phase detector operation is shown in Fig. 29b. The difference frequency of the two signals in the absence of modulation causes the relative phases to drift in one direction, and modulation causes a change in the opposite direction. The result is that the adjusted phase oscillates in sawtooth fashion about the correct adjustment with a maximum error approximately equal to the phase-modulator resolution.

6. Interference-Occurrence Detector

The first detector constructed to measure the time of occurrence of interference was an envelope detector attached to the output of the 104 kHz QLS filter, and having a threshold slightly above the background noise level. This detector was adequate to check the operation of all other circuits for cancellation of laboratory-generator pulse or FM-CW

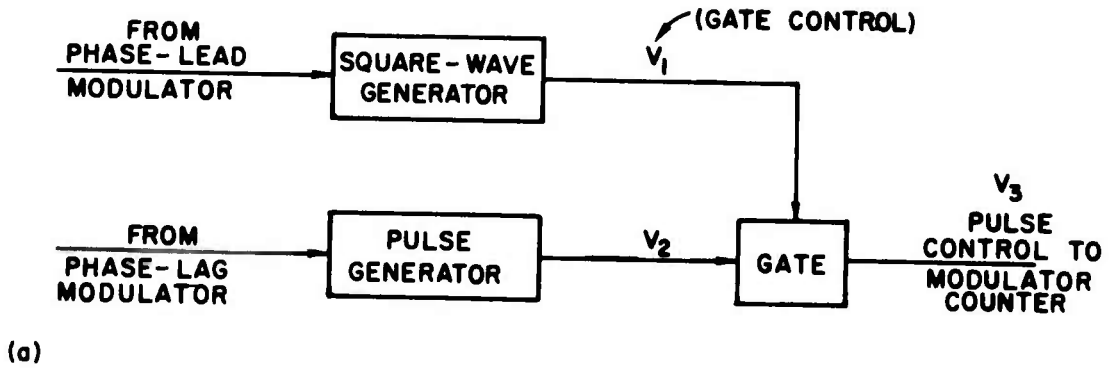

(a)

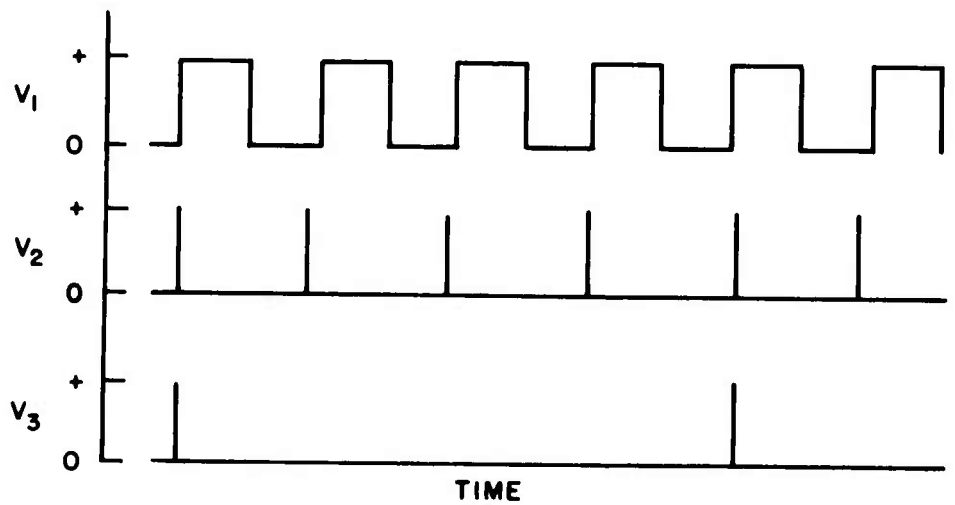

(b)

Fig. 29. PHASE DETECTOR AS USED IN QLS.
a. Block diagram.
b. Waveforms from (a).

interference. The envelope response from the filter rises quite slowly with FM-CM interference, so that the measured time of interference occurrence is very dependent on interference amplitude and would be useful only in the minimum-output cancelling method where time accuracy is not required.

The circuit of Fig. 30 was designed to provide improved accuracy in measuring the time of FM-CW interference occurrence. The two filters are tuned to slightly different frequencies, f_1 and f_2, so that their envelope responses cross as the FM-CW interference sweeps through. At the envelope crossing the comparator changes states. By selecting the average frequency of f_1 and f_2, the comparator switching is made to occur at the correct time to initiate the cancelling action by removing a positive voltage from the reset line of the binary counter. The comparator output is not used directly to control the counter because the length of time of the cancelling operation would be too variable with the amplitude of the interference. A pulse is generated from the comparator switching and stretched to obtain a fixed-length counter-enabling

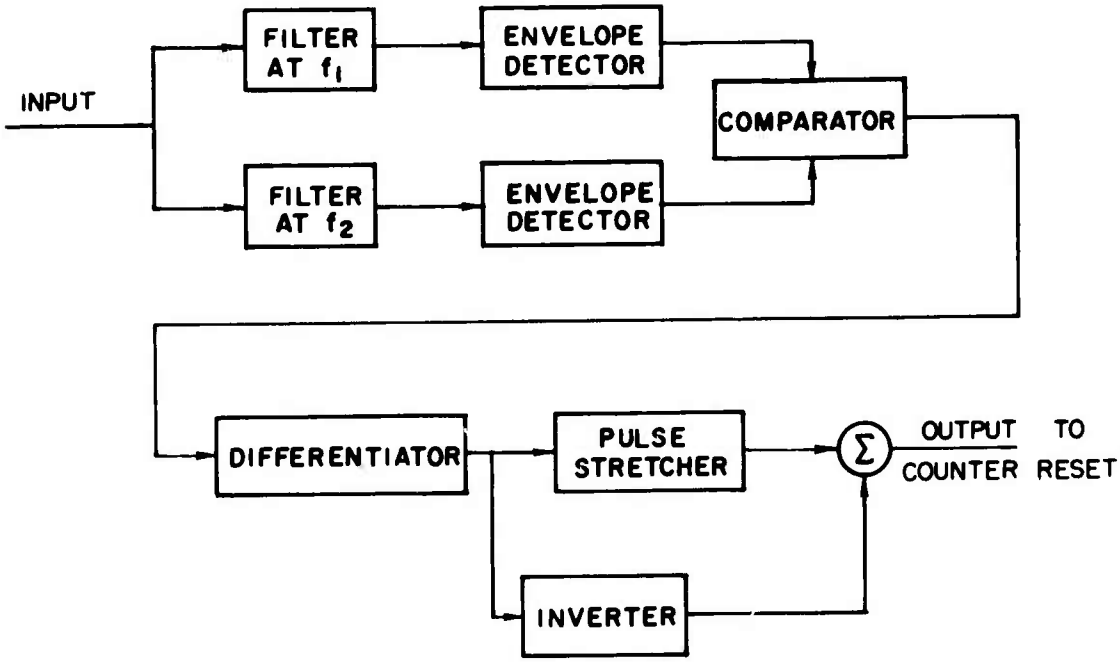

Fig. 30. BLOCK DIAGRAM OF FM-CW INTERFERENCE-OCCURRENCE DETECTOR.

pulse. The unstretched pulse is inverted and added to the stretched pulse to reset the counter at the comparator switching time in case the counter has been turned on by a previous comparator switching.

Figure 31a shows an oscillogram of the two envelope-detector outputs. The filter with the later response has a long discharge time constant to prevent additional crossings from the ripple caused by the beat between the input sweep and the filter natural frequency. Figure 31b shows an oscillogram of the comparator output with the filter output having the later response. (The oscillograms shown in Figs. 31b and c were taken under slightly different network adjustments than Fig. 31a, as can be noted by the differing filter envelope responses. The basic properties of the waveforms are representative, however.) Figure 31c shows the counter control with the reset pulses. The counter enabling pulse width is 5 msec measured from the last reset pulse. (The latter does not show in the picture.)

B. THE BLANKING CIRCUIT

Two types of blanking are required in the test evaluation of the QLS. Self blanking is required after the QLS to blank those stations whose wide bandwidth modulation prevents cancelling. Separate-channel blanking is used for comparison purposes as a measure of the effectiveness of the QLS. Figure 32a and b show the block diagrams for the circuits which were used for self blanking and separate-channel blanking respectively. The delay network and filters used in separate-channel blanking are part of the QLS. A photograph of the breadboard circuitry of the QLS and blanking circuits is shown in Fig. 33.

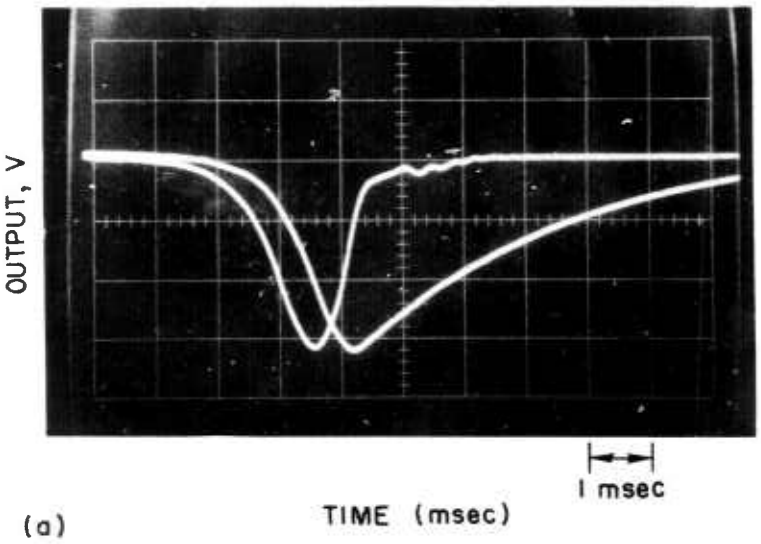

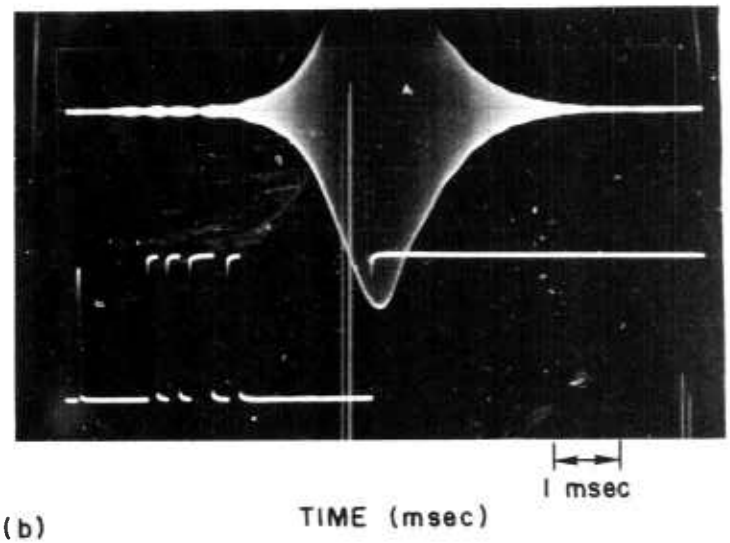

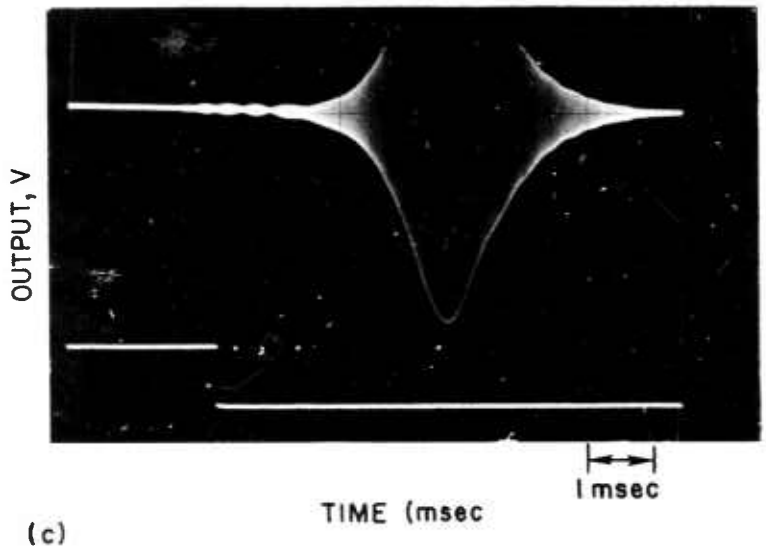

Fig. 31. INTERFERENCE DETECTOR WAVEFORMS.
a. Envelope detector outputs.
b. Comparator output.
c. Counter reset control.

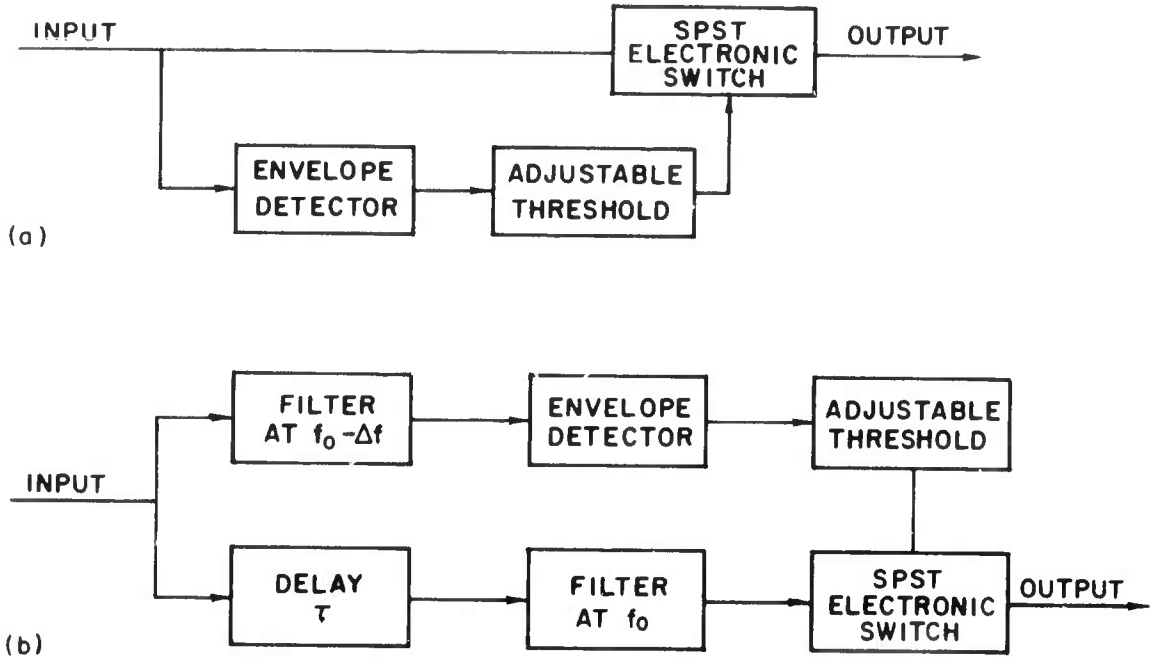

Fig. 32. BLOCK DIAGRAMS OF BLANKING CIRCUITS.
a. Self blanking.
b. Separate-channel blanking.

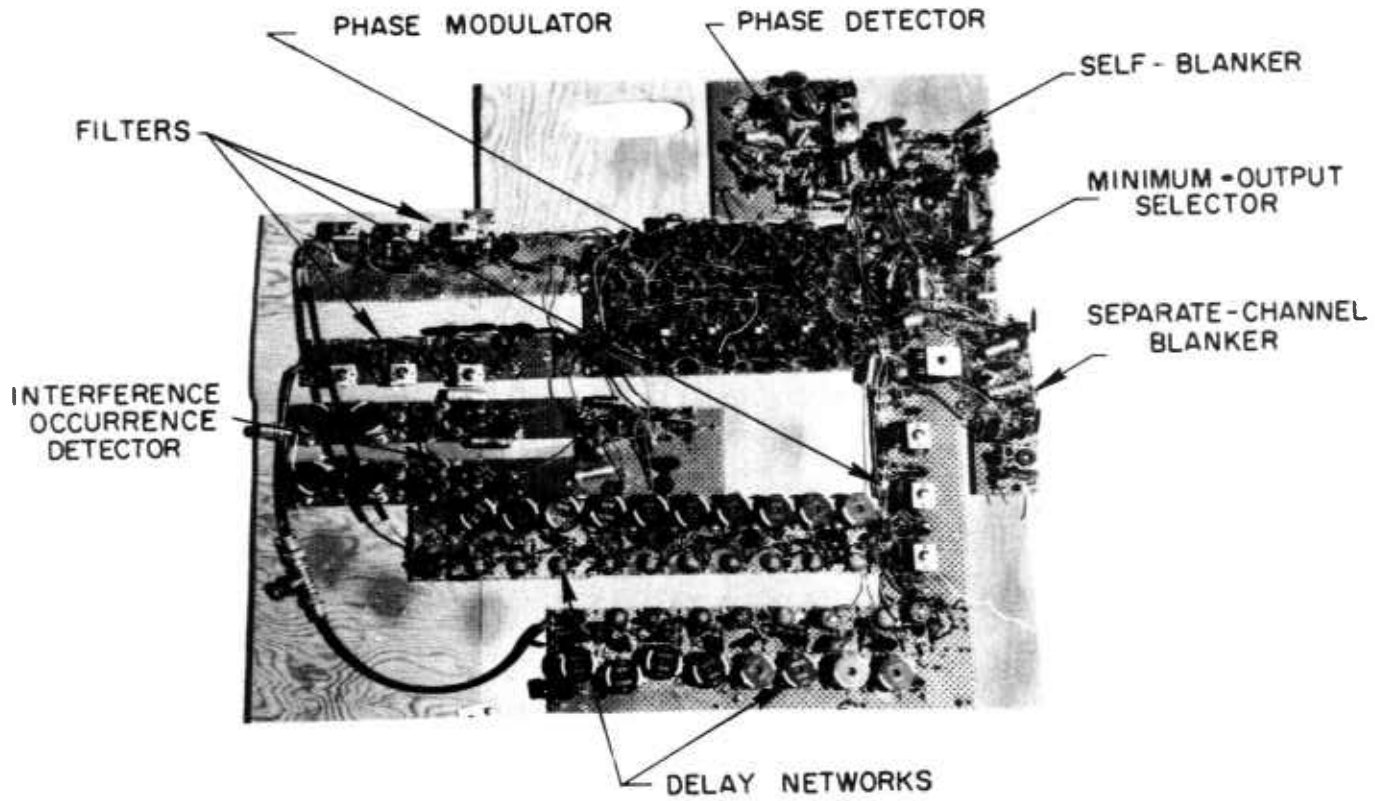

FIG. 33. BREADBOARD CIRCUITRY FOR QLS WITH BLANKER.

VI. RESULTS OF TESTS ON QLS

A. RESULTS USING LABORATORY-GENERATED INTERFERENCE

The QLS, described in Chapter V, was adjusted and tested using laboratory-generated interference to determine whether circuit operation was satisfactory. The first tests made were pulse tests. These tests did not use delay networks. They were performed to verify proper circuit performance, which in turn would justify building the delay networks for FM-CW cancellation. The system adjustments for optimum operation are: (1) the frequency of the filters in the interference detector; (2) the phase of variable-phase networks in the two cancelling signal paths; and (3) the gain after the summation of the cancelling voltages.

All of the QLS tests using laboratory interference relied on the accuracy of the time reference provided by the interference-occurrence detector. The free-running oscillator method of phase adjustment was also used, since the need for the phase detector method was not apparent at the time the tests were made. It is felt that no significant differences would result in rerunning the tests with the improved features of the QLS which are needed for FM-CW receiver signals.

1. Pulse Interference

The impulse QLS was tested using the block diagram shown in Fig. 34a. The pulse generator simulates an interfering impulse and the oscillator simulates a desired CW signal. The upper trace of the oscillogram in Fig. 34b shows the output V_u of the center-channel filter. This output is the CW signal plus the pulse interference. The lower trace is the output V_c after cancellation, showing the CW relatively unaltered during the time when a large pulse response was present before cancellation.

2. FM-CW Interference

The FM-CW QLS was tested using the block diagram of Fig. 35. The upper trace of the oscillogram in Fig. 36a shows the responses, V_u, from a simulated interfering sweep with no simulated desired signal applied.

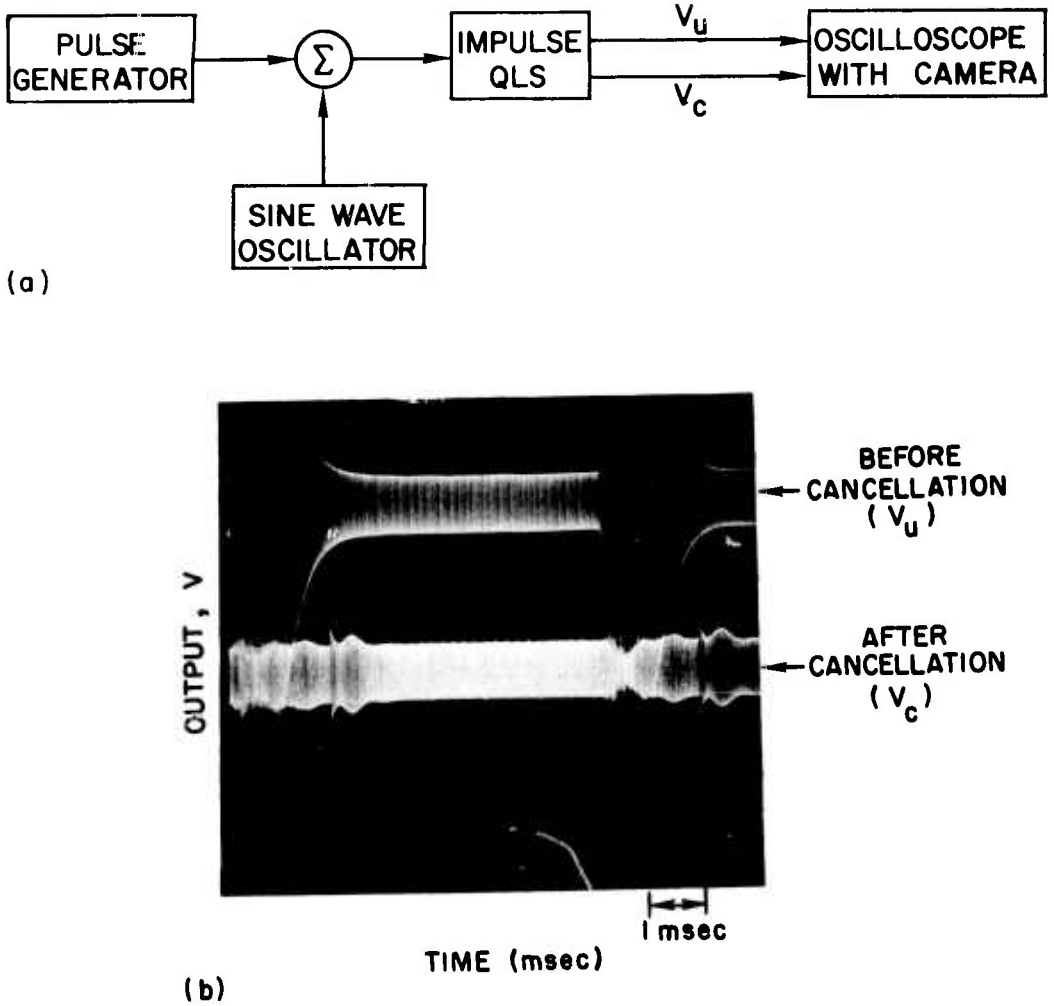

Fig. 34. PULSE INTERFERENCE TEST OF IMPULSE QLS.
a. Block diagram of pulse-test equipment.
b. Pulse-test waveforms.

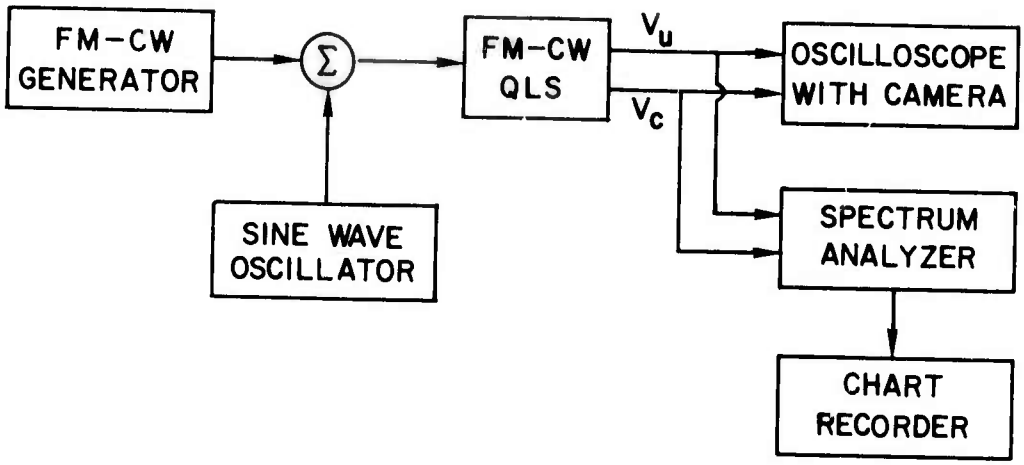

Fig. 35. BLOCK DIAGRAM FOR TEST OF FM-CW QLS.

The lower trace is the output, V_c, after cancellation. The ripple responses following the main response are caused by a phase discontinuity in the FM-CW sweep at 100 kHz. Figure 36b shows in similar fashion the results with an added CW voltage simulating the desired signal.

A scanning spectrum analysis was also made (Fig. 37) while a repeating FM-CW interference was applied. Three spectrum-analysis sweeps are shown in each part of Fig. 37. The first sweep is with the desired CW signal applied but no FM-CW interference; the second is with the FM-CW interference added but the QLS disabled by disconnecting the interference detector; the third is also with both FM-CW interference and CW signal applied but with the QLS enabled by reconnecting the interference detector. To demonstrate the wide dynamic range possessed by the QLS, the spectrum analysis data are shown at three different signal and interference levels, as follows: Fig. 37a, at reference level (near the maximum of the QLS dynamic range); Fig. 37b, at 20 dB below reference level; and Fig. 37c, at 40 dB below reference level.

B. RESULTS USING FM-CW RECEIVER

The major motivation for building the QLS was to determine its performance in reducing fixed-station interference in an FM-CW ionosphere sounder. The FM-CW receiver shown in Fig. 38 was assembled to duplicate

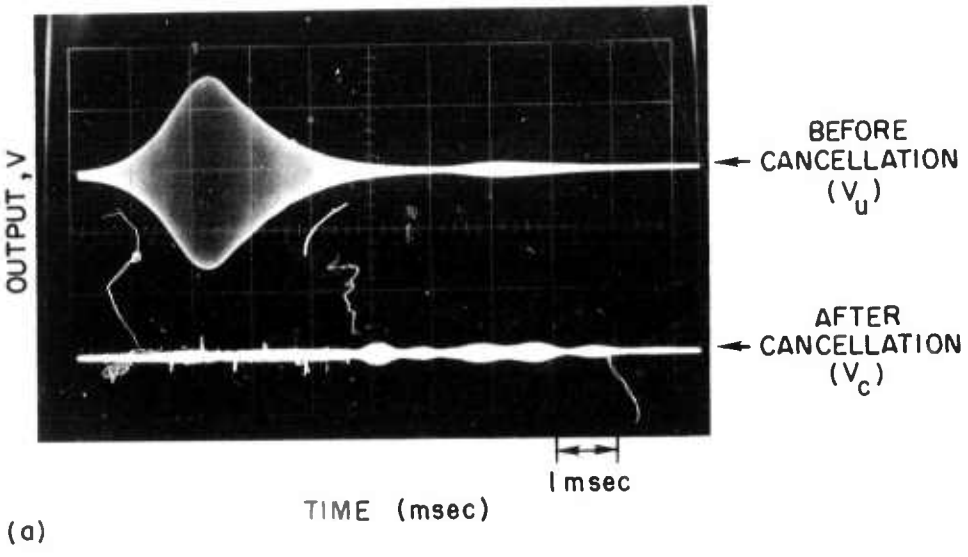

(a)

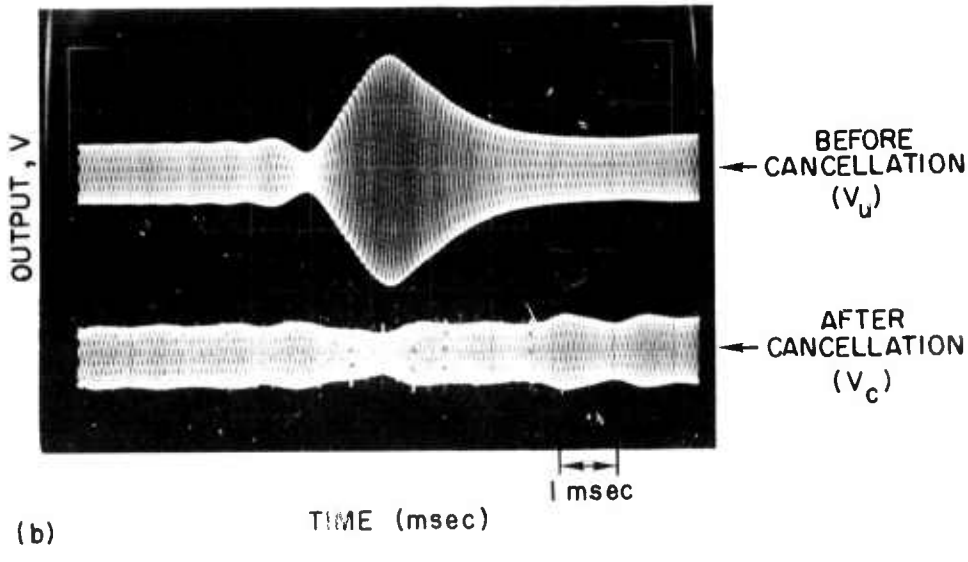

(b)

Fig. 36. FM-CW QLS WAVEFORMS.
a. Interference with no desired signal.
b. Interference plus CW desired signal.

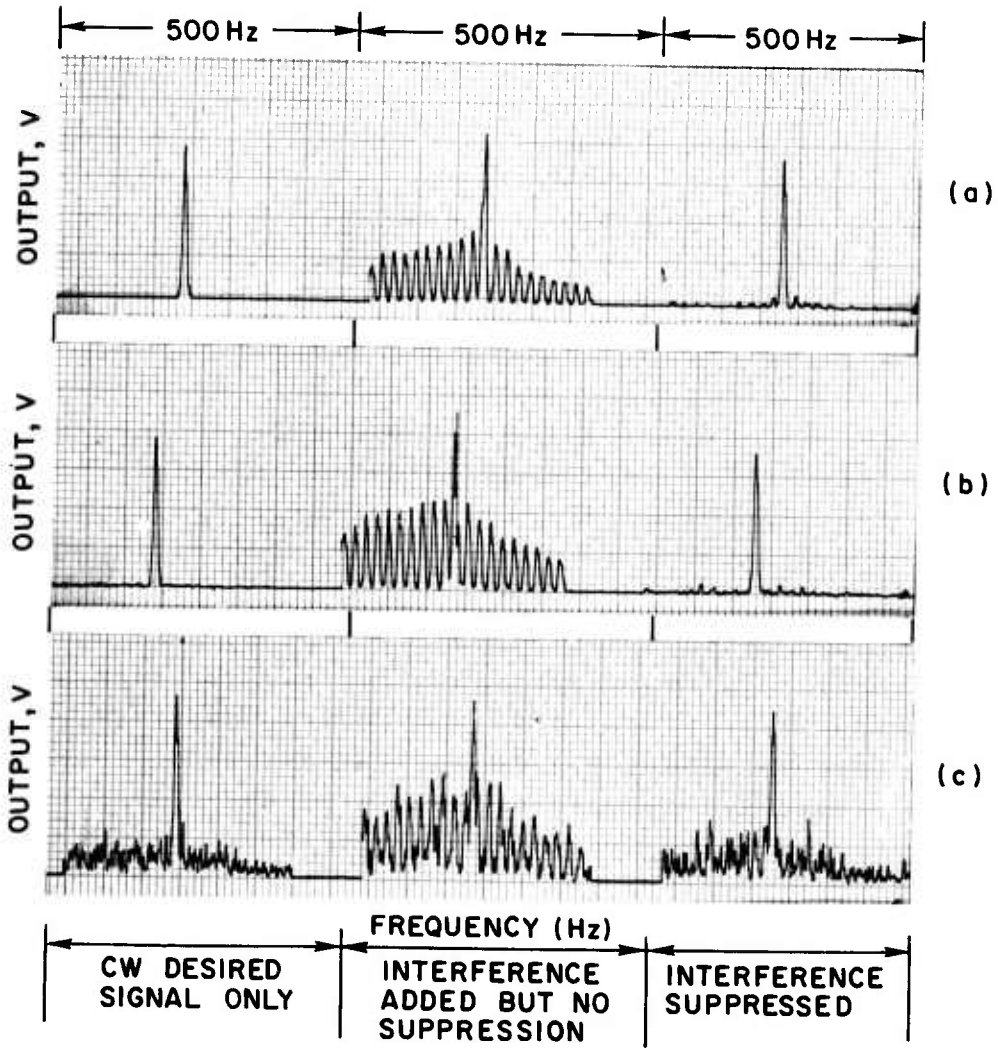

Fig. 37. RESULTS OF SPECTRUM ANALYSIS OF FM-CW TESTS ON QLS.
a. Reference level.
b. 20 dB below reference level.
c. 40 dB below reference level.

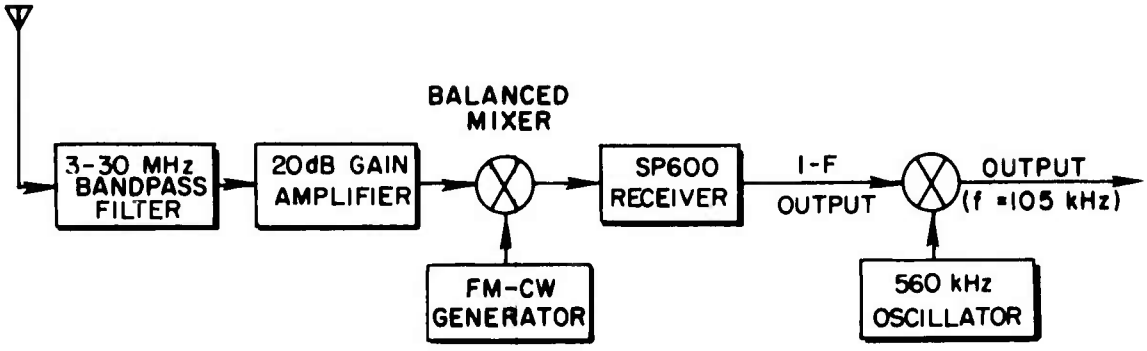

Fig. 38. BLOCK DIAGRAM OF FM-CW RECEIVER.

conditions encountered in a sounding system. If the receiver were being used to obtain an ionogram, the desired signal at the antenna would be an FM-CW with a sweep rate equal to the sweep rate of the local oscillator for the FM-CW receiver. At the output of the mixer, the desired signal for a fixed target becomes fixed in frequency.

Signals from fixed-frequency stations within the interval of the spectrum being swept become FM-CW signals at the output of the receiver balanced mixer. Most HF stations transmit modulated signals, however, so that the results of Section A-2 on unmodulated FM-CW signals are not directly applicable to the sounder receiver situation. The objective of the FM-CW receiver tests described in the present section was to determine the performance of the QLS in a situation identical with its primary intended use.

The FM-CW receiver was assembled at a Stanford Radioscience Laboratory field site using the equipment shown in the block diagram of Fig. 38. Two receiving antennas located near the site were employed, a rhombic antenna aimed east and a rotatable, log periodic antenna (LPA). The 3 to 30 MHz bandpass filter was used to prevent spurious responses caused by transmissions outside the HF band. In the block diagram, a transistor amplifier having 20 dB gain with low noise precedes the balanced mixer to provide a good receiver noise figure. The linear FM sweep (FM-CW) is a modified Hewlett-Packard (H-P) 5100A-5110A synthesizer whose frequency is controlled by the digital controller developed at Stanford. Frequency conversion from the receiver IF output to the QLS operating frequency is

accomplished by a balanced mixer driven by a 560 kHz transistor crystal oscillator. The oscillator circuit is described in the Appendix. The test equipment and the FM-CW receiver are shown in the photograph, Fig. 39.

The FM-CW receiver results were obtained with the QLS in the minimum-output-selecting mode. Negligible differences in the results of the spectrum analysis were noted when the oscillator method of serrodyne drive was used. In the tests of individual station performance, however, it was observed that the time reference given by the detector was inadequate to prevent interference addition on an occasional interfering station.

To be consistent, minimum-output mode was used in all data presented. Suggestions for improving the detector are given in Chapter VII, the adoption of which may make it possible to obtain the required time accuracy, in the interference detector, thus eliminating the need for the less desirable minimum-output mode of operation.

1. Individual-Station Performance of the QLS

Equipment was connected as shown in Fig. 40 to obtain data demonstrating the performance of the QLS in cancelling individual HF stations received by the FM-CW receiver. An amplifier and a detector were attached to the center-filter uncancelled output V_u and to the cancelled output V_c. As the FM-CW receiver swept through the HF spectrum the detector outputs were recorded at 15 inches per second (IPS) on an FM tape recorder. The tape recorder was then played back at 1-7/8 IPS and the output was recorded on a chart recorder. A calibrating signal was recorded at the beginning of each test so that the chart recorder gain could be set for equal gain in the two channels.

A short stretch of the resulting chart record is shown in Fig. 41. Frequency markers (added to V_u) permit calibrating the HF signal-frequency being received. Each positive spike in the record is the response caused by an interfering station. The upper-channel spikes indicate the amplitude V_u before cancelation, and the lower-channel spike indicates the amplitude V_c after cancellation. The positive spike at 15 MHz is the radio station WWV. It was not cancelled significantly in this record, although it often is depending on the type of modulation

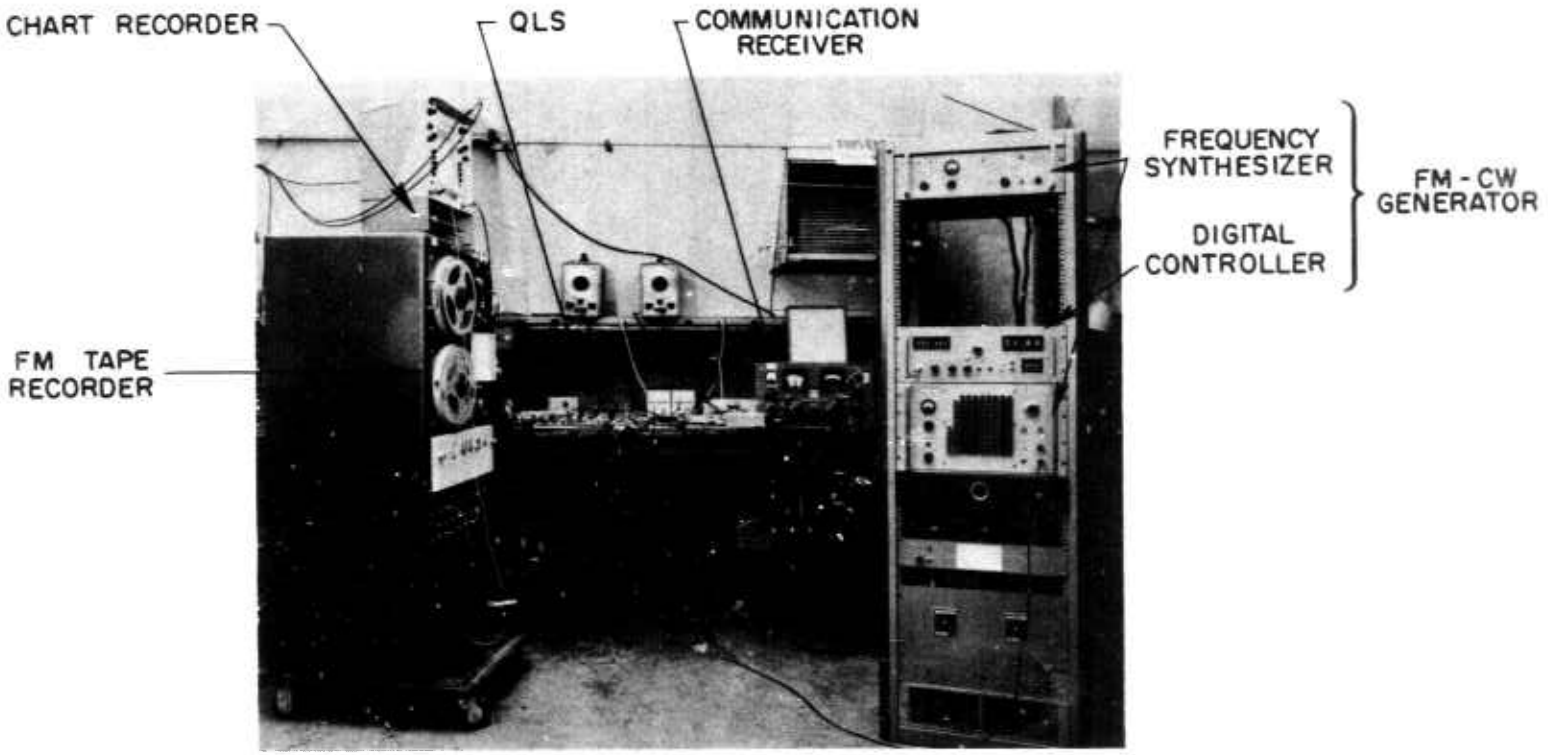

Fig. 39. EQUIPMENT FOR FM-CW RECEIVER TESTS OF THE QLS.

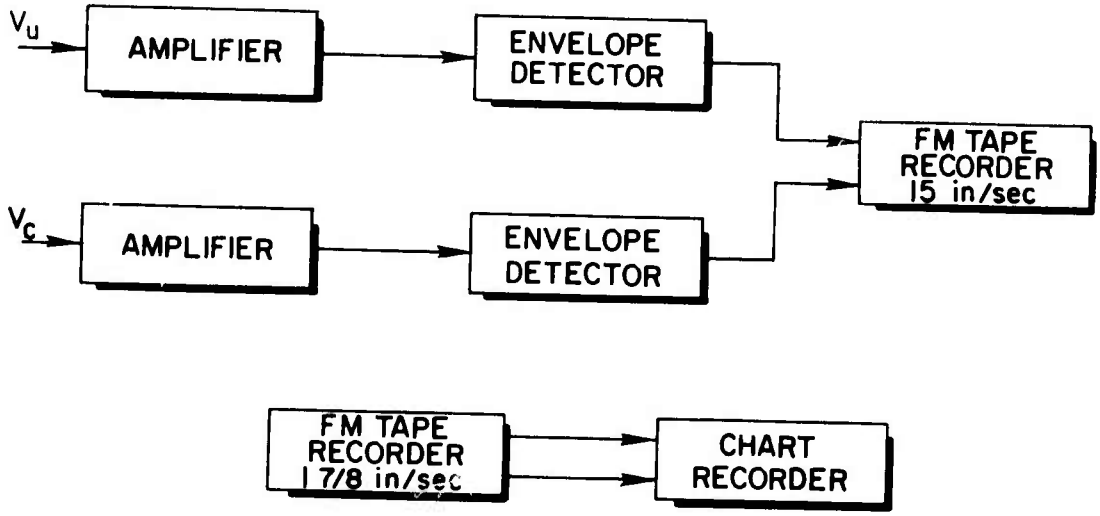

Fig. 40. BLOCK DIAGRAM FOR TEST OF QLS PERFORMANCE IN CANCELLING INDIVIDUAL STATIONS.

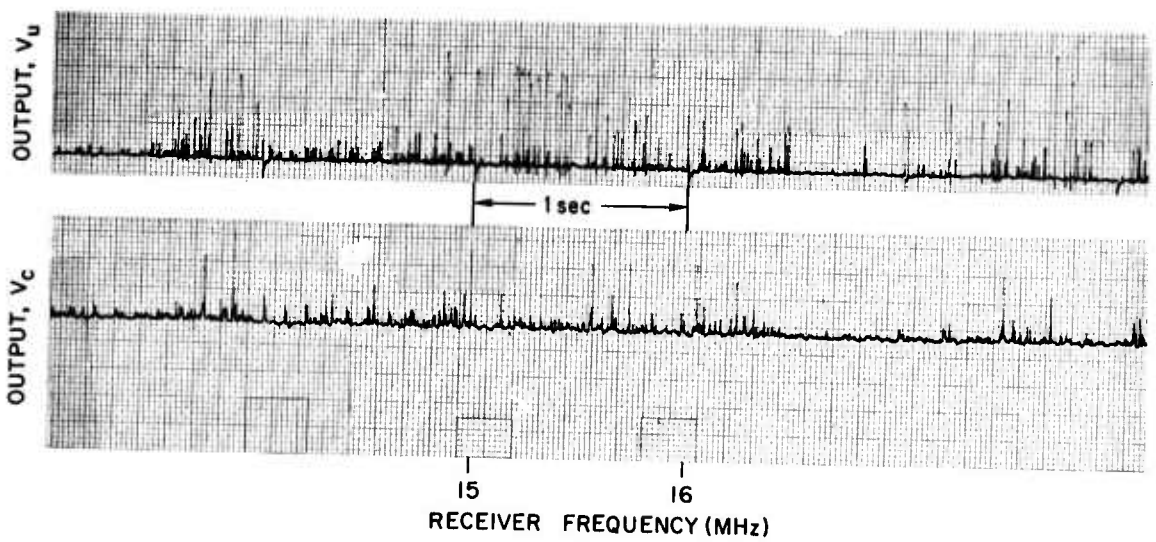

Fig. 41. CHART RECORD SHOWING CANCELLATION OF INDIVIDUAL STATIONS.

being broadcast at the time of the sweep. The international short-wave broadcast band transmissions are those that start at 15.1 MHz and extend to 15.45 MHz. As can be seen, these are cancelled quite well. The stations at about 14.9 MHz are simplex FSK and are also cancelled to a considerable degree.

Chart records such as that shown in Fig. 41 were made by ten sweeps through the frequency range of 5 to 25 MHz. Two sweeps each were made using the eastbound rhombic and the LPA aimed north, south, east and west. Immediately after each pair of sweeps the receiver was manually tuned to identify the types of stations received, so that the performance of the QLS could be assessed for the different classes of stations.

The stations are divided into three classes, as follows: (1) broadcast voice; (2) simplex FSK, on-off-keyed; and (3) complex telegraphy. Cumulative probability distributions showing the QLS performance are presented in Fig. 42. The vertical scale of each plot gives the probability that an interference of the type specified will be cancelled at least as thoroughly as the corresponding horizontal-scale value would indicate. The "all stations" class includes all stations whose signal amplitude exceed 1 cm on the uncancelled channel of the chart record. The number of station indications which were used to plot the curves of Fig. 42 are shown in Table 1.

The probability distributions show that the QLS is very effective in reducing interference caused by "broadcast, voice" or "simplex FSK, on-off-keyed" signals. The probability is about 0.7 that these stations will be cancelled by at least 20 dB. The "complex telegraphy" stations were the only type of transmissions which were not significantly cancelled. Hence the relative performance of a QLS-equipped sounder could be estimated quite closely by counting the number of such stations relative to others received at a particular receiver location. The reason the "complex telegraphy" signals do not cancel is that their wideband, comparatively noise-like spectrum develops uncorrelated responses in the three symmetrical filters.

For the "all stations" data the percent of the station indications which are of the "complex telegraphy" type can be approximately

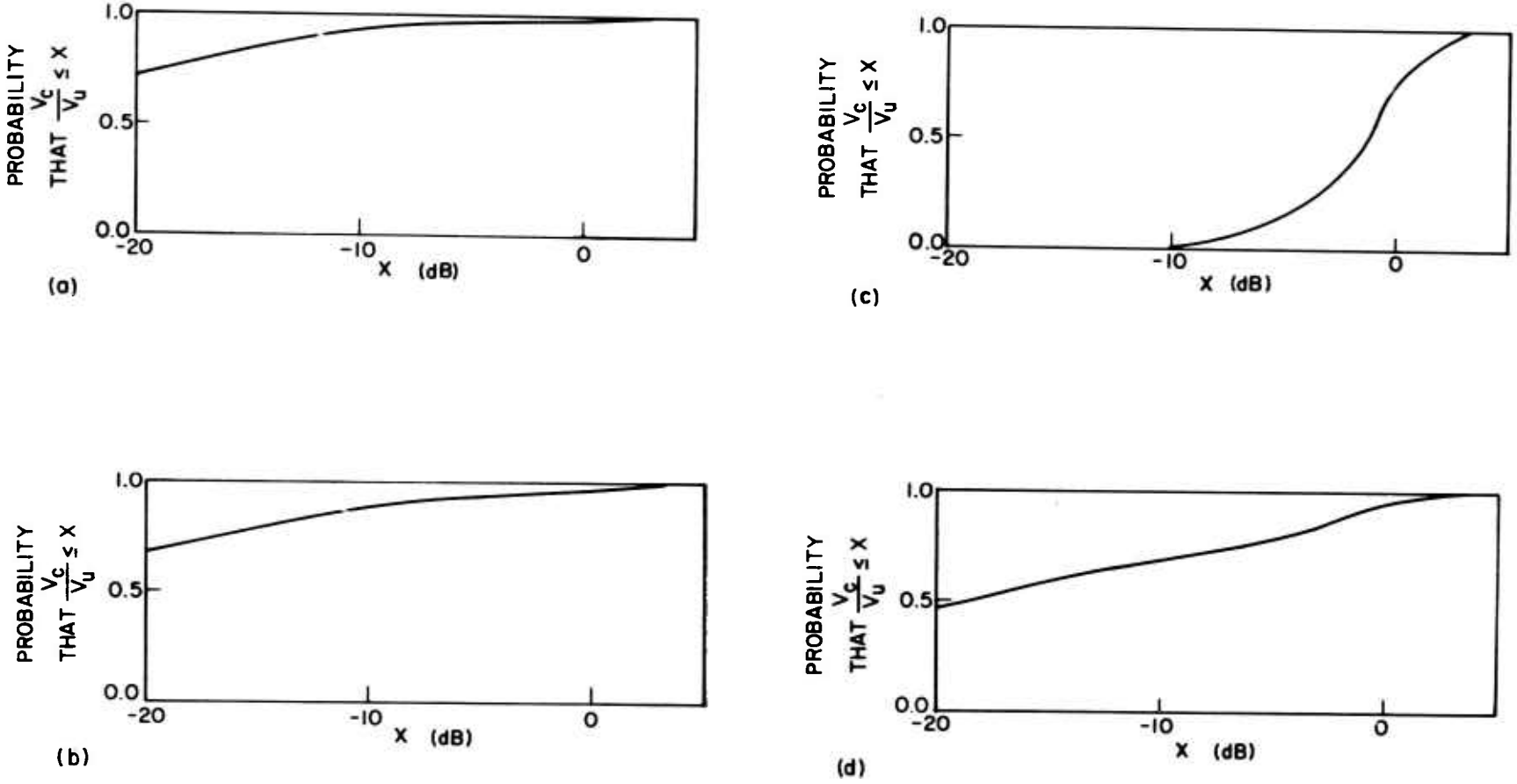

Fig. 42. CUMULATIVE PROBABILITY DISTRIBUTIONS OF QLS CANCELLATION. (Based on 10 sweeps 5.25 MHz.)
a. Broadcast, voice.
b. Simplex FSK, on-off keyed.
c. Complex telegraphy.
d. All stations.

Table 1

NUMBER OF STATION INDICATIONS USED TO PLOT PROBABILITY CURVES OF FIG. 42

TYPE OF STATION	NUMBER OF STATION INDICATIONS
Broadcast, voice	162
Simplex FSK, on-off keyed	167
Complex telegraphy	62
All stations	462

calculated. The probability P_T of cancelling the "complex telegraphy" signal by 20 dB is zero, while the probability P_0 of cancelling any other signal by 20 dB is approximately 0.7. Given the total number of stations, N_A, and the number of stations, N_C, which are "complex telegraphy," the probability P_A of cancelling a randomly selected station by 20 dB is

$$P_A = \frac{P_0(N_A - N_C)}{N_A} \quad . \tag{6.1}$$

$$N_C = N_A\left(1 - \frac{P_A}{P_0}\right) \quad . \tag{6.2}$$

Using Eq. (6.2), the number of "complex telegraphy" station indications included in the "all stations" category of Fig. 42 is found to be 140, or approximately 30 percent of the total number of station indications.

2. Spectrum-Analysis Comparison of Interference-Suppression Methods

As was described in Chapter III, the data produced in an FM-CW sounder is processed by spectrum analysis. The value of an interference-suppression method for the FM-CW receiver is measured by the amount of improvement obtained in the ratio of the desired signal responses in the final output to the response due to interference. Spectrum-analysis comparisons between the performance of the QLS and that of a separate-channel blanking system were made.

The block diagram shown in Fig. 43 illustrates the circuit interconnections used to obtain the spectrum-analysis data. Inherent in the blanking circuits is an adjustable threshold which, when exceeded, causes the blanking operation to occur. To compare the results using different threshold levels, spectrum analysis data were taken for three different separate-channel blanking threshold levels 0.5, 1 and 2 times the CW which simulated a desired signal. The data conclusively showed that the greatest ratio between the analyzer response at the CW desired-signal frequency and the analyzer responses at other frequencies caused by the interference was obtained with the blanking threshold set equal to the CW desired signal. The separate-channel blanking threshold was therefore so set in obtaining the spectrum-analysis data.

It seems likely that the self-blanking threshold giving the greatest ratio between the analyzer response at the CW desired-signal frequency and the analyzer responses due to interference at other frequencies, would also be approximately equal to the CW desired signal. A self-blanking threshold equal to the desired signal could not be used, however, without danger of signal self-blanking, which would cause undesirable intermodulation in the usual ionosphere sounder situation where the signal is more complex than a single CW desired signal. To give a reasonable immunity against intermodulation caused by signal self-blanking,

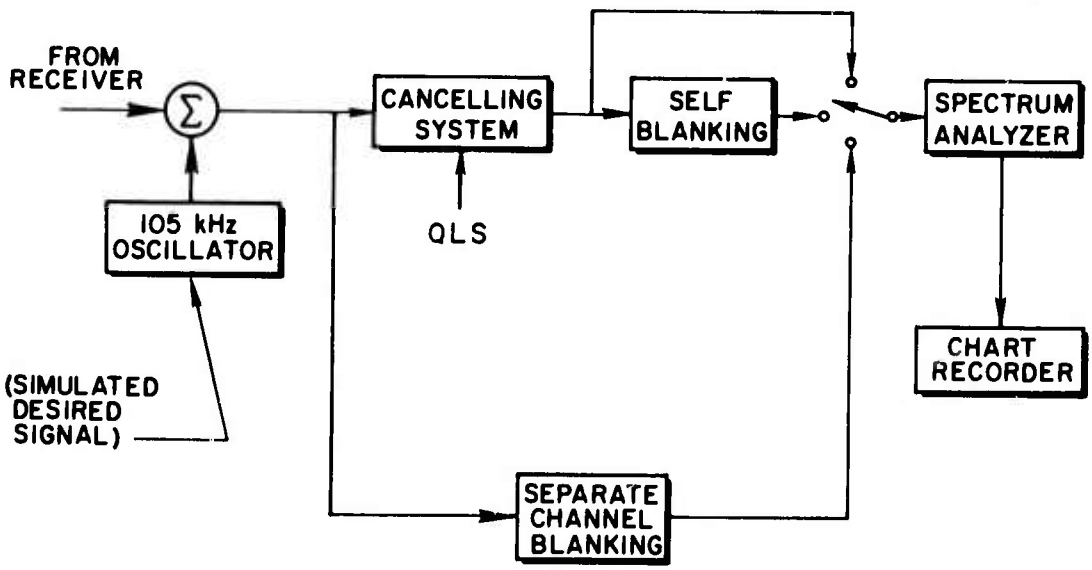

Fig. 43. BLOCK DIAGRAM OF SPECTRUM-ANALYSIS TEST.

the self-blanking threshold of the blanking following the QLS (cancelling system) was set equal to 2 times the CW desired signal.

The spectrum analyzer available for this test was a scanning filter type, so that the analysis of differing frequencies is not simultaneous. The relative amplitudes of the analyzer response at the desired-signal frequency and the responses due to interference at other frequencies is not very meaningful, since the amplitude of the desired signal response will depend on the amount of blanking caused by the interference at the time the desired-signal frequency is within the spectrum analyzer filter bandwidth. Therefore when two systems are compared which involve blanking, a separate measure of the desired signal is made in a non-scanning filter while interference is applied. In the spectrum analysis the filter bandwidth selected was 1 Hz, since this is a typical value for sounder signal processing. The minimum analyzer range of 50 Hz was selected because this is adequate to compare desired-signal and interference responses and also results in minimum data-taking time. For the desired-signal measurement in a non-scanning filter, the bandwidth was widened to 10 Hz to ease the problem of keeping the desired-signal frequency within the filter bandwidth.

The results of a spectrum analysis of the QLS output is shown in Fig. 44. These records were being taken while the receiver was being swept from 15 to 23 MHz by the FM-CW generator. Figure 44a shows the analysis with the QLS disabled. Figure 44b shows the improved ratio between the desired-signal and the interference responses when the cancelling action is restored. No blanking is performed here so that the desired-signal height does represent desired signal amplitude. Figure 44c shows a spectrum analysis demonstrating the further improvement obtained with the addition of self blanking. At the right of the spectrum analysis is a measure of the desired signal using a non-scanning filter. For calibration purposes approximately 1 cm of the desired-signal measurement is without interference. The periodicity of the measurement after the calibration is caused by the repeating sweeps of the receiver from 15 to 23 MHz

Figure 44d shows a similar spectrum analysis and signal measurement for the separate-channel blanking system. The difference between the minimum desired-signal amplitude in the cancel and self-blanking measurement,

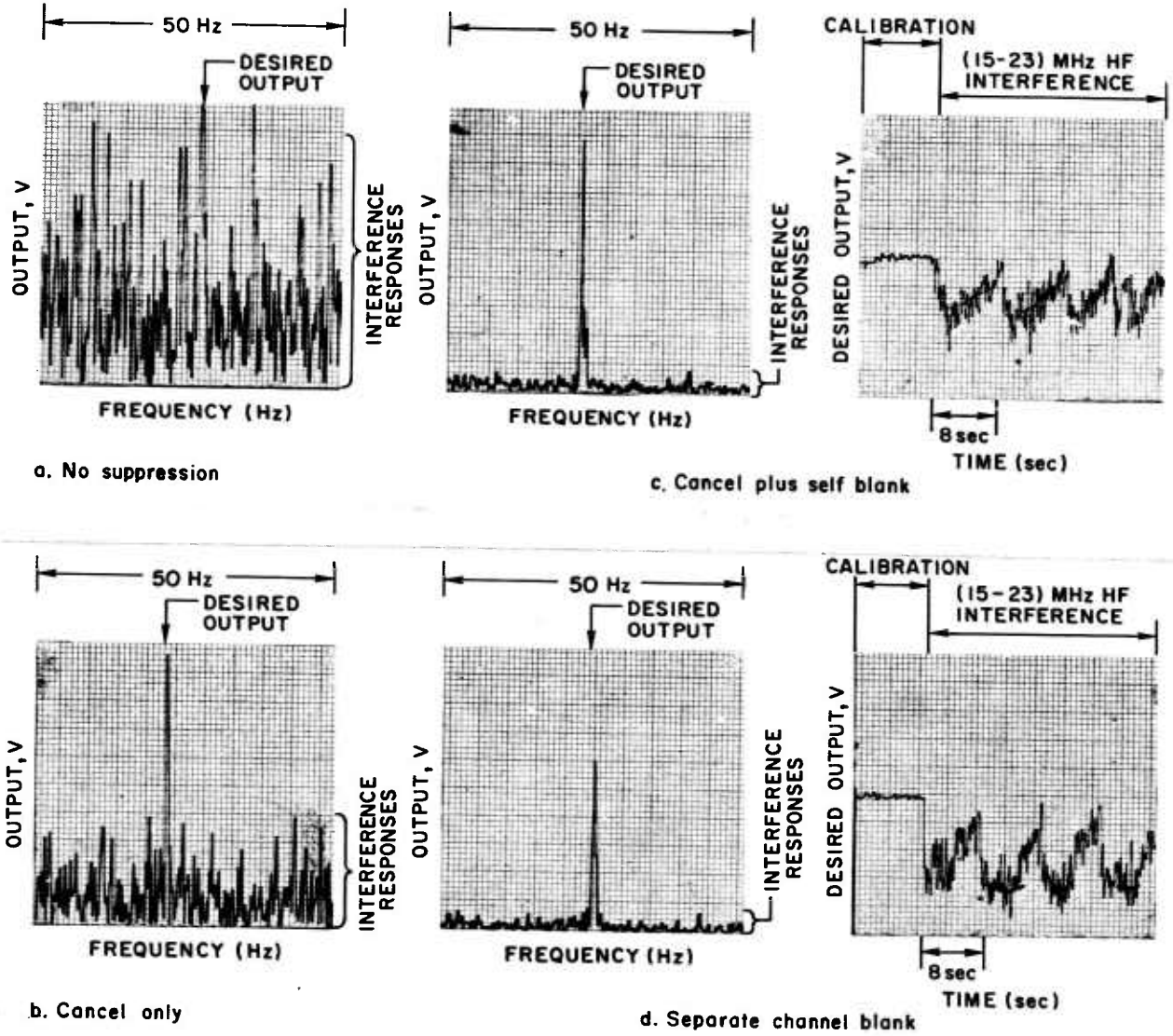

Fig. 44. RESULTS OF SPECTRUM ANALYSIS OF QLS OUTPUT.

and the separate-channel blanking measurement, is about 6 dB. The interference sideband responses in the separate-channel-blanking analysis are no more than 3 dB less than in the cancel-plus-self-blanking analysis, so that it can be seen that at least 3 dB improvement results from using the QLS as compared with separate-channel blanking.

3. FM-CW System Problems

The spectrum-analysis results of the QLS using the HF FM-CW receiver vary considerably when data are taken at times separated by an hour or more. This is not surprising in view of the fact that propagation varies from day to day, and so does the amount of traffic handled by spectrum users. In about ten days of taking spectrum analysis data, only two days resulted in performance as favorable as that illustrated by Fig. 44. The improvement provided during other days ranged from none at all to that of Fig. 44. More data of this type are not shown because it is felt that deficiencies of the present experimental FM-CW generator cause a considerable increase in the number of interfering signals present in the IF of the FM-CW receiver which cannot be suppressed by the QLS. Spurious signals in the FM-CW generator, and spurious responses from the mixer, cause a given strong interfering signal to be converted into a plurality of signals, some of which cannot be cancelled regardless of the type of transmission causing the interference.

A test was made to determine the number of spurious responses which result from a simulated single strong station. A crystal oscillator was inserted in place of the antenna and the amplitude was attenuated until the receiver signal-strength meter read the same as for a strong signal received by the antenna. A chart record of the envelope of the uncancelled and cancelled QLS outputs was made in the same manner as in finding the individual station performance (Fig. 40). This chart record is shown in Fig. 45. The gain between the QLS and the recording process was increased 30 dB from the earlier individual-station performance tests. However, the desired signal in the spectrum-analysis tests was about 40 dB below the strong interference, so that any response greater than about one large division is larger than the desired signal for the spectrum analysis tests. This record shows that one strong station of the

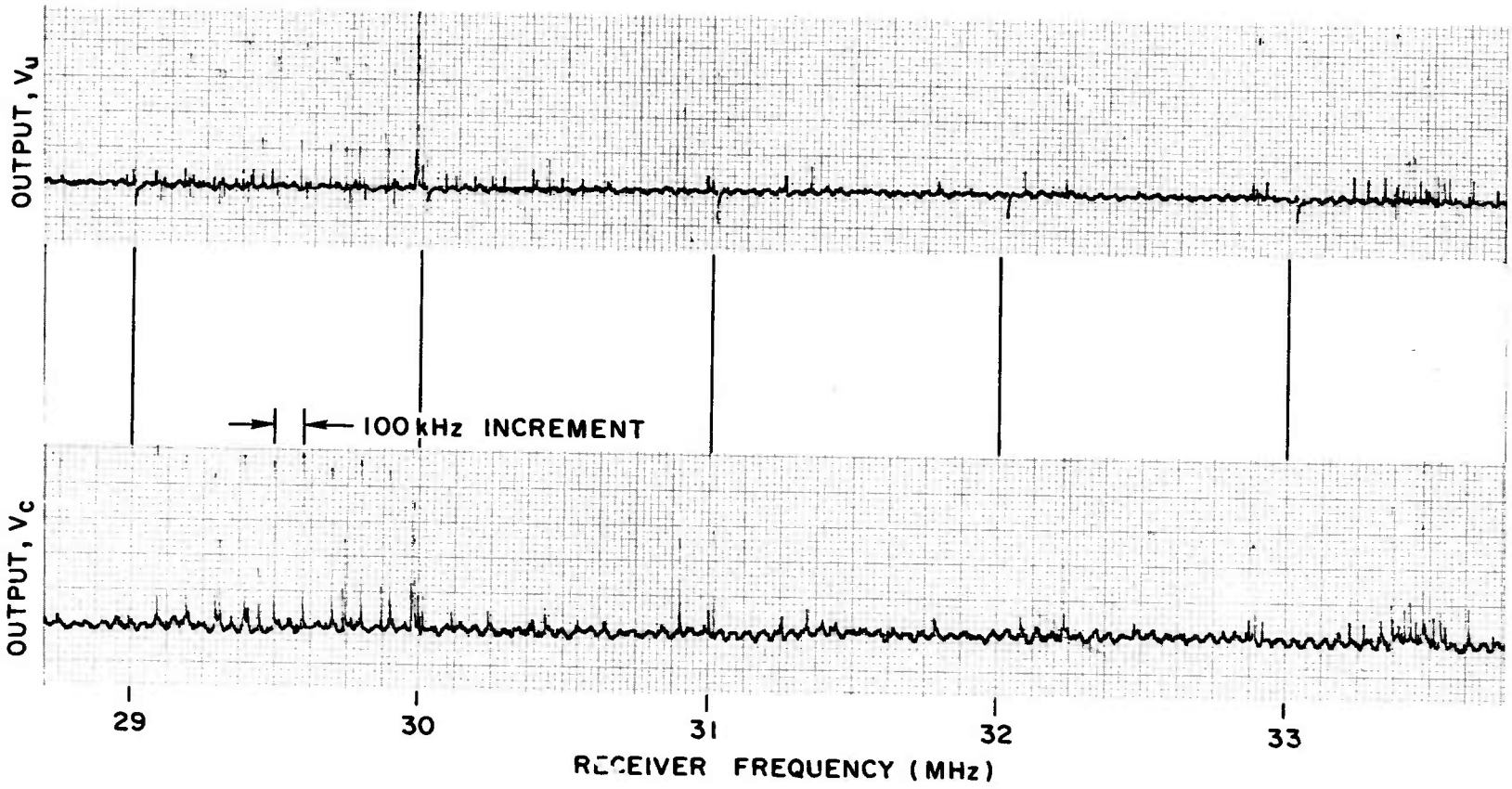

Fig. 45. EVIDENCE OF PROBLEM IN FM-CW SYSTEM.

type the QLS can cancel may result in more than 15 spurious responses which cannot be cancelled. The spurious responses are not cancelled because they are not caused by FM-CW signals of the correct sweep rate and sweep direction. Desired-signal energy is lost because of the resulting self blanking, and the undesired spectrum analyzer responses are made larger by the desired-signal modulation associated with the blanking and by the interference whose amplitude is insufficient to operate the blanker.

The spurious responses shown in Fig. 45, which occur every 100 kHz, are caused by the FM-CW generator; but the exact reason for their existence has not been determined. Since the QLS cannot cancel them, they must be caused by a waveform other than FM-CW, or by an FM-CW of incorrect sweep rate or sweep direction. It seems likely in the future that improved FM-CW generators will be designed. In that case, the QLS will be of greater benefit in FM-CW sounders than it is with the generators presently being used.

VII. CONCLUSION

A. SUMMARY OF RESULTS

A new method of interference suppression has been devised and has been shown capable of cancelling certain types of interference with negligible effect on the desired signal. The method translates interference energy from outside the signal bandwidth into the signal bandwidth in a phase-coherent manner so that the interference included with the signal can be balanced out. Other than at times of switching from the cancelling to the noncancelling mode, the system can be considered approximately linear, and hence the name Quasi-Linear Suppressor (QLS) has been used.

A requirement enabling a possible application of the QLS is that the interference which is to be cancelled must have frequency components outside as well as within the desired signal bandwidth. Pulse and FM-CW are examples of such interference. The block diagram for a QLS of a configuration to cancel pulse interference is shown in Fig. 18. Figure 20 shows a block diagram similar to Fig. 18 except for the addition of two delay networks. This addition results in a configuration of the QLS suitable for cancelling FM-CW interference.

An important application of the FM-CW version of the QLS is to reduce the interference caused by fixed stations in an FM-CW ionosphere sounder. The FM-CW sounder application was the major motivation for this work.

An experimental implementation of the system demonstrated the feasibility of the QLS, although this implementation did not include all the capabilities that would be desired in an actual FM-CW sounder receiver installation. Some of the circuits involved represent original design which has not previously been published to the author's knowledge. The digital phase modulator (Fig. 25b) is perhaps the best example of original design.

The results of testing the breadboard version of the QLS using laboratory-generated signals are in accordance with prediction. Figure 34b is an oscillogram illustrating the waveforms obtained when testing the pulse QLS. This oscillogram shows the CW desired signal combined

with pulse interference, before cancellation (V_u) and after cancellation (V_c). Figure 36b is an oscillogram obtained in like manner using the FM-CW configuration of the QLS. The same signals are shown in Fig. 36a as in Fig. 36b except for the absence of the CW desired signal.

The signal obtained by the FM-CW ionosphere sounder is processed by spectrum analysis. Therefore an appropriate test of the QLS is to spectrum-analyze a CW signal combined with the FM-CW interference. Figure 37 shows the results of such a test at three different levels of CW signal and FM-CW interference.

An even more meaningful test of the QLS for sounder purposes is to use FM-CW interference generated by HF radio stations in an FM-CW sounder receiver. Figure 41 shows a chart record of the envelope of such HF radio interference before (V_u) and after (V_c) the QLS cancellation. This chart record demonstrates that a majority of the received responses arising from HF station interference have been cancelled by more than 20 dB. The results of spectrum analysis tests using HF radio interference are shown in Fig. 44. The text explains how the spectrum analyses shown in Fig. 44 were used to deduce that the QLS gave 3 dB better performance than a hitherto preferred nonlinear interference suppression technique.

B. DISCUSSION AND EVALUATION

The QLS is designed to be effective in eliminating FM-CW interference having a known sweep rate and direction. It was found that the FM-CW generator that was used in the QLS tests contained output energy other than FM-CW of the correct sweep rate and direction. These undesired FM-CW signal components cause a multiplicity of receiver responses from a single HF station signal. Many of these responses will not be cancelled by the QLS; in fact, on the average they will be increased. The result is that many interfering stations, having properties such that the QLS can cancel the expected receiver response produced by the stations, will cause considerable interference energy at the QLS output due to the FM-CW generator spurious outputs. The QLS may prove to be of much greater benefit as compared with the best nonlinear interference-suppression technique when FM-CW generators are available that are more free from spurious responses.

A desirable configuration of the QLS which requires an accurate time reference for the interfering FM-CW signal was not used in the test results presented in Chapter VI. The time reference is obtained from the interference-occurrence detector of Fig. 20. The interference-occurrence detector which was used in the QLS breadboard was adequate for unmodulated FM-CW signals, but did not perform well for the HF radio-station interference. The function performed by the detector is to measure the time at which a scanning (FM-CW) modulated interference may be said to have reached a particular frequency. This could probably best be done by scanning spectrum-analysis techniques using compressive filters.

The construction of an improved interference-occurrence detector using compressive filters would require considerable time and expense. Since the spurious responses of the FM-CW generator being used in the tests were the major limiting factor in the QLS performance, this added time and expense did not seem justified for the present.

In some FM-CW systems it may be desirable to vary the sweep rate. This would require some means of adjusting the QLS. The only major adjustment needed would be an adjustment in the delay of the time-delay networks. A method of making an easily adjusted delay would be to convert analog information to digital form and then obtain delay in shift registers. The amount of delay is determined by the rate the register is advanced. Recent developments in integrated-circuit fabrication of shift registers using metal oxide silicon-field effect transistors (MOSFETS) may make it easy to construct the adjustable delays.

C. CONCLUSION

The QLS can effectively cancel FM-CW or pulse interference with negligible effect on a desired narrow-band signal. The interference-rejection capability of an FM-CW ionosphere sounder can be improved by approximately 3 dB by using the QLS. It is expected that the improvement afforded in the interference rejection capability of the sounder will be increased beyond 3 dB if FM-CW generators are developed which are more free from spurious responses.

D. RECOMMENDATIONS FOR FUTURE WORK

During the progress of this work it was determined that the spurious outputs of the FM-CW generator seriously degrade the interference-rejection properties of the FM-CW ionosphere sounder. In addition, these spurious responses are particularly detrimental to the QLS performance, since they are not FM-CW signals of a correct sweep rate and direction. Therefore a primary effort in improving the interference rejection of the FM-CW ionosphere sounder would consist in finding either methods of building spurious-free FM-CW generators, or methods to eliminate the spurious responses of the presently available generators.

The improved FM-CW generators would probably increase the effectiveness of the QLS and thus justify further experimentation to optimize the QLS performance. This, in turn, would be likely to entail building the improved interference-occurrence detector. The development of the variable delay mentioned in the discussion above would also be desirable in order to increase the versatility of the QLS.

Appendix

BASIC CIRCUITS USED IN THE QLS

The circuits discussed in this appendix perform the functions of switching, detection, amplification, and signal generation as indicated on the block diagrams of the QLS. In some cases the criterion for selecting a particular circuit was that almost identical versions are available in integrated-circuit form. If further realizations of the QLS are constructed in the future, a greater use of integrated circuits should reduce cost and simplify construction.

1. Unity-Gain Amplifier

Figure 46 shows the feedback-pair amplifier which is used where circuit isolation and unity voltage gain are required. This circuit is similar to versions appearing in transistor-circuit texts, except for the addition of the diode CR1 which compensates for the base-emitter voltage drop in the input transistor Q1 resulting in nearly zero DC voltage offset between the input and the output. The compensation is not particularly precise (it is accurate to within about 0.1 V); but it is adequate for the usage required in the QLS.

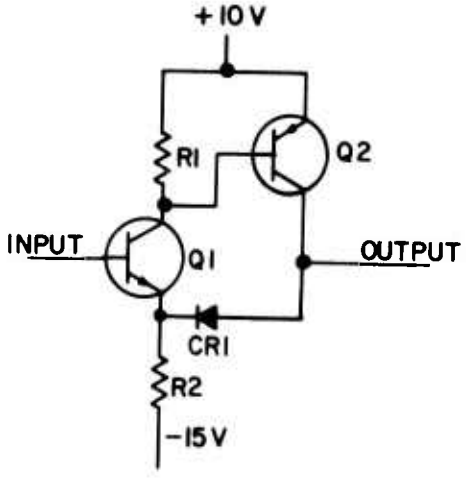

Fig. 46. UNITY-GAIN AMPLIFIER.

2. Dr

The driver circuit shown in Fig. 47 is suitable for increasing the voltage range of logic signals from the less than 3 V level used with integrated-circuit logic, to approximately 25 V. This circuit was chosen because an integrated circuit containing up to five circuits equivalent to Fig. 47 is available from Siliconix, Inc.

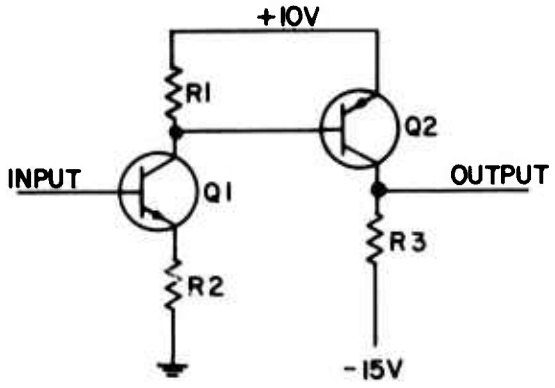

Fig. 47. DRIVER CIRCUIT.

3. Electronic Switches

The schematic diagram for an electronic SPDT switch is shown in Fig. 48. The complementary control input signals are obtained from either a bi-stable or a comparator. For purposes of illustration, control 2 is assumed to be "low," causing the output of Driver No. 2 to be negative. This forward-biases CR2 and (overriding any effect of the output of the amplifier through R2) turns off the Field Effect Transistor (FET) Q_2. The "high" input at Driver 1 causes a positive output which back-biases CR1, enabling the amplifier output to control the gate of Q_1 through R_1. The "on" resistance of Q1 is negligible compared to the amplifier input impedance. The gate current of Q1 plus the leakage current of CR1 causes negligible voltage drop in R1. Therefore, equal potentials exist at input 1, at all three terminals of Q1, and at the amplifier output.

As in the case of the driver, equivalent integrated circuit versions of the SPDT switch are available from Siliconix, Inc. New versions which became available in March 1968 have up to five SPST switches, including drivers, in a single integrated circuit package.

When an SPST switch was needed in the QLS, one of the drivers of Fig. 48 with its associated diode, resistor and FET was omitted, and a resistor was added from the amplifier input to ground to give zero voltage in the switch "off" position.

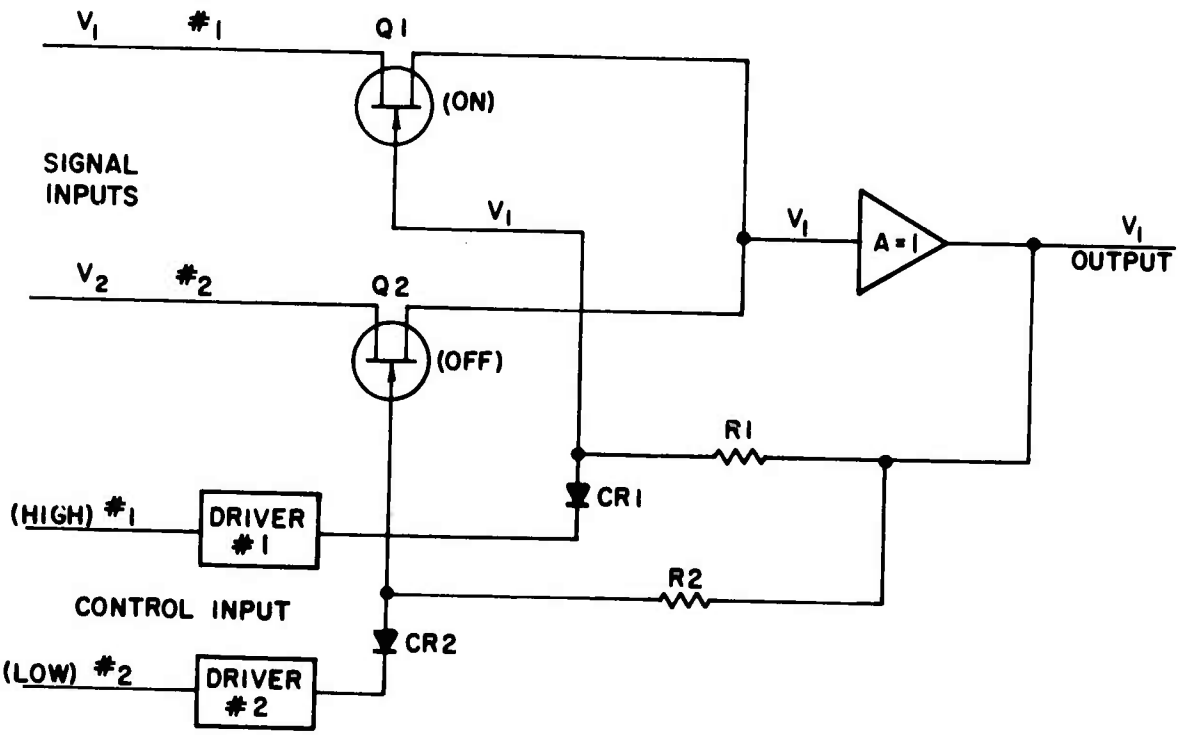

Fig. 48. SPDT SWITCH.

4. Envelope Detector

A conventional diode detector would fail to have the required dynamic range needed for the QLS applications. The circuit shown by the schematic diagram in Fig. 49 has much greater dynamic range than does the conventional diode detector. Wide dynamic range is assured by two

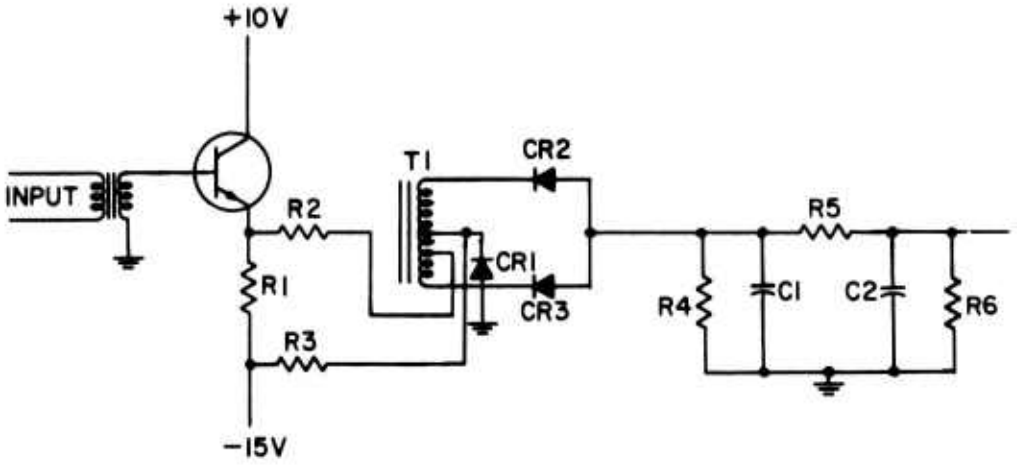

Fig. 49. ENVELOPE DETECTOR.

features: First, the forward threshold of diodes CR2 and CR3 is compensated by forward-biased diode CR1; and second, any uncompensated threshold is made less objectionable by stepping up the signal AC potential by a factor of about ten in the autotransformer T1.

5. Crystal Oscillator

The local oscillator signal for the mixer which converted the FM-CW receiver IF output to the QLS operating frequency was provided by the circuit shown by the schematic diagram in Fig. 50. This is a particularly appropriate circuit for a transistor crystal oscillator because the crystal terminating resistances are very low, resulting in little degradation of the Q of the crystal in the series-resonant mode. The tank circuit (T1, C1, R1) is of very low Q, but has sufficient selectivity to prevent oscillation on an undesired crystal overtone.

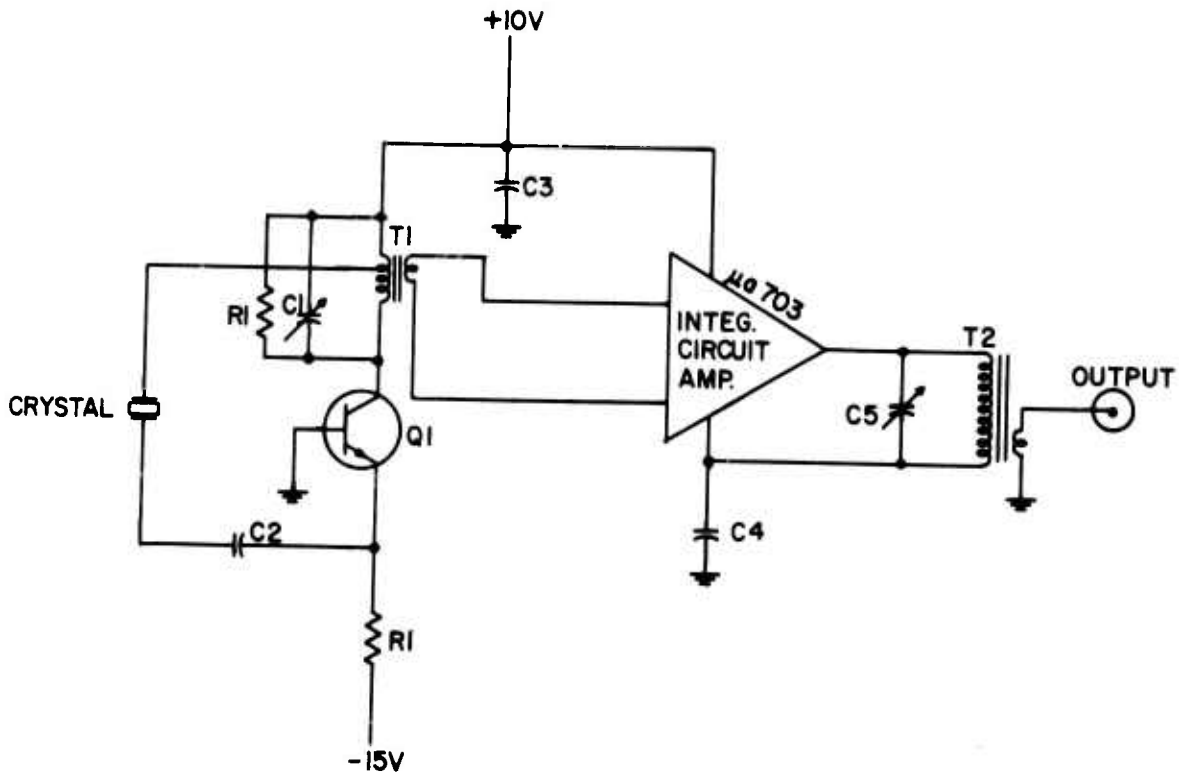

Fig. 50. CRYSTAL OSCILLATOR.

REFERENCES

1. T. A. Potemra, "Acoustic-Gravity Waves in the Atmosphere," Rept. SU-SEL-65-097 (TR 110), Stanford Electronics Laboratories, Stanford, Calif., Nov 1965.

2. W. C. Headrick and E. W. Ward, "High Frequency Channel Occupancy," Unofficial Advance Copy of Report, U.S. Naval Research Laboratory, Washington, D. C., Apr 1966.

3. R. N. Bracewell, The Fourier Transform and Its Applications, McGraw-Hill Book Co., Inc., New York, 1965.

4. G. Breit and M. Tuve, "A Test of the Existence of the Conducting Layer," Phys. Rev. 28, p. 554, Sep 1926.

5. H. A. Hall, "A New Model for "Impulsive" Phenomena: Application to Atmospheric-Noise Communication Channels," Rept. SU-SEL-66-052 (TR 3412-8, TR 7050-7), Stanford Electronics Laboratories, Stanford, Calif., Aug 1966.

6. B. Widrow, P. E. Mantey, L. J. Griffiths, and B. B. Goode, "Adaptive Antenna Systems," Proc. IEEE, Dec 1967, pp. 2143-2159.

7. D. O. North, "Analysis of the Factors Which Determine Signal/Noise Discrimination in Radar," Rept. PTR-6C, RCA Laboratories, Jun 1943.

8. G. L. Turin, "An Introduction to Matched Filters," IRE Transactions on Information Theory, Jun 1960, pp. 311-329.

9. J. S. Rochefort, "Matched Filters for Detecting Pulse Signals in Noise," IRE Nat'l. Conv. Rec. 2, pt. 4, pp. 30-34, 1954.

10. D. C. Coll and J. R. Storey, "Ionospheric Sounding Using Coded Pulse Signals," Radio Science (J. Res., NBS/USNC-URSI), 680, 10 Oct 1964, pp. 1155-1159.

11. R. M. Lerner, "Design of Signals," Lectures on Communication System Theory, E. J. Baghdady ed., McGraw-Hill Book Co., Inc., New York, 1961, pp. 243-277.

12. S. Gnanalingam, "An Apparatus for The Detection of Weak Ionospheric Echoes," Proc. IEE, Mar 1954 (Paper No. 1670) pp. 243-248.

13. R. B. Fenwick and G. H. Barry, "HF Measurements Using Extended Chirp-Radar Techniques," Rept. SU-SEL-65-058 (TR 103), Stanford Electronics Laboratories, Stanford, Calif., Jun 1965.

14. E. J. Baghdady, "Analog Modulation Systems," Lectures on Communication System Theory, E. J. Baghdady ed., McGraw-Hill Book Co., Inc. New York, 1961, pp. 439-555.

15. S. J. Jennings and A. A. Winkeljohann, "Fundamentals of System Analysis," Handbook of Automation Computation and Control, E. M. Grabbe, S. Rambo, and D. E. Wooldridge, eds., John Wiley & Sons, Inc., New York, 1958, pp. (20-01) (20-84).

16. D. R. Jackson and R. W. Orth, "A Frequency Selective Limiter Using Nuclear Magnetic Resonance," Proc. IEEE, 55, Jan 1967, pp. 36-45.

17. R. A. Weagant, "Reception Thru Static and Interference," Proc. IRE, Jun 1919, pp. 207-244.

18. M. Wald, "Noise Suppression by Means of Amplitude Limiters," Wireless Eng., Vol. 17, p. 432, Oct 1940.

19. A. J. Nicholson and M. J. Kay, "Reduction of Impulse Interference in Voice Channels," IEEE Trans. on Communication Technology, Dec 1964.

20. E. H. Armstrong, "Methods of Reducing the Effect of Atmospheric Disturbances," Proc. IRE, Jan 1928, pp. 15-26.

21. J. R. Carson, "The Reduction of Atmospheric Disturbances," Proc. IRE, Jul 1928, pp. 966-975.

22. R. C. Cumming, "The Serrodyne Frequency Translator," Proc. IRE, Feb 1957, pp. 175-186.

23. R. C. Cumming, "Serrodyne Performance and Design," Microwave Journal, Sep 1965.

24. W. R. Kincheloe, Jr., "The Measurement of Frequency with Scanning Spectrum Analyzers," Rept. SEL-62-098 (TR 557-2), Stanford Electronics Laboratories, Stanford, Calif., Oct 1962.

25. C. V. Smith and E. V. Phillips, "MOS-FET Clutter Canceller," Rept. SRS-678, Hughes Aircraft Co., Culver City, Calif., Apr 1967.

26. W. L. Black, "An Impulse Noise Canceller," IEEE Trans. on Communications Systems, CS-11, p. 506, Dec 1963.

27. G. Hok, "The Response of a Linear Resonant System to Excitation of a Frequency Varying Linearly with Time," J. Applied Phys., 19, Mar 1948, pp. 242-250.

DISTRIBUTION LIST

U-Series

NAVY

Chief of Naval Research
Department of the Navy
Washington, D. C. 20360
2 Attn: Code 418
1 Attn: Code 2027

Director
U.S. Naval Research Lab
Washington, D. C. 20390
1 Attn: Code 5320
(Mr. E. Zettle)
1 Attn: Code 5320
(Mr. J.M. Headrick)
1 Attn: Code 5432C
(Mr. F.A. Polinghorn)

Chief of Naval Operations
Department of the Navy
The Pentagon
Washington, D. C. 20350
1 Attn: OP-07TE
1 Attn: OP-723E

Commander
U.S. Naval Missile Center
Point Mugu, California 93041
1 Attn: Code N03022

Commander
Naval Weapons Center
China Lake, California 93555
1 Attn: Code 4025
(Mr. R.S. Hughes)

Commander
Naval Command Control Communications Laboratory Center
San Diego, California 92152
1 Attn: Mr. H.J. Wirth
1 Attn: Library

Commander
Naval Weapons Center
Corona Laboratories
Corona, California 91720
1 Attn: Mr. V.E. Hildebrand

Director
Office of Naval Research
Branch Office
495 Summer Street
Boston, Massachusetts 02210
1 Attn: Mr. Stan Curley

AIR FORCE

Headquarters, USAF
The Pentagon
Washington, D.C. 20330
1 Attn: AFNICAD
(MAJ Nyquist)
1 Attn: AFRDDF

Headquarters, USAF
Office of Assistant Chief of Staff, Intelligence
Washington, D. C. 20330
1 Attn: AFNICAA

Commander
Rome Air Development Center
Research & Technology Div.
Griffiss AFB, New York 13442
1 Attn: EMASO
(Mr. S. DiGennaro)
1 Attn: EMAES
(MAJOR D.R. Wipperman)
1 Attn: EMASR
(Mr. V.J. Coyne)
1 Attn: EMASA

Headquarters, AF Systems Command
Foreign Technology Division
Wright-Patterson AFB.
Ohio 45433
1 Attn: TDC (Mr. Zabatakas)
1 Attn: TDEED
(Mr. W. L. Picklesimer)
1 Attn: TDCES
1 Attn: TDCE
(Mr. M.S.J. Grabener)

Headquarters
AF Systems Command
Research & Technology Division
Bolling AFB, Washington,
D.C. 20332
1 Attn: RTTC
(Mr. Philip Sandler)

Headquarters
USAF Security Service (OSA)
San Antonio, Texas 78241
1 Attn: Mr. W. L. Anderson
ODC-R

Headquarters
Air Defense Command
Ent AFB, Colorado Springs,
Colorado 80912
1 Attn: NPSD-A
1 Attn: ADLPC-2A
(LCOL R.J. Kaminski)
1 Attn: ADOAC-ER
1 Attn: NELC-AP

Electronics Systems Div. (ESSL)
L. G. Hanscom Field
Bedford, Massachusetts 01731
1 Attn: 440L

Headquarters SAC (OAI)
Offutt AFB
Omaha, Nebraska 68113
1 Attn: Mrs. E. G. Andrews

Headquarters, AFCRL
L.G. Hanscom Field
Bedford, Massachusetts 01731
1 Attn: CRUI
1 Attn: CRUP (Dr. G.J. Gassman)

U.S. Air Force
Western Test Range
Vandenberg AFB,
California 93437
1 Attn: WTGT
(Mr. Stanley Radom)

Headquarters, USAF AFTAC
Washington, D. C. 20333
1 Attn: TD-3

Major T.D. Damon
Hqtrs. Air Weather Service
(AWVDC)
1 Scott Air Force Base, Illinois
62265

ARMY

Office of the Assistant Chief
of Staff for Intelligence
Department of the Army
The Pentagon, Room 2B 457
Washington, D. C. 20310
1 Attn: Mr. Joseph Grady

U. S. Army SLAG
The Pentagon, Room 1B 657
Washington, D. C. 20310
1 Attn: Mr. N. R. Garofalo

Chief, Army Security Agency
Arlington Hall Station
Arlington, Virginia 22212
1 Attn: Mr. R. R. Neill
1 Attn: IAOPS-O(SA)

Commanding Officer
U.S. Army Security Agency
Processing Center
Vint Hill Farms Station
Warrenton, Virginia 22186
1 Attn: LT Alan Bagully
1 Attn: Technical Library

Commander, Electronics
Warfare Lab
Mt. View Office, USAEC
P.O. Box 205
Mt. View, California 94040
1 Attn: Mr. Joseph Bert

U. S. Army Foreign Science &
Technology Center
Munitions Building
Washington, D. C. 20315
1 Attn: Communications &
Electronics Division

Commanding General
U. S. Army Missile Command
Redstone Arsenal, Alabama 35809
1 Attn: AMSMI-RES

DEPT. OF DEFENSE

Director
Advanced Research Projects Agency
The Pentagon
Washington, D. C. 20301
1 Attn: Mr. Alvin Van Every

Office of the Assistant Director
Intelligence & Reconnaisance
Office of the Director of Defense
Research & Engineering
The Pentagon, Room 3E 119
Washington, D. C. 20301
1 Attn: Mr. H. A. Staderman

Director
National Security Agency
Ft. George G. Meade
Maryland 20755
1 Attn: K-344 (Mr. C. Gandy)
1 Attn: C3-TDL

Deputy Director
Research & Technology
Office of the Director of
Defense Research & Engineering
The Pentagon, Room 3E 1030
Washington, D. C. 20301
1 Attn: Dr. C. W. Sherwin

Office of the Assistant
Director (Defense Systems)
Defense Research & Engineering
The Pentagon, Room 3D 138
Washington, D. C. 20301
1 Attn: Mr. Daniel Fink

Director, Defense
Intelligence Agency
The Pentagon, Room 3B 259
Washington, D. C. 20301
1 Attn: DIACO-4
1 Attn: DIAST-2B

Director, Weapons Systems
Evaluation Group
Office of the Director of
Defense, Research & Engineering
1 Washington, D. C. 20301

Defense Documentation Center
Cameron Station
20 Alexandria, Virginia 22314

National Aeronautics & Space
Administration
Ames Research Center
Moffett Field, California 94035
1 Attn: Dr. Kwok-Long Chan
1 Attn: Mr. Lawrence Colin

OTHER

ITT Electro-Physics Labs Inc.
3355 - 52nd Avenue
Hyattsville, Maryland 20781
1 Attn: Mr. W. T. Whelan

Institute for Defense Analyses
400 Army-Navy Drive
Arlington, Virginia 22202
1 Attn: Dr. Louis Wetzel

MITRE Corporation
E Bldg., Room 353
Bedford, Massachusetts 01730
1 Attn: Mr. W.A. Whitcraft, Jr.
1 Attn: Mr. Bill Talley

RAND Corporation
1700 Main Street
Santa Monica, California 90406
1 Attn: Dr. Cullen Crain
1 Attn: Library

Raytheon Company
Spencer Laboratory
2 Wayside Road
Burlington, Massachusetts 01803
1 Attn: Mr. L. C. Edwards

U-Series - Other (Cont)

Stanford Research Institute
Menlo Park, California 94025
1 Attn: Dr. David Johnson

Sylvania Electronics Systems
Electronics Defense Laboratory
P. O. Box 205
Mt. View, California
1 Attn: Mr. John DonCarlos

Mr. Thurston B. Soisson
Box 8164 SW Station
1 Washington, D. C. 20024

Astrophysics Research Corporation
10889 Wilshire Blvd.
Los Angeles, California 90024
1 Attn: Dr. Alfred Reifman

Institute of Science & Technology
The University of Michigan
P. O. Box 618
Ann Arbor, Michigan 48105
1 Attn: BAMIRAC Library

Bendix Corporation
Bendix Radio Division
Baltimore, Maryland 21204
1 Attn: Mr. John Martin

AVCO Systems Division
Lowell Industrial Park
Lowell, Massachusetts 01851
1 Attn: Mr. Sidney M. Bennett

U.S. Department of Commerce
ITSA - ESSA
Boulder, Colorado 80302
1 Attn: Mr. William Utlaut
1 Attn: Mr. L. H. Tveten
1 Attn: Mr. W. A. Klemperer,
Div. 530, ESSA

Page Communications, Inc.
3300 Whitehaven St., NW
Washington, D. C. 20008
1 Attn: Mr. David Fales, III

Massachusetts Institute of
Technology
Lincoln Laboratory
P. O. Box 73
Lexington, Massachusetts 02173
1 Attn: Dr. J. H. Chisholm

Massachusetts Institute
of Technology
Center for Space Research
Building 33-109
Cambridge, Massachusetts 02138
1 Attn: Dr. J.V. Harrington

Princeton University
James Forrestal Research Center
Plasma Physics Laboratory
P. O. Box 451
Princeton, New Jersey 08540
1 Attn: Dr. Edward Frieman

University of California
Mathematics Department
Berkeley, California 94720
1 Attn: Dr. E. J. Pinney

Electronics Research Laboratory
University of California
Berkeley, California 94720
1 Attn: Prof. D. J. Angelakos

Battelle-Defender
Battelle Memorial Institute
505 King Avenue
1 Columbus, Ohio 43201

HRB-Singer, Inc.
Science Park
P.O. Box 60
State College, Pennsylvania 16801
1 Attn: Library

Bickard & Burns,
Research Department
103 Fourth Avenue
Waltham, Massachusetts 02154
1 Attn: Dr. J. C. Williams

Other U-Series (Cont)

Sylvania Electronic Systems
Applied Research Laboratory
40 Sylvan Road
Waltham, Massachusetts 02154
1 Attn: Library

Department of Electrical
Engineering
Radiolocation Research Laboratory
University of Illinois
Urbana, Illinois 61803
1 Attn: 311 EERL (Mr. D.G. Detert)

Arecibo Ionospheric Observatory
Box 995
Arecibo, Puerto Rico 00613
1 Attn: Librarian

The University of Texas
Electrical Engineering Research
Laboratory
Route 4, Box 189
Austin, Texas 78756
1 Attn: Mr. C. W. Tolbert

Rice University
Fondren Library
P.O. Box 1892
1 Houston, Texas 77001

Purdue University
Library
1 West Lafayette, Indiana

Telcom, Incorporated
5801 Lee Highway
Arlington, Virginia 22207
1 Attn: Mr. J. D. Ahlgren,
Vice President

UNCLASSIFIED

Security Classification

DOCUMENT CONTROL DATA - R & D

(Security classification of title, body of abstract and indexing annotation must be entered when the overall report is classified)

1. ORIGINATING ACTIVITY *(Corporate author)*
Stanford Electronics Laboratories
Stanford University
Stanford, California

2a. REPORT SECURITY CLASSIFICATION
UNCLASSIFIED

2b. GROUP

3. REPORT TITLE
QUASI-LINEAR INTERFERENCE SUPPRESSOR

4. DESCRIPTIVE NOTES *(Type of report and inclusive dates)*
Technical Report No. 150

5. AUTHOR(S) *(First name, middle initial, last name)*
A. C. Phillips

6. REPORT DATE
August 1968

7a. TOTAL NO. OF PAGES
102

7b. NO. OF REFS
27

8a. CONTRACT OR GRANT NO.
Nonr-225(64), NR 088 019

b. PROJECT NO.

c.

d.

9a. ORIGINATOR'S REPORT NUMBER(S)
SEL-68-052

9b. OTHER REPORT NO(S) *(Any other numbers that may be assigned this report)*

10. DISTRIBUTION STATEMENT This document is subject to special export control and each transmittal to foreign governments or foreign nationals may be made only with prior approval of the Office of Naval Research, Field Projects Programs, Washington, D.C. 20360.

11. SUPPLEMENTARY NOTES

12. SPONSORING MILITARY ACTIVITY
Office of Naval Research

13. ABSTRACT The purpose of this research was to devise and test new interference suppression techniques. A major motivation was the desire to minimize the deleterious effects of HF radio-station interference to an ionosphere sounder. Previous research has shown that the FM-CW waveform is particularly attractive for ionosphere sounding because of the ability to generate waveforms having very large time bandwidth products using electronically controlled frequency synthesizers. In studying interference problems during this research it was appreciated for the first time that simple nonlinear processing (e.g., clipping) in the FM-CW sounder is directly analogous to the much more complicated nonlinear processing (e.g., frequency-by-frequency limiting) necessary in the corresponding simple-pulse or coded-pulse sounding systems.

A new interference suppression method has been devised and shown to be effective in removing pulse or FM-CW interference from narrow-band signals. Interference energy at frequencies outside the desired-signal bandwidth is processed and used to balance out the interference energy included with the desired signal. The balancing action is intermittent and the principle of operation is to switch from one linear mode to another, hence the name quasi-linear suppressor (QLS).

The performance of the quasi-linear suppressor in removing pulse or FM-CW signals generated in the laboratory, was shown to be very satisfactory. An FM-CW sounder receiver was tested at a field site where antennas of a type typically used for ionosphere sounding were available. It was found that the new suppressor was able to decrease the amplitude of the IF response due to interference at least 20 dB for about 70 percent of the stations. The FM-CW receiver was also used to compare the suppression of HF radio-station interference by means of the new quasi-linear suppressor, with a hitherto

DD FORM 1 NOV 65 1473 (PAGE 1)

S/N 0101-807-6801

UNCLASSIFIED

Security Classification

14. KEY WORDS	LINK A		LINK B		LINK C	
	ROLE	WT	ROLE	WT	ROLE	WT
INTERFERENCE SUPPRESSION IONOSPHERE SOUNDER HF RADIO COMMUNICATION IMPULSE INTERFERENCE						

(Abstract Contd)

preferred nonlinear technique. A CW signal, to simulate a desired sounder signal, was added to the interference background received from the antenna. The criterion for performance in this test was the ratio of the spectrum analyzer response at the desired CW frequency, to analyzer responses caused by the interference. (The interference usually affects all filters in the analyzer roughly alike.) The improvement in this ratio when using the quasi-linear suppressor was found to be approximately 3 dB. It is felt that this is a pessimistic result because in the process of testing, it was observed that the laboratory FM-CW generator contained spurious outputs which greatly increased the effects of the interference in a way which reduced the advantage of the quasi-linear scheme over nonlinear methods.